SANDIA REPORT

SAND2014-18206
Unlimited Release
Printed September 2014

Characterization of U.S. Wave Energy Converter (WEC) Test Sites: A Catalogue of Met-Ocean Data

Ann R. Dallman, Vincent S. Neary

Prepared by
Sandia National Laboratories
Albuquerque, New Mexico 87185 and Livermore, California 94550

Sandia National Laboratories is a multi-program laboratory managed and operated by Sandia Corporation, a wholly owned subsidiary of Lockheed Martin Corporation, for the U.S. Department of Energy's National Nuclear Security Administration under contract DE-AC04-94AL85000.

Issued by Sandia National Laboratories, operated for the United States Department of Energy by Sandia Corporation.

Available to DOE and DOE contractors from
U.S. Department of Energy
Office of Scientific and Technical Information
P.O. Box 62
Oak Ridge, TN 37831

Telephone: (865) 576-8401
Facsimile: (865) 576-5728
E-Mail: reports@adonis.osti.gov
Online ordering: http://www.osti.gov/bridge

Available to the public from
U.S. Department of Commerce
National Technical Information Service
5285 Port Royal Rd.
Springfield, VA 22161

Telephone: (800) 553-6847
Facsimile: (703) 605-6900
E-Mail: orders@ntis.fedworld.gov
Online order: http://www.ntis.gov/help/ordermethods.asp?loc=7-4-0#online

SAND2014-18206
Unlimited Release
Printed September 2014

Characterization of U.S. Wave Energy Converter (WEC) Test Sites: A Catalogue of Met-Ocean Data

Ann R. Dallman, Vincent S. Neary
Water Power Technologies
Sandia National Laboratories
P.O. Box 5800
Albuquerque, New Mexico 87185-MS1124

Abstract

This report presents met-ocean data and wave energy characteristics at three U.S. wave energy converter (WEC) test and potential deployment sites. Its purpose is to enable the comparison of wave resource characteristics among sites as well as the selection of test sites that are most suitable for a developer's device and that best meet their testing needs and objectives. It also provides essential inputs for the design of WEC test devices and planning WEC tests, including the planning of deployment and operations and maintenance. For each site, this report catalogues wave statistics recommended in the (draft) International Electrotechnical Commission Technical Specification (IEC 62600-101 TS) on Wave Energy Characterization, as well as the frequency of occurrence of weather windows and extreme sea states, and statistics on wind and ocean currents. It also provides useful information on test site infrastructure and services.

ACKNOWLEDGMENTS

This study was supported by the Department of Energy (DOE), Office of Energy Efficiency and Renewable Energy (EERE), Wind and Water Power Technologies Office (WWPTO). Sandia National Laboratories is a multi-program laboratory managed and operated by Sandia Corporation, a wholly owned subsidiary of Lockheed Martin Corporation, for the U.S. Department of Energy's National Nuclear Security Administration under contract DE-AC04-94AL85000.

The following people provided valuable input to this project:

- The bulk of the methodology for wave resource characterization used in this catalogue came from the draft International Electrotechnical Commission (IEC) Technical Specification (TS) on Wave Energy Characterization (to be released soon; the TS is described in Folley et al. 2012). Much of this originated from work done at OSU (Lenee-Bluhm et al. 2011, Lenee-Bluhm 2010).
- Luis Vega (HINMREC, University of Hawaii (UH)), who provided information on the Wave Energy Test Site (WETS) and facilitated data analysis of the UH hindcast dataset for this catalogue. Kwok Fai Cheung and Ning Li at the University of Hawaii for providing the analysis of their hindcast dataset.
- Belinda Batten (OSU, NNMREC), who provided information on the North Energy Test Site (NETS) offshore of Newport, OR and feedback on the site description.
- Tuba Özkan-Haller, Merrick Haller, and Gabriel García-Medina, (OSU), who provided helpful suggestions and feedback regarding the characterization methodology.
- Gabriel García-Medina (OSU), who provided the Oregon coast hindcast dataset (García-Medina et al. 2014) to Sandia National Laboratories for use in this catalogue.
- Pukha Lenee-Bluhm and Ken Rhinefrank, Columbia Power Technologies, for providing feedback on the methodology and data presented in the catalogue.
- Colin Sheppard, Humboldt State University, who provided information on the potential Humboldt Site and suggestions on the characterization methodology and presentation of data.
- Diana Bull, Water Power Technologies, Sandia National Laboratories, for providing information from previous wave resource assessment efforts near Humboldt Bay.
- Jenessa Duncombe, summer student intern at Sandia National Laboratories, for gathering and organizing information for site descriptions, and developing site maps.
- Alex Campbell, summer student intern at Sandia National Laboratories, for processing surface current and wind data.

CONTENTS

FIGURES

TABLES

NOMENCLATURE

CFSR	Climate Forecast System Reanalysis
CFSv2	Climate Forecast System version 2
DOE	Department of Energy
EquiMar	Equitable Testing and Evaluation of Marine Energy Extraction Devices in terms of Performance, Cost and Environmental Impact
EMF	Electromagnetic Fields
ESA	Environmental Site Assessment
FERC	Federal Energy Regulatory Commission
HINMREC	Hawaii National Marine Renewable Energy Center
HNEI	Hawaii National Energy Institute
HSU	Humboldt State University
HWC	Humboldt WaveConnect
IEC	International Electrotechnical Commission
MCBH	Marine Corps Base Hawaii
NETS	North Energy Test Site
NAVFAC	Naval Facilities Engineering Command
NNMREC	Northwest National Maine Renewable Energy Center
OSCAR	Ocean Surface Current Analyses - Real time
OSU	Oregon State University
OWC	Oscillating Water Column
PG&E	Pacific Gas & Electric
PMEC	Pacific Marine Energy Center
PPLP	Pilot Project Licensing Process
SETS	South Energy Test Site
SNL	Sandia National Laboratories
TS	Technical Specification
UH	University of Hawaii
WEC	Wave Energy Converter
WETS	Wave Energy Test Site
WET-NZ	Wave Energy Technology – New Zealand

1. INTRODUCTION

1.1. Motivation

This study was motivated by the lack of a single information source that catalogues, with documented and consistent methodologies, met-ocean data and wave energy characteristics at U.S. wave energy converter (WEC) test sites and potential deployment sites. Such information allows WEC developers to compare wave resource characteristics among test sites as well as select test sites that are most suitable for their device and that best meet their testing needs and objectives. It also serves as an initial data set and framework to support a wave classification system, much like the wind classification system, which has become a standard for wind turbine design.

This catalogue includes wave statistics recommended in the (draft) International Electrotechnical Commission Technical Specification (IEC 62600-101 TS) on Wave Energy Characterization (Folley et al. 2012); but it also provides additional information on wave resource characteristics, including the frequency of occurrence of weather windows and extreme sea states, and statistics on wind and ocean currents. This additional information can assist developers in planning WEC tests, servicing their test devices, and assessing opportunities and risks at the test site.

1.2. Wave Resource Characterization

Wave energy resources are analyzed and presented in various ways throughout the literature. For example, efforts have included analyses of measured buoy data and/or hindcast simulation data; some consider full directional spectra while others only consider bulk parameters; extreme event analyses are often neglected or considered in separate studies. This ambiguity and difficulty in comparing assessments are some of the reasons that the IEC began the process of creating a technical specification (Folley et al. 2012). The IEC Technical Specification (TS) on Wave Energy Characterization is nearly completed, with a draft version currently released. The TS provides guidelines for a "design" resource assessment, which is the most detailed stage and is appropriate for particular test sites compared to broader assessments suitable for large regional areas.

Wave energy resource is defined in the IEC TS as "the amount of energy that is available for extraction from surface gravity waves," (IEC 62600-101 TS). The TS specifies three classes of resource assessment. Class 1, or *reconnaissance*, is the lowest level and produces estimates with high uncertainty. This would be appropriate for large areas as the first assessment in a region. Class 2, or *feasibility*, produces estimates with greater certainty, and is appropriate for refining a reconnaissance assessment before a Class 3 assessment is done. Class 3, or *design*, produces an assessment with the least uncertainty and would be the final and most detailed assessment for small areas. This catalogue provides a Class 3 (*design*) assessment for the three sites considered. For a detailed resource assessment at a particular site of interest, the energy characterization should be based on the analysis of directional wave spectra produced from a simulated hindcast. Measurements (e.g., from buoys) can be useful for boundary conditions, and independent

measured data should be used to validate the hindcast model. Future versions of this catalogue may include lower classes of assessments for other sites based on data availability.

In a related effort to the IEC TS, EquiMar (Equitable Testing and Evaluation of Marine Energy Extraction Devices in terms of Performance, Cost and Environmental Impact), published wave resource assessment guidance, Deliverable 2.7 (Davey et al. 2010), available at http://www.equimar.org/equimar-project-deliverables.html. According to this protocol, an assessment should provide an estimate of the available energy and the operating and survival characteristics of a site, which can be achieved by using a combination of in-situ measurements and numerical modelling. Similarly to the IEC TS, three stages of resource assessment are addressed, and the one closest to the IEC TS 'design' would be the EquiMar 'Project Development,' which should provide "detailed information on a deployment site including information on spectra and extremes," (Davey et al. 2010). The period of record of data considered should be 10 years, and many cases would use numerical modeling. This is in general consistent with the IEC TS and the methodology applied to this catalogue. The EquiMar project also produced a brief catalogue of sorts (O'Connor and Holmes 2011), where several test sites were characterized with the best data available.

The IEC TS, and recent papers regarding the U.S. Pacific Northwest coast (Lenee-Bluhm et al. 2011, García-Medina et al. 2014), recommend six parameters to characterize the wave resource at a test site. In addition, they advocate calculating these parameters from simulated hindcast spectral wave data. These six parameters are omnidirectional wave power, significant wave height, energy period, spectral width, direction of maximum directionally resolved wave power, and directionality coefficient. Equations for calculating these statistics are provided in the Methodology section.

The IEC TS recommends that seasonal variation of wave statistics be considered, and monthly plots of the six parameters, along with seasonal cumulative distributions, should be provided. It is also recommends that wave roses and time histories of the six parameters for one representative year be included. Wave roses provide a direct and intuitive means to visualize wave directions for corresponding wave bulk properties, typically omnidirectional wave power and significant wave height.

Although extreme sea states are not addressed in the IEC TS, they provide critical information needed to assess the risks of deploying a WEC at the test site and to design a WEC to survive wave loads associated with extreme sea states of a given return period. For this reason, the 100-year environmental contours are provided, as explained in Section 2.2. Although 100-year recurrence intervals (return periods) are common for marine structures, lower return periods can be used, if acceptable for survivability, when the design service life is less than 100 years (DNV 2005).

Additional wave statistics and met-ocean data, not specified in the IEC TS, but provided in this report, include weather windows as well as wind and ocean current statistics. This information is also valuable to developers for the purpose of assessing risks at the site and planning for testing and servicing of the WEC test device.

1.3. Format of Report

Three high energy wave sites will be included in the catalogue: (1) the Pacific Marine Energy Center (PMEC) North Energy Test Site (NETS) offshore of Newport, Oregon, (2) Kaneohe Bay Naval Wave Energy Test Site (WETS) offshore of Oahu, HI, and (3) a potential test site offshore of Humboldt Bay (Eureka, CA).

Following this chapter, there is a Methodology section, describing the data presented, analysis procedures, and data sources. Next is a chapter for each site that includes a description of the site and testing infrastructure, and a discussion of the results of the met-ocean data. A summary of the study and conclusions are presented in the final chapter. Additional data is provided in plots and tables in the appendices.

2. METHODOLOGY

2.1. Overview

For this study, the wave model SWAN (Simulating Waves Nearshore) was used to generate all simulated hindcast wave data. For NETS, hindcast data was generated by researchers at the Northwest National Marine Renewable Energy Center (NNMREC) (García-Medina et al. 2014). The dataset for WETS was generated by the Hawaii National Marine Renewable Energy Center (HINMREC) (Stopa et al. 2013, Li & Cheung 2014), and that for the Humboldt Site by Sandia National Laboratories (Dallman et al. 2014). All hindcast simulations were validated by comparing predicted wave statistics against buoy observations prior to processing data and plots presented in this catalogue. Sandia National Laboratories (SNL) analyzed hindcast wave data for the NETS and Humboldt sites, while HINMREC analyzed those for WETS.

2.2. Data Presented

The six parameters recommended by Lenee-Bluhm et al. (2011) and specified in the TS are defined below as in Lenee-Bluhm et al. (2011) and García-Medina et al. (2014). Equations for these parameters are repeated below for completeness.

The omnidirectional wave power, J, which indicates the resource available, is the sum of the contributions to energy flux from each of the components of the wave spectrum,

$$J = \sum_i \rho g c_{g,i} S_i \Delta f_i \tag{1}$$

where ρ is the density of sea water, g is the acceleration due to gravity, $c_{g,i}$ is the group velocity, S_i is the variance density, and Δf_i is the frequency bin width at each discrete frequency index i. Significant wave height, H_{m0}, estimated from spectra, is commonly used to describe the sea state and is defined as

$$H_{m0} = 4\sqrt{m_0} \tag{2}$$

where m_0 is the zeroth moment of the variance spectrum. The moments of the variance spectrum are

$$m_n = \sum_i f_i^n S_i \Delta f_i. \tag{3}$$

The energy period, T_e, is also widely used to describe the sea state and is more robust than the peak period (due to a high sensitivity to spectral shape). The energy period is calculated as

$$T_e = \frac{m_{-1}}{m_0}. \tag{4}$$

The spectral width,

$$\epsilon_0 = \sqrt{\frac{m_0 m_{-2}}{{m_{-1}}^2} - 1}, \tag{5}$$

characterizes the spreading of energy along the wave spectrum. The directionally resolved wave power is the sum of the wave power at each direction θ

$$\begin{gathered} J_\theta = \sum_{i,j} J_{ij} \Delta f_i \, \Delta\theta_j cos(\theta - \theta_j)\delta \\ \begin{cases} \delta = 1, & cos(\theta - \theta_j) \geq 0 \\ \delta = 0, & cos(\theta - \theta_j) < 0 \end{cases} \end{gathered} \tag{6}$$

where J_θ is the directionally resolved wave power in direction θ. The maximum time averaged wave power propagating in a single direction, J_{θ_J}, is the maximum value of J_θ. The corresponding direction, θ_J, is the direction of maximum directionally resolved wave power and describes the characteristic direction of the sea state. The directionality coefficient, d_θ, is the ratio of maximum directionally resolved wave power to the omnidirectional wave power,

$$d_\theta = \frac{J_{\theta_J}}{J}, \tag{7}$$

which is a characteristic measure of directional spreading of wave power (i.e., larger values approaching unity signify narrow directional spread). It is also recommended in the IEC TS that annual and seasonal values be reported.

The average monthly values of the above parameters, along with 5th and 95th percentiles, are presented to capture their variation over a typical year. This information is useful for planning deployments and tests. Optimal deployment windows, for example, are generally in summer months when sea states are less energetic than winter months. For similar reasons, testing of a scaled model WEC is generally more suitable in summer months.

Joint probability distribution (JPD) plots are presented to provide an overall depiction of the wave climate at each site and help inform the design of the WEC test device. These plots also include the mean, 5th and 95th percentiles of wave steepness, defined in this study as the ratio of the significant wave height to length, H_{m0}/λ, where the wavelength is calculated using the Newton-Raphson method to solve the dispersion relation (Holthuijsen 2007) using T_e. Steepness is important because it is related to wave breaking, and it affects wave forces on marine structures such as a WEC (Bitner-Gregersen 2001).

JPD plots, also known as bi-variate scatter plots (Cahill and Lewis 2013), can be used to present the frequency of occurrence of sea states (H_{m0}, T_e pairings) at a site, or the percentage contribution of each sea state to the total annual energy or power density. Wave characterization studies have shown (e.g., Cahill and Lewis 2011, Cahill and Lewis 2013, Lenee-Bluhm et al.

2011) that the sea states that occur most often do not necessarily correspond to those contributing the most to annual energy.

Cumulative distributions of H_{m0} and T_e are shown to describe the percentage of time these parameters are equal to or less than a threshold value. In order to account for duration, weather windows for wave heights equal to or less than threshold values are calculated for multiples of 6-hour periods. Weather windows quantify the number of opportunities in a given season or year to access the site for installation of a test device, or for operations and maintenance, based on their specific device, service vessels, and diving operation constraints.

Following suggestions from the IEC TS, wave roses are generated to visualize the spread and predominant directions of omnidirectional wave power and significant wave height. Rose plots for wind and ocean currents are also generated to examine the spread and predominant direction of wind and ocean currents. From these rose plots, one can also determine the percentage of time that a given statistical parameter (e.g., omnidirectional wave power) is equal or less than a given value at a specified direction sector. The radial thickness of a given bin represents the percentage of the time that the given omnidirectional wave power and direction occurs. Wave, wind, and current directions are defined as degrees clockwise from North. When directions are concentrated around North (0°), plots show positive directions (clockwise from North) and negative directions which are counter-clockwise from North. For example, -45° is equivalent to 315°.

Estimates of extreme sea states (H_{m0}, T_e pairings) are determined from 100-year environmental contours calculated using a modified version of the inverse first order reliability method (IFORM). The IFORM, as described by Winterstein et al. (1993), is standard design practice for generating environmental contours used for estimating extreme sea states of a given recurrence interval or return period (DNV 2014). It provides developers, not only with an estimate of the largest significant wave height, but also extreme sea states at other significant wave heights with energy periods that could compromise the survival of a marine structure or service vessel. The modified IFORM used in this study (Eckert-Gallup et al. 2014) improves the original fitting method by implementing principal components analysis.

Estimates of applied wave loads and power response under a diverse range of sea states is required for designing and siting a WEC. Since running simulations for a WEC response to all frequency spectra occurring at a site would take an unfeasibly long amount of time, it is beneficial to synthesize a fixed number of spectra which can be used to represent each expected sea state (e.g., Lenee-Bluhm 2010). Therefore, representative spectra for the most common sea states at a site (found in the JPD) were calculated by averaging all measured spectra within each sea state. Standard spectra (Bretschneider and JONSWAP) were included for comparison.

The Bretschneider spectrum, which is meant for developing seas, was computed according to the unified form described in Chakrabarti (1987),

$$S(\omega) = \frac{A}{4} {H_{m0}}^2 {\omega_s}^4 \omega^{-5} exp\left(-A\left(\frac{\omega}{\omega_s}\right)^{-4}\right), \quad (8)$$

where $A = 0.675$ is a nondimensional constant and $\omega_s = T_p/1.167$ is the significant frequency. The JONSWAP spectrum (Hasselmann et al. 1973), is an extension of the Pierson-Moskowitz spectrum (for fully developed wind seas) to include fetch-limited wind seas, and therefore describes developing seas. It was computed according the DNV Recommended Practices on Environmental Conditions and Environmental Loads (DNV-RP-C205 2014),

$$S(\omega) = A_\gamma \frac{5}{16} {H_{m0}}^2 {\omega_p}^4 \omega^{-5} exp\left(-\frac{5}{4}\left(\frac{\omega}{\omega_p}\right)^{-4}\right)\gamma^{exp\left(-0.5\left(\frac{\omega-\omega_p}{\sigma\,\omega_p}\right)^2\right)}, \quad (9)$$

where $\omega_p = 2\pi/T_p$ is the angular spectral peak frequency, $A_\gamma = 1 - 0.287\, ln(\gamma)$ is a normalizing factor, $\gamma = 3.3$ is a non-dimensional shape parameter, and σ is a spectral width parameter where $\sigma = 0.07$ for $\omega \leq \omega_p$ and $\sigma = 0.09$ for $\omega \geq \omega_p$. If the wind speed and fetch were known, the JONSWAP spectrum could be calculated according to the equation in Hasselmann et al. (1973). Use of this equation, however, does not ensure the spectrally estimated H_{m0} would match the input value. Although a better fit could be achieved if a least squares fit was applied to the mean of the measured spectrum, it is assumed that the actual spectral shape would not be known *a priori* and a standard spectrum would be fit to a sea state (H_{m0}, T_e or T_p). Therefore, this comparison shows how well an assumed standard spectrum fits an actual measured spectrum without knowing the shape *a priori*.

As well as wave statistics, monthly averages of wind speed and direction, along with seasonal and annual wind roses are provided for each site. Monthly averages of ocean surface current speed and direction, along with seasonal and annual current roses are provided for each site.

2.3. Data Sources

The majority of the wave data (e.g., the six parameters of interest described above) was generated from a validated hindcast model simulation at each site, as recommended in the IEC TS. These hindcast datasets are described in the Data Used section for each site.

In general, hindcast models do not reproduce extreme events well (for example the hindcast by Garcia-Medina et al. 2014, represents significant wave height only up to $H_{m0} \approx 8\,m$), unless specialized input data and versions of models are used for specific storms (e.g., the National Weather Service's National Hurricane Center specialized models). Therefore the hindcast models utilized in this catalogue may not be reliable data sources for estimations of extreme events. The location of a buoy at each site does not necessarily coincide with the actual test site, but it is the most reliable data source for this calculation, and will be used herein. In addition, results in Feld & Mork (2004) indicate that hindcast model spectra are less peaked than measured buoy data, and therefore representative spectra are also calculated from buoy data. The location and POR of buoys used will be described in each chapter.

Wind data for each site was obtained from 0.5 degree spatial resolution and 6-hour temporal resolution datasets available at the National Centers for Environmental Prediction's (NCEP) Climate Forecast System Reanalysis (CFSR) (covering 1979-2010) and CFSv2 (covering 2011-

present) (Saha et al. 2010, Saha et al. 2014). Data was selected at a single point or multiple points closest to the site. When multiple points were selected a simple arithmetic average of the data reported at each time step was computed. The wind data available from buoys or onshore meteorological stations greatly varies between sites, so using CFSR allows for a consistent data source between all sites. In addition, CFSR data generally has better spatial coverage than buoy data, as well as longer periods of record (POR).

Surface currents near the test sites were obtained from Ocean Surface Current Analyses – Real time (OSCAR), part of the National Oceanic and Atmospheric Administration (NOAA). OSCAR calculates near real-time global sea surface currents from NASA satellite data and reports the data publically on their website. Sea surface currents are calculated from (1) sea surface height derived from Satellite altimeter and (2) ocean near-surface wind speed and direction from satellite scatterometers. The result is a global-scale sea surface current speed and direction dataset with a spatial resolution of 1 degree and a temporal resolution of 5 days.

OSCAR current data has been shown to be accurate for time-mean measurements by Johnson et al. (2007). Compared to moored current meters, drifters and shipboard current profilers, OSCAR mean sea surface currents closely match observed data at all latitudes and longitudes. High frequency (HF) radar has a higher resolution and is often a preferred data source for real-time applications and short term analyses, but is unavailable at the Hawaii site and has a much shorter period of record compared to OSCAR. As more systems are setup along the U.S. coast and the POR increases, HF radar will likely become a viable data source for long term characterization. For the purpose of this catalogue, OSCAR data was used because it provides data at each site to maintain consistency, has periods of record of at least 10 years at each site, and has been shown to be accurate for mean current speed and direction.

3. PACIFIC MARINE ENERGY TEST CENTER (PMEC): NORTH ENERGY TEST SITE (NETS)

3.1. Site Description

The Pacific Marine Energy Center (PMEC) is the name of the Northwest National Marine Renewable Energy Center's (NNMREC) marine energy converter testing facilities located in the Pacific Northwest region. NNMREC is a Department of Energy funded entity designed to facilitate development of marine renewable energy technology. Ultimately PMEC will facilitate testing a broad range of technologies being produced by the marine energy industry (NNMREC 2014). The North Energy Test Site (NETS) is an off-grid WEC test site that became operational in the summer of 2012. As shown in Figure 1, it encompasses an area of 1-square nautical mile (roughly 3 square kilometers) within state waters at 44.6899 N, 124.1346 W.

NETS is located near the City of Newport, Oregon and Yaquina Bay. At the test site, the water depth is approximately 45-55 m (25-30 fathoms), the bathymetry is gently sloping, and the sea bed consists of soft sand. Figure 2 shows the bathymetry surrounding promontory Yaquina Head and the test site. The wave climate at the test site varies seasonally, with calmer seas in the summer compared to more energetic seas in the winter. The wave environment at NETS is characterized by an annual average power flux of about 37 kW/m, including a number of events with significant wave heights exceeding 7 m each winter.

NNMREC offers a wide range of technical and testing infrastructure support services for WEC developers, including access to a fully instrumented test buoy and grid connection emulator at NETS. NETS has full scale wave energy resources, and can accommodate devices up to 100 kW connected to the mobile ocean test berth, the Ocean Sentinel, and larger devices if no grid emulation or connection is required.

NNMREC is currently designing a utility-scale, grid-accessible test site, the South Energy Test Site (SETS), which is planned to be operational in 2017.

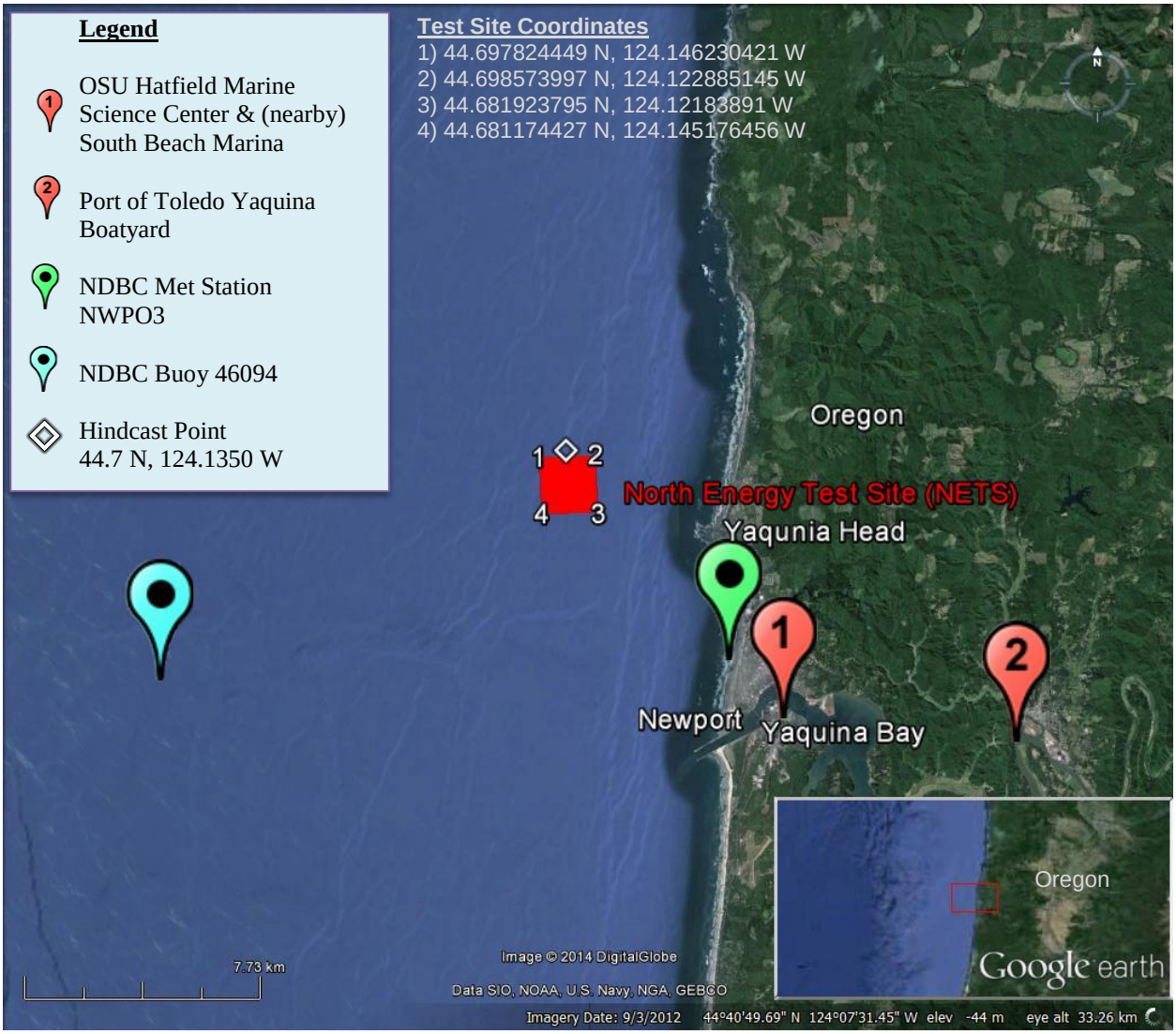

Figure 1. NETS is located in the coastal waters of Oregon near the City of Newport. The test site is 3-5 km off-shore in 45–55 m depth water. One National Data Buoy Center (NDBC) ocean buoy and one NDBC meteorological station are close to the site (see Table 1), as well as Oregon State University's (OSU) test instrumentation buoy (see Section 3.2.7). The South Beach Marina, Port of Toledo Yaquina Boatyard, and OSU Hatfield Marine Science Center offer services valuable for WEC testing. The point of reference for the hindcast simulation is on the north edge of NETS. Image modified from Google Earth (Google Earth 2014).

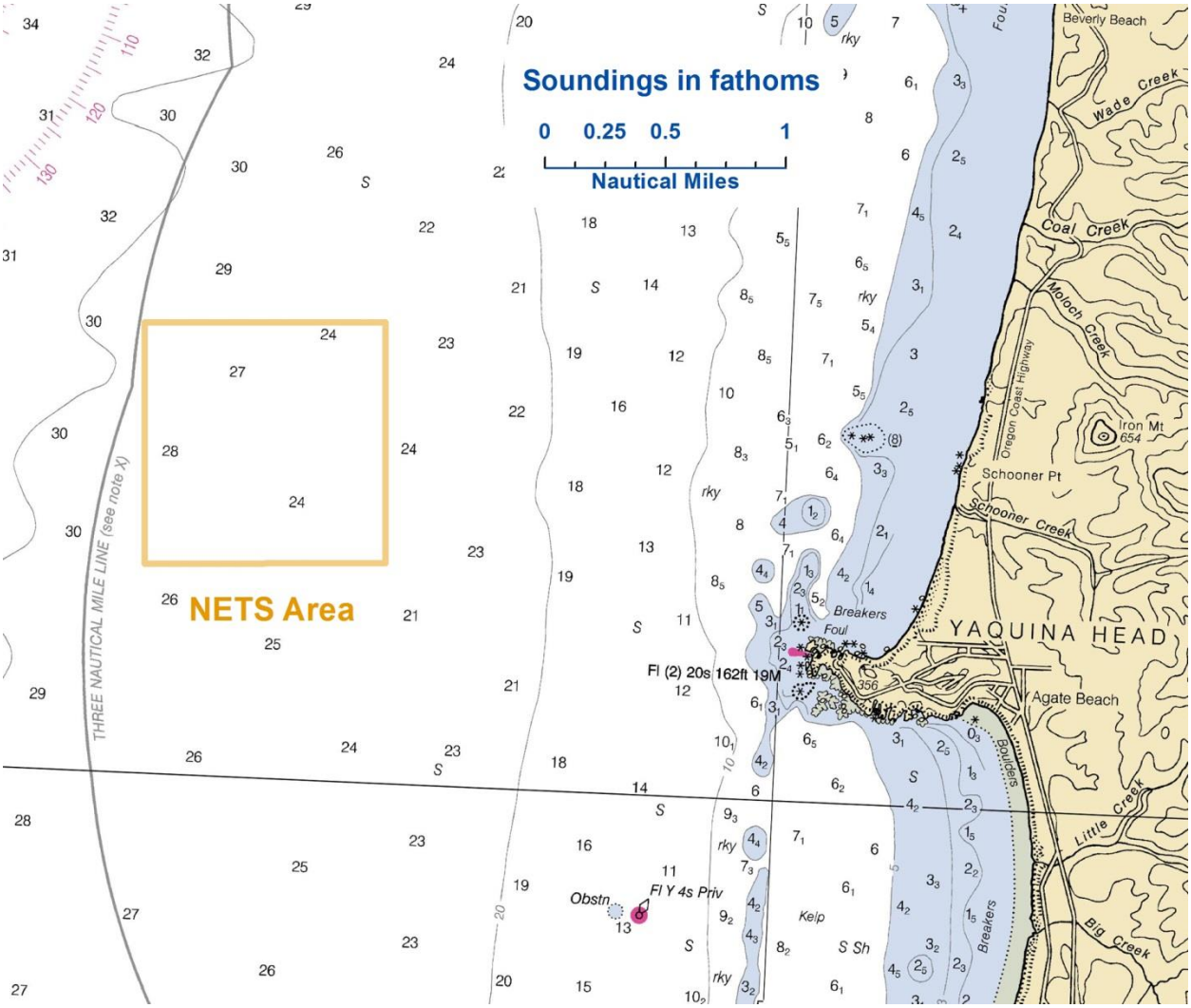

Figure 2. Nautical chart of Yaquina Head and surrounding area shows the gradually sloping bathymetry around NETS. Soundings in fathoms (1 fathom = 1.8288 m). Image modified from nautical chart #18561 (Office of Coast Survey 2011).

3.2. WEC Testing Infrastructure

3.2.1. Mooring Berths

NETS is permitted to test up to two WECs concurrently within the 45-55 m depth site. Mooring systems are not provided and would need to be installed according to the developer's design. As an example, a six-point mooring system was used for the WET-NZ during their 2012 test. A layout of their test site mooring is provided in von Jouanne et al. (2013). A three point mooring system is used for OSU's Ocean Sentinel buoy (described in Section 3.2.2) during device deployment in order to hold a tight watch circle along the device and to maintain the connection of the power and communication umbilical with the Ocean Sentinel (NNMREC 2014). During

more energetic winter months, the Ocean Sentinel uses a single point mooring system and can be used for environmental testing, but will not be connected to the device. WEC testing can be done in "stand alone" mode (no electrical connection) during the winter.

3.2.2. Electrical Grid Connection

There is no electrical grid connection at NETS, but the Ocean Sentinel test buoy (Figure 3) was designed as an electrical grid emulator to allow assessment of WEC device performance (von Jouanne et al. 2013). The Ocean Sentinel serves several purposes: (1) it consumes the electrical power generated by the WEC device with an onboard resistor element, (2) it measures the electrical power generated (voltage, current), and (3) it collects year-round met-ocean data, as described in Section 3.2.7.

The Ocean Sentinel can currently accommodate one device with an average power output up to 100 kW during the months May through October (NNMREC 2014). The data collected by the Ocean Sentinel is communicated wirelessly to OSU's Hatfield Maine Science Center, which is located in Yaquina Bay next to the South Beach Marina (Waypoint #1 in Figure 1). This data can be accessed remotely.

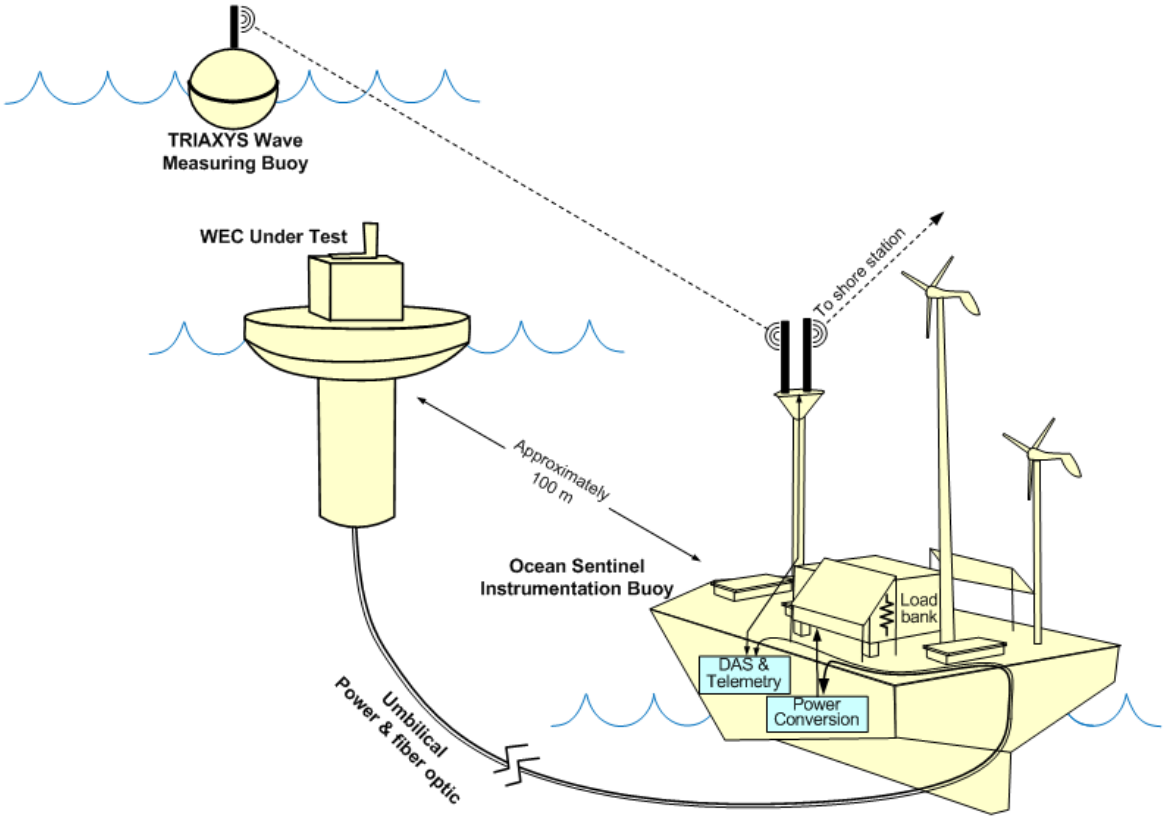

Figure 3. The Ocean Sentinel acts as a grid emulator for WEC devices, as well as records electricity output and monitors surrounding environmental data. The WEC device is connected to the Ocean Sentinel via an umbilical cord.

3.2.3. Facilitating Harbor

NETS is approximately 9 km north/northwest of the entrance to Yaquina Bay, the mouth of the Yaquina River. The South Beach Marina is located near the outlet of Yaquina Bay and offers year-round boat mooring (near Waypoint #1 in Figure 1).

3.2.4. On-Shore Office Space

The fishing and tourist City of Newport, Oregon, where approximately ten thousand people live, is on the north side of Yaquina Bay (U.S. Census Bureau 2012). At this time, developers at NETS are responsible for renting office space in Newport, Oregon or Toledo, Oregon, which is a town up the Yaquina River. Meeting rooms and temporary office space through PMEC are planned to be available in the future following the completion of the South Energy Test Site (SETS) (Batten 2014).

3.2.5. Service Vessel and Engineering Boatyard Access

No dedicated service vessel is available at this time, but following the completion of SETS, more resources may be available through PMEC. Service vessels for hire are likely available in the Newport/Toledo area. The Port of Toledo's Yaquina Boatyard (Waypoint #2 in Figure 1) services boats and provides space for self-service. Yaquina Boatyard hauls boats up to 300 tons and has capabilities that include steel fabrication, carpentry, painting, haul-out, and project management (Port of Toledo 2014).

3.2.6. Travel and Communication Infrastructure

Portland International Airport (PDX) is a two and a half hour drive from Newport, Oregon. Eugene Airport is located closer and is a one hour and forty minute drive. Cellular service offers consistent coverage; three Federal Communication Commission (FCC) registered cell phone towers are located in and around Newport, Oregon.

3.2.7. Met-Ocean Monitoring Equipment

The Ocean Sentinel test buoy reports environmental data (waves, currents and winds), and other signals from the installations onboard the WEC test device (NNMREC 2014). As with electrical power data, met-ocean data is communicated wirelessly to OSU's Hatfield Marine Science Center (Waypoint #1 in Figure 1) and is available for remote access.

In addition, there are two National Buoy Data Center (NDBC) buoys that measure and collect ocean data and one NDBC station reporting meteorological data (see Figure 1 for location). Instrument and data specifications for this monitoring equipment are summarized in Table 1. Buoy data is accessible online at the NDBC database. NDBC46050 (Stonewall Bank) is located

30 km seaward from the test site and provides spectral wave data. NDBC46094 (NH-10) is slightly closer to the site at only 14 km away and reports standard ocean wave data (Figure 4 (a)). The land based meteorological station is situated directly on the shoreline (Figure 4 (b)).

Figure 4. (a) Moored buoy NDBC46094 located 14 km southwest of the test site, (b) meteorological station NWPO3 on the coastline 8 km southeast of the test site (National Data Buoy Center 2014).

Table 1: Wave monitoring equipment in close proximity to NETS.

Instrument Name (Nickname)	NDBC Station 46094 (also called NH-10)	NDBC Station 46050 (Stonewall Bank)			NWPO3	
Type	Moored buoy	3-meter discus buoy			C-MAN station (MARS payload)	
Measured parameters	-std. met. data -continuous winds -sea surface temp, salinity, density -current measurements	-std. met. data -continuous winds -spectral wave density -spectral wave direction			-std. met. data -continuous winds	
Variables reported, including derived variables (Sampling interval)	*Std Met.:* WDIR WSPD BAR ATMP (10 min sampling period)	*Std Met.:* WDIR WSPD GST WVHT DPD APD PRES ATMP WTMP (1 hr sampling period)	*Contin. Winds:* WDIR WSPD GDR GST GTIME (10 min sampling period)	-Spectral Wave Density -Spectral Wave direction (1 hr sampling period)	*Std Met.:* WD WSPD GST BAR ATMP DEWP (1 hr sampling period)	*Contin. Winds:* WDIR WSPD GDR GST GTIME (10 min sampling period)
Location	directly west of Newport, 14 km southwest from NETS	20 nm (nautical miles, 1 nm = 1.852 km) directly west of Newport, 30 km west pf NETS			on the shoreline, near Newport, 8 km southeast of NETS	
Coordinates	44.633 N 124.304 W (44°38'0" N 124°18'13" W)	44.639 N 124.534 W (44°38'20" N 124°32'2" W)			44.613 N 124.067 W (44°36'48" N 124°4'0" W)	
Depth	-depth: 81 m -air temp 2.5 m above site -anemometer 3 m above site	-depth: 128 m -air temp: 4 m above water -anemometer: 5 m above water -barometer: sea level -sea temp depth: 0.6 m below water			-site: 9.1 m above sea level -air temp: 6.4 m above site -anemometer: 9.4 m above site -barometer: 11 m above sea level	
Data Start	2/5/2007	-std met: 11/16/1991 -contin winds: 09/07/1997 -spect wave dens: 01/01/1996 -spect wave dir: 03/05/2008			-std met: 1/10/1985 -contin winds: 1/12/1997	
Data End	present; several winters missing data	present			present	
Period of Record	~7.5 yrs	-std met: ~23 yrs -contin winds: ~17 yrs -spect wave dens: ~19 yrs -spect wave dir: ~6.5 yrs			std met: ~30 yrs contin winds: ~18 yrs	
Owner / Contact Person	Oregon Coastal Ocean Observing System/ National Data Buoy Center	National Data Buoy Center			National Data Buoy Center	

3.2.8. Environmental Monitoring

Environmental conditions have been characterized at the site by Oregon State University, NOAA, and NNMREC. The information gathered includes baseline measurements of benthic habitat and organisms, marine mammal populations, electromagnetic fields (EMF), and acoustics (Batten 2013). Developers can contract with NNMREC to monitor environmental effects of WEC deployments during testing. Required environmental monitoring of WEC deployments includes acoustics, electromagnetic fields (EMF), benthic ecosystems, and opportunistic marine mammal observations.

3.2.9. Permitting

The site is fully permitted through the NEPA process, Department of State Lands, the U.S. Coast Guard, and the Army Corp of Engineers (NNMREC 2014). Developers interested in testing WECs at NETS are required to provide plans and present information to show compliance with test center standards and regulatory requirements. Each test requires its own permits for WEC testing in Oregon state waters. The approval process has been streamlined, but it should be noted that completed permit applications and supporting documentation should be submitted at least six months prior to the desired deployment site. More information can be found at NNMREC's website http://nnmrec.oregonstate.edu/permitting-requirements.

3.3. Data used

Researchers at the Northwest National Marine Renewable Energy Center (NNMREC) produced a 7 year hindcast dataset for the area offshore of Oregon (García-Medina et al. 2014) in order to complement the study of temporal and spatial variability in the wave resource over the Pacific Northwest region by Lenee-Bluhm et al. (2011). This dataset was used to calculate statistics of interest for the wave resource characterization at NETS. The hindcast data at the grid point on the north side of NETS was analyzed (see Figure 1). Although a 10 year hindcast would be preferred, García-Medina et al. (2014) showed that the probability density function (PDF) of significant wave height from their hindcast compared to NDBC46029 buoy data were in agreement up to ~7 m, and, therefore, the hindcast is at least representative of the twenty-seven years of buoy operation, 1985-2011.

In addition to the hindcast data set, historical data from buoy NDBC46050 was used to calculate extreme sea states and representative spectra. Wind data was available from NDBC46050 and a Coastal-Marine Automated Network (C-MAN) station, NWPO3 located just on-shore. However, to be consistent with the other sites, Climate Forecast System Reanalysis (CFSR) winds were used, as explained in Section 2.3. As with the other sites, current data was downloaded from OSCAR.

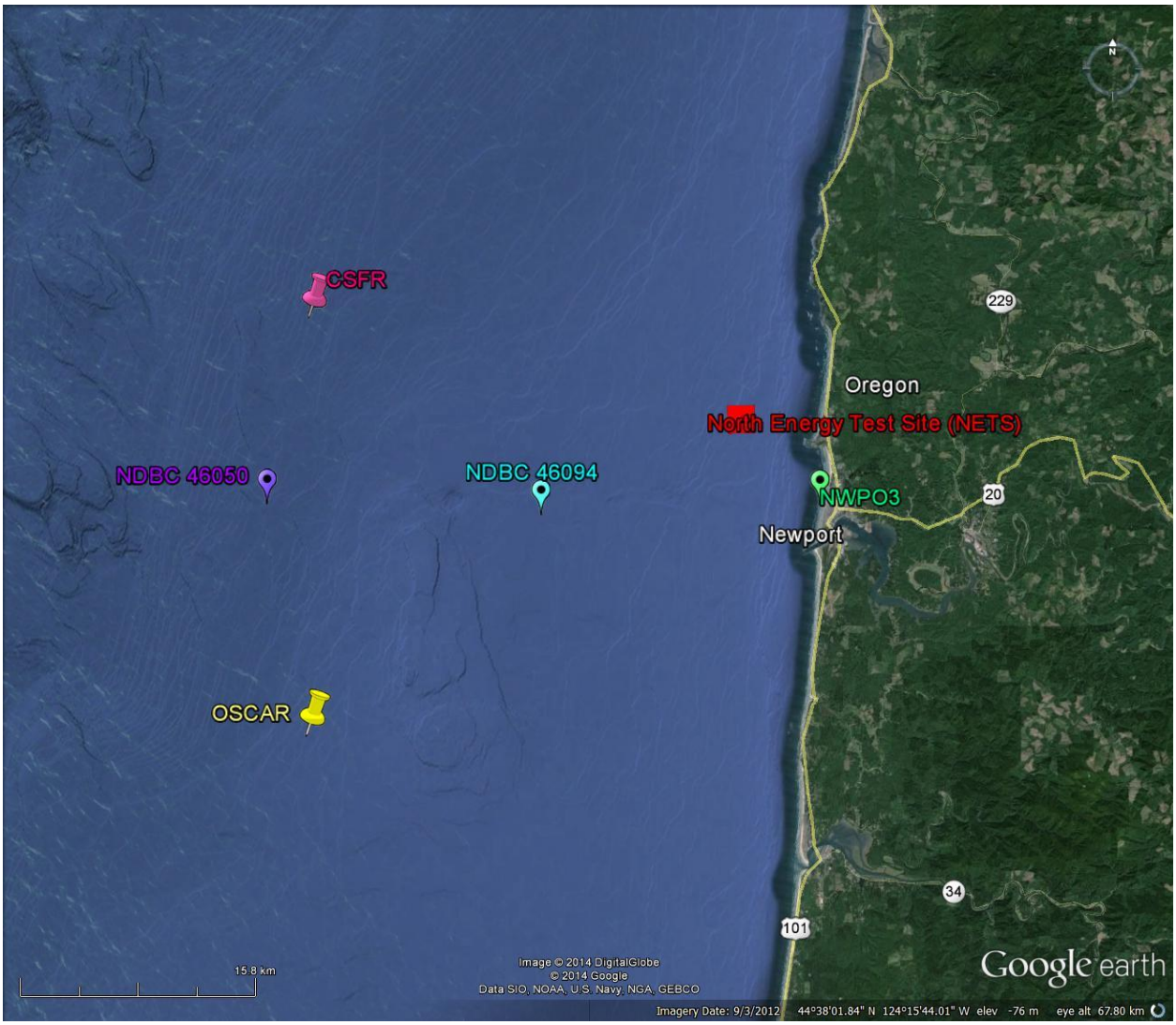

Figure 5. NETS location map showing CSFR wind data points, OSCAR current data points, and NDBC buoy locations (Google Earth 2014).

3.4. Results

The following sections provide information on the joint probability of sea states, the variability of the IEC TS parameters, cumulative distributions, weather windows, extreme sea states, and representative spectra. This is supplemented by wave roses as well as wind and surface current data in Appendix A. The wind and surface current data provide additional information to help developers plan installation and operations & maintenance activities.

3.4.1. Sea States: Frequency of Occurrence and Contribution to Wave Energy

Joint probability distributions of the significant wave height, H_{m0}, and energy period, T_e, are shown in Figure 6. Figure 6 (top) shows the frequency of occurrence of each binned sea state and Figure 6 (bottom) shows the percentage contribution to the total wave energy. Figure 6 (top) indicates that the majority of sea states are within the range 1 m < H_{m0} < 3.5 m and 7 s < T_e < 11 s; but a wide range of sea states are experienced at NETS, including extreme sea states caused by severe storms where H_{m0} exceeded 7.5 m. The site is well suited for testing WECs at various scales, including full-scale WECs, and testing the operation of WECs under normal sea states. Although the occurrence of an extreme sea state for survival testing of a full scale WEC is unlikely during a normal test period, the NETS wave climate offers opportunities for survival testing of scaled model WECs.

As mentioned in the methodology (Section 2.2. Data Presented), previous studies show that sea states with the highest frequencies of occurrence do not necessarily correspond to those with the highest contribution to total wave energy. The total wave energy in an average year is 322,250 kWh/m, which corresponds to an average annual omnidirectional wave power of 36.8 kW/m. The most frequently occurring sea state is within the range 1 m < H_{m0} < 1.5 m and 8 s < T_e < 9 s, while the sea state that contributes most to energy is within the range 3 m < H_{m0} < 3.5 m and 10 s < T_e < 11 s. Several sea states occur at a similar frequency, and sea states within 2 m < H_{m0} < 4.5 m and 9 s < T_e < 11 s contribute a similar amount to energy.

Frequencies of occurrence and contributions to energy of less than 0.01% are considered negligible and are not shown for clarity. For example, the sea state within 0.5 m < H_{m0} < 1 m and 5 s < T_e < 6 s has an occurrence of 0.02%. The contribution to total energy, however, is only 0.001% and, therefore, does not appear in Figure 6 (bottom). Similarly, the sea state within 8.5 m < H_{m0} < 9 m and 12 s < T_e < 13 s has an occurrence of 0.004%, but the contribution to total energy is 0.06%.

Curves showing the mean, 5th and 95th percentiles of wave steepness, H_{m0}/λ, are also shown in Figure 6. The mean wave steepness at NETS is 0.0165 (≈1/61), and the 95th percentile approaches 1/34.

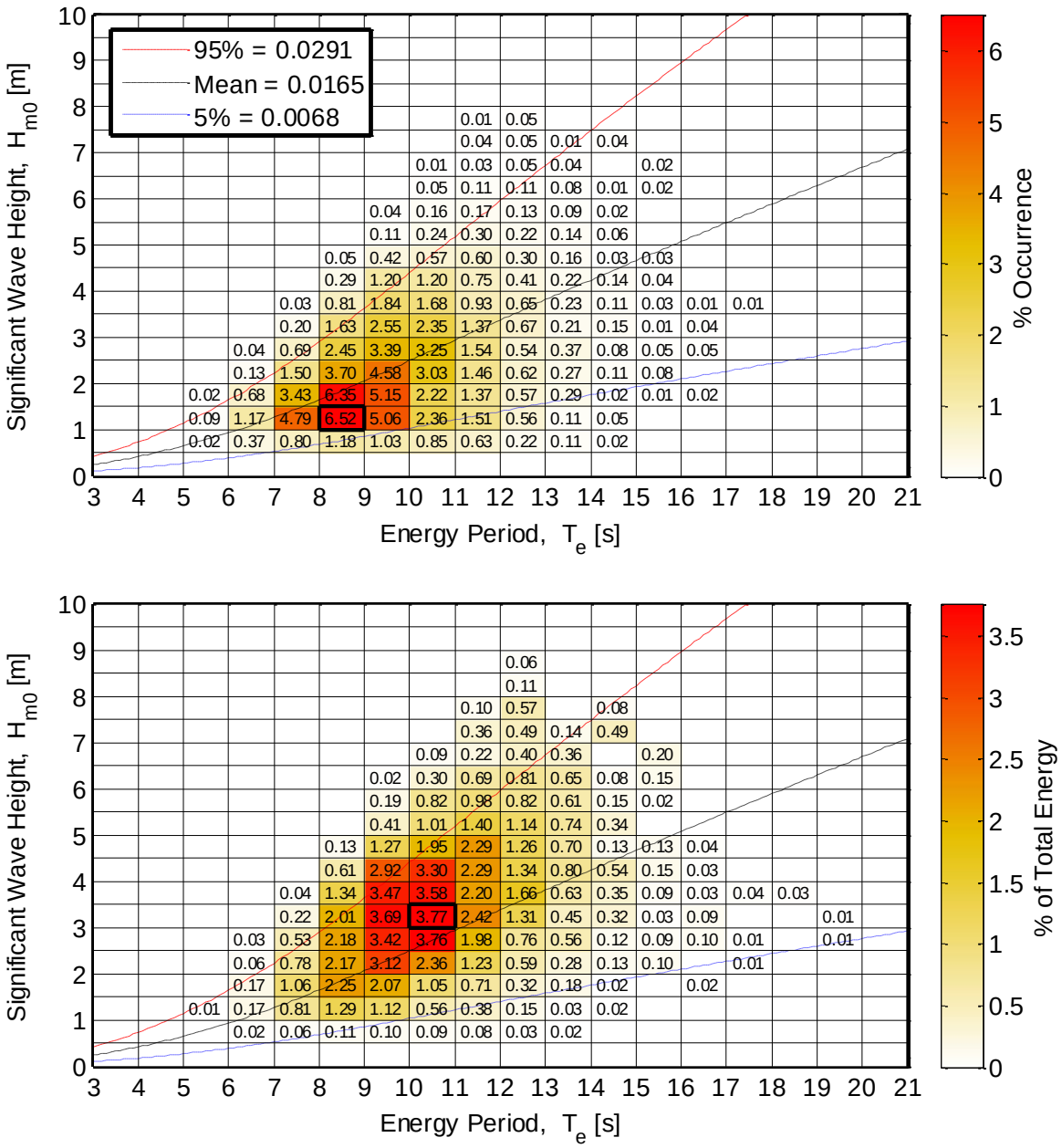

Figure 6. Joint probability distribution of sea states for NETS. The top figure is frequency of occurrence and the bottom figure is percentage of total energy, where total energy in an average year is 322,250 kWh/m.

3.4.2. IEC TS Parameters

The monthly means of the six IEC TS parameters, along with the 5th and 95th percentiles, are shown in Figure 7. The values in the figure are summarized in Table 4 in Appendix A.

Monthly means of the significant wave height, H_{m0}, and the omnidirectional wave power density, J, show the greatest seasonal variability compared to the other parameters. Values are largest and vary the most during the winter months. The same trend is observed for the monthly mean energy period, T_e, but its variation is less pronounced. These observations are consistent with the relationship between wave power density, significant wave height and energy period, where wave power density, J, is proportional to the energy period, T_e, and the square of the significant wave height, H_{m0}.

Seasonal variations of the remaining parameters, ϵ_0, θ_J, and d_θ, are much less than J, H_{m0}, and T_e, and are barely discernable. Monthly means for spectral width, ϵ_0, remain nearly constant at ~0.4. Similarly, monthly means for wave direction, θ_J, remains nearly constant from west at ~275°, and directionality coefficient, d_θ, remains at ~0.9. In summary, the waves at NETS, from the perspective of monthly means, have a fairly consistent spectral width, are predominantly from the west, and exhibit a wave power that has a narrow directional spread.

Wave roses of wave power and significant wave height, presented in Appendix A, Figure 45 and 46, also show the predominant direction of the wave energy at NETS, which is west, with frequent but small shifts to the north and occasional but small shifts to the south. Figure 45 shows two dominant wave direction sectors, west (at 270°) and west/northwest (WNW) at 285°. Along the predominant wave direction, 285°, the omnidirectional wave power density is at or below 35 kW/m about 24% of the time, but greater than 35 kW/m nearly 15% of the time. Along the west direction (270°), wave power density is at or below 35 kW/m about 18% of the time, and greater than 35 kW/m nearly 10% of the time.

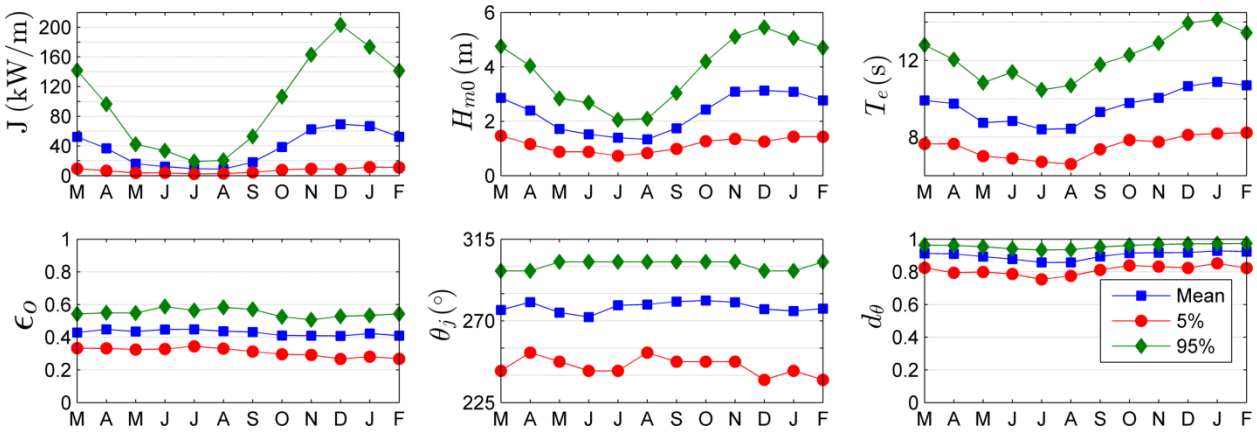

Figure 7. The average, 5th and 95th percentiles of the six parameters at NETS.

Monthly means, however, smear the significant variability of the six IEC parameters over small time intervals as shown in plots of the parameters at 1-hour intervals in Figure 8 for a representative year. While seasonal patterns described for Figure 7 are still evident, these plots show how sea states can vary abruptly at small time scales with sudden changes, e.g., jumps in the wave power as a result of a storm.

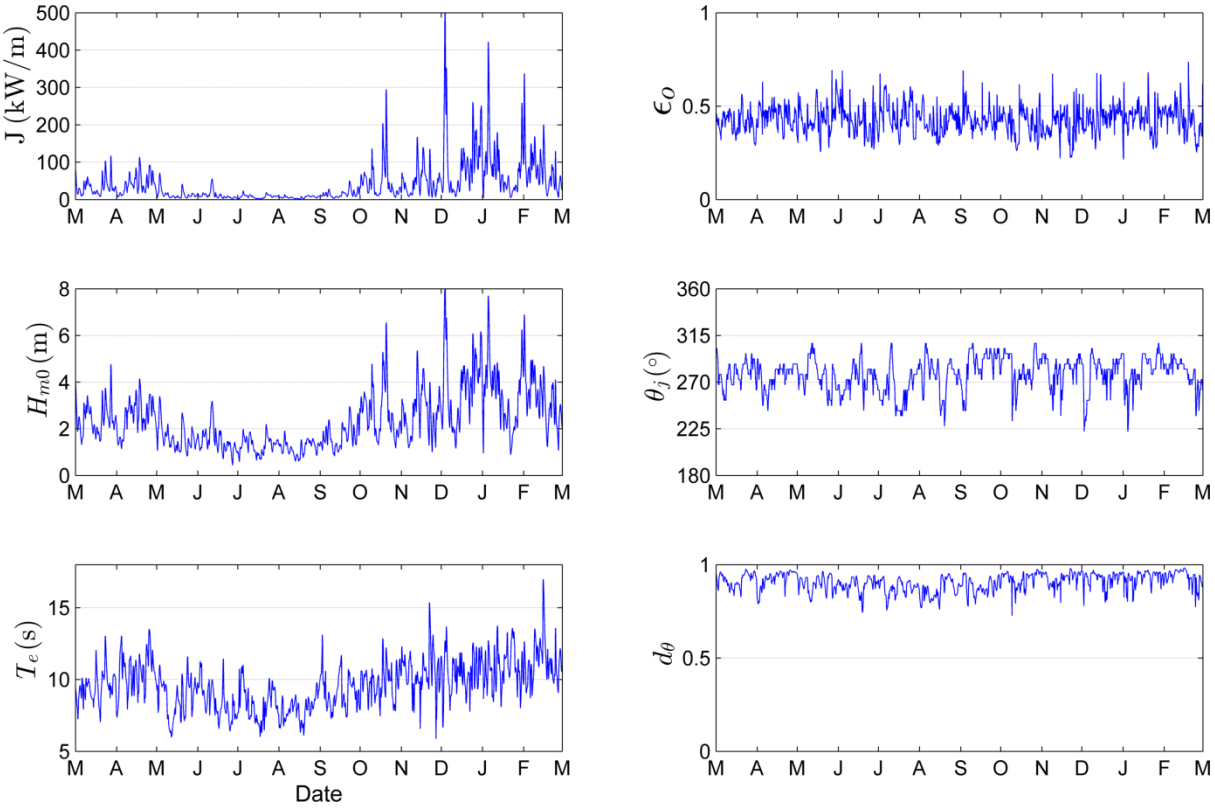

Figure 8. The six parameters of interest over a one-year period, March 2007 – February 2008 at NETS.

3.4.3. Cumulative Distributions

Annual and seasonal cumulative distributions (a.k.a., cumulative frequency distributions) are shown in Figure 9. Note that spring is defined as March – May, summer as June – August, fall as September – November, and winter as December – February. The cumulative distributions are another way to visualize and describe the frequency of occurrence of individual parameters, such as H_{m0} and T_e. A developer could use cumulative distributions to estimate how often they can access the site to install or perform operations and maintenance based on their specific device, service vessels, and diving operation constraints. For example, if significant wave heights need to be less than or equal to 1 m for installation and recovery, according to Figure 9, this condition occurs nearly 6% of the time on average within a given year. If significant wave heights need to be less than or equal to 2 m for emergency maintenance, according to Figure 9, this condition occurs about 49% of time on average within a given year. Cumulative distributions, however, do not account for the duration of a desirable sea state, or weather window, which is needed to plan deployment and servicing of a WEC device at a test site. This limitation is addressed with the construction of weather window plots in the next section.

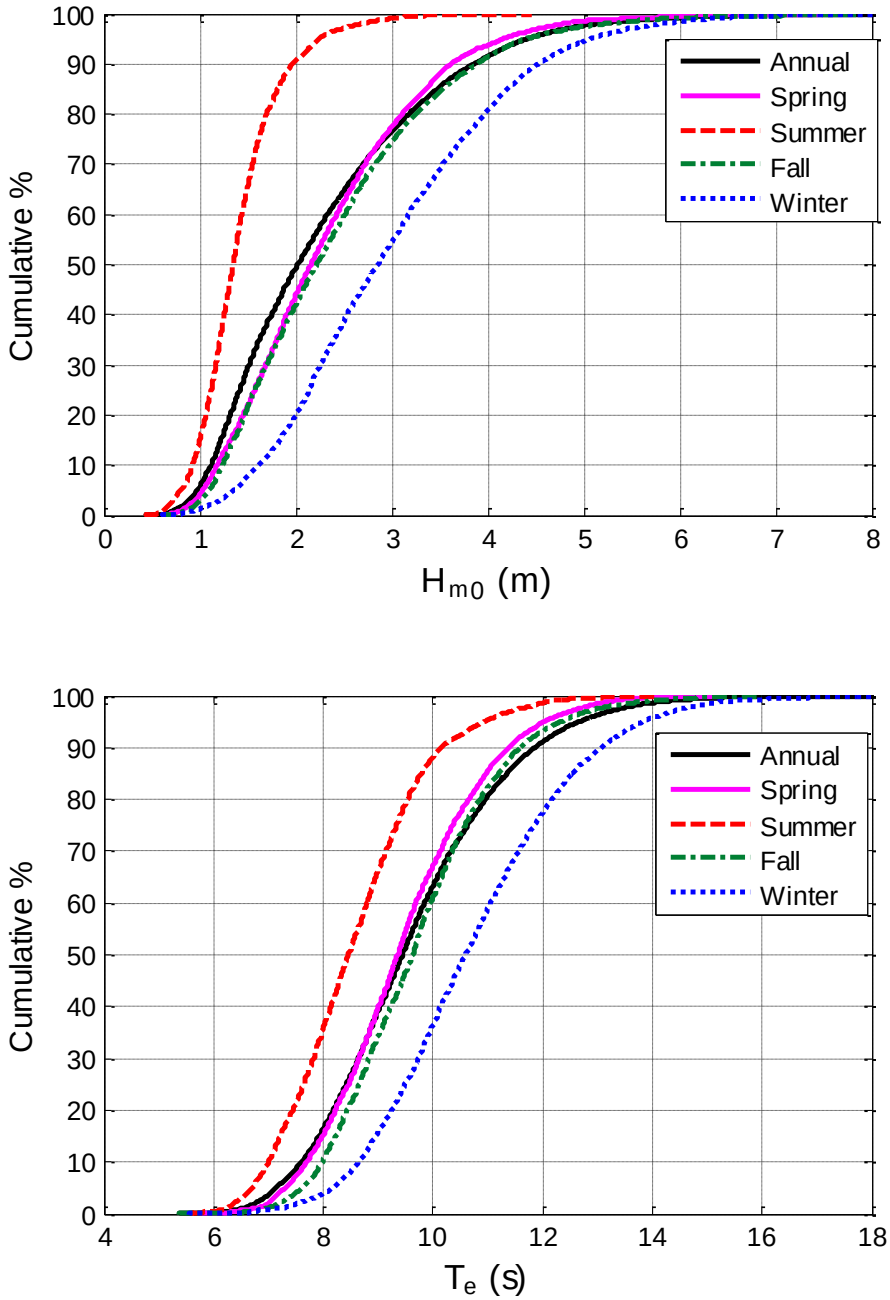

Figure 9. Annual and seasonal cumulative distributions of the significant wave height (top) and energy period (bottom) at NETS.

3.4.4. Weather Windows

Figure 10 shows the number of weather windows at NETS, when significant wave heights are at or below some threshold value for a given duration, for an average winter, spring, summer and fall. In these plots, each occurrence lasts a duration that is some multiple of 6-hours. The

minimum weather window is, therefore, 6-hours in duration, and the maximum is 96-hours (4 days). The significant wave height threshold is the upper bound in each bin and indicates the maximum significant wave height experienced during the weather window. Note that the table is cumulative, so, for example, an occurrence of $H_{m0} \leq 1$ m for at least 30 consecutive hours in the fall is included in the count for 24 consecutive hours as well. It is clear that there are significantly more occurrences of lower significant wave heights during the summer than winter, which corresponds to increased opportunities for deployment or operations and maintenance.

Weather window plots provide useful information at test sites when planning schedules for deploying and servicing WEC test devices. For example, if significant wave heights need to be less than or equal to 1 m for at least 12 consecutive hours to service a WEC test device at NETS with a given service vessel, there would be, on average, twenty-three weather windows in the summer, but only one in the winter. When wind speed is also considered, Figure 11 shows the average number of weather windows with the additional restriction of wind speed, U<15 mph. The local winds (which are not necessarily driving the waves) are used in these weather windows, and are given in Appendix A.4. That wind data was not available from the hindcast, so data from CFSR was used (see Section 2.3, Appendix A.4). For shorter durations (6- and 12-hour windows), daylight is necessary. Windows with U <15 mph and only during daylight hours are shown in Figure 12. Daylight was estimated as 5am – 10pm Local Standard Time (LST).

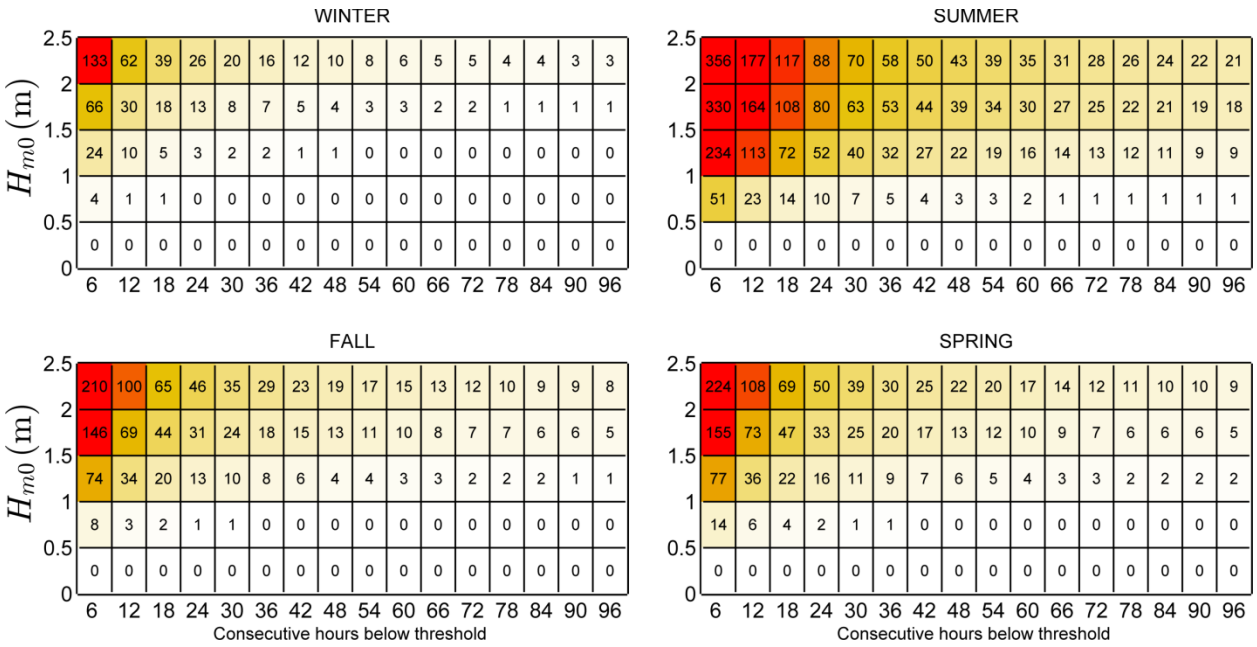

Figure 10. Average cumulative occurrences of wave height thresholds (weather windows) for each season at NETS. Winter is defined as December – February, spring as March – May, summer as June – August, and fall as September – November.

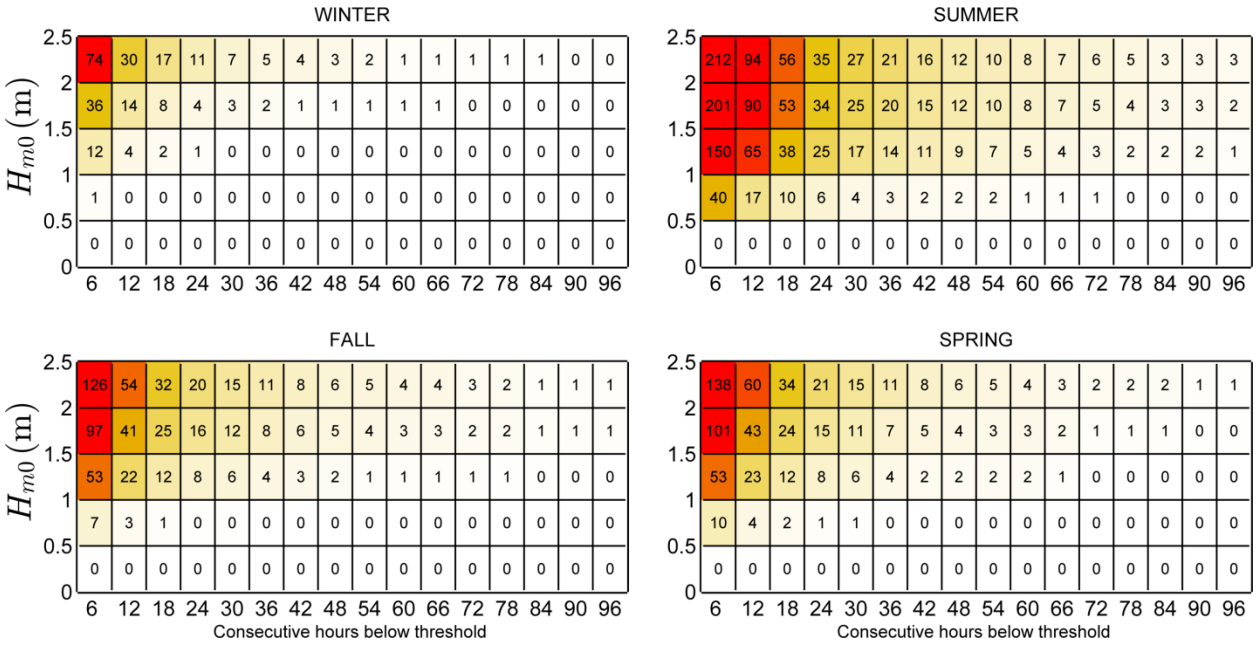

Figure 11. Average cumulative occurrences of wave height thresholds (weather windows) for each season at NETS with an additional restriction of U < 15 mph.

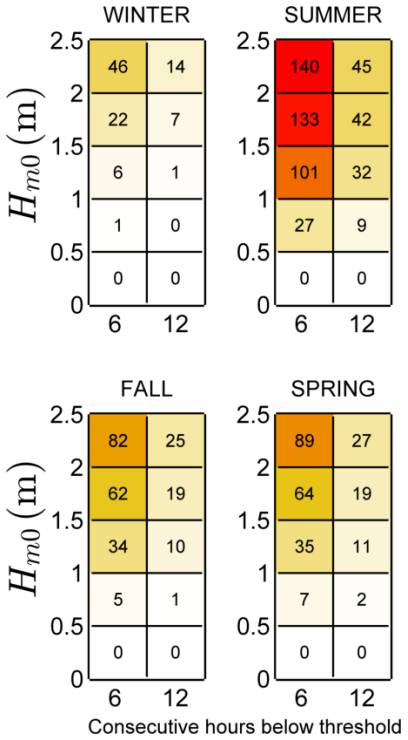

Figure 12. Average cumulative occurrences of wave height thresholds (weather windows) for 6- and 12-hour durations with U < 15 mph and only during daylight hours (5am – 10pm LST) at NETS.

3.4.5. Extreme Sea States

The modified IFORM was applied using NDBC46050 data (see Table 1 for buoy information) to generate the 100-year environmental contour for NETS shown in Figure 13. Selected sea states along this contour are listed in Appendix A, Table 5. As stated in Section 1.2, environmental contours are used to determine extreme wave loads on marine structures and design these structures to survive extreme sea states of a given recurrence interval, typically 100-years. For NETS, the largest significant wave height estimated to occur every 100-years is over 17.5 m, and has an energy period of about 16.3 s. However, significant wave heights lower than 17.5 m, with energy period less than or greater than 16.3 s, listed in Table 5, could also compromise the survival of the WEC test device under a failure mode scenario in which resonance occurred between the incident wave and WEC device, or its subsystem. For comparison, a 50-year return period results in a similar contour where the largest significant wave height is over 16.5 m with an energy period of about 16.1 s. A 25-year return period also results in a similar contour where the largest significant wave height is over 15.6 m with an energy period of about 15.9 s.

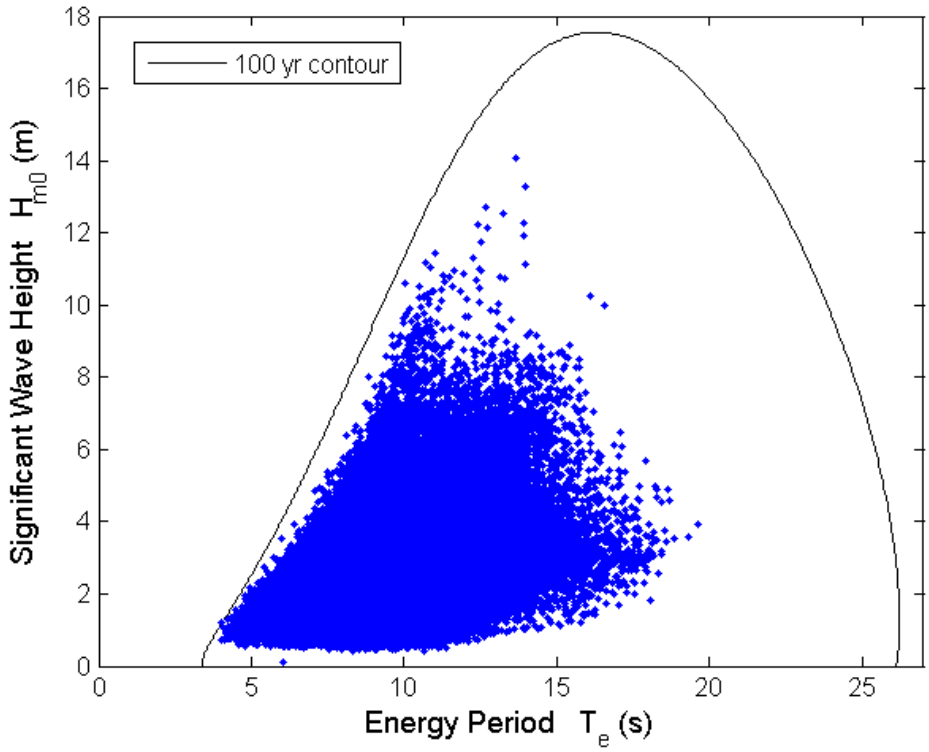

Figure 13. 100-year contour for NDBC 46050 (1996-2012).

3.4.6. Representative Wave Spectrum

All hourly discrete spectra measured at NDBC46050 for the most frequently occurring sea states are shown in Figure 14. The most frequently occurring sea state, which is within the range 1.5 m < H_{m0} < 2 m and 7 s < T_e < 8 s, was selected from a JPD similar to Figure 6 in Section 3.4.1, but based on the NDBC46050 buoy data. As a result, the JPD, and therefore the most common sea states, generated from buoy data are slightly different from that generated from hindcast data.

For example, the most frequently occurring sea state for the JPD generated from hindcast data is in the same range for H_{m0} (1.5 m < H_{m0} < 2 m), but one second higher on bounds for T_e (8 s < T_e < 9 s). Often several sea states will occur at a very similar frequency, and therefore plots of hourly discrete spectra for several other sea states are also provided for comparison. Each of these plots includes the mean spectrum and standard wave spectra, including Bretschneider and JONSWAP, with default constants as described in Section 2.2.

For the purpose of this study, the mean spectrum is the 'representative' spectrum for each sea state, and the mean spectrum at the most common sea state, shown in Figure 14 (bottom-right plot), is considered the 'representative' spectrum at the site. The hourly spectra vary considerably about this mean spectrum, but this is partly reflective of the bin size chosen for H_{m0} and T_e. Comparisons of the representative spectra in all plots with the Bretschneider and JONSWAP spectra illustrate why modeled spectra with default constants, e.g., the shape parameter $\gamma = 3.3$ for the JONSWAP spectrum, should be used with caution. Using the constants provided in Section 2.2, the Bretschneider spectra are, at best, fair representations of the mean spectra in Figure 14. If these modeled spectra were to be used at this site, it is recommended that the constants undergo calibration against some mean spectrum, e.g., the representative spectrum constructed here.

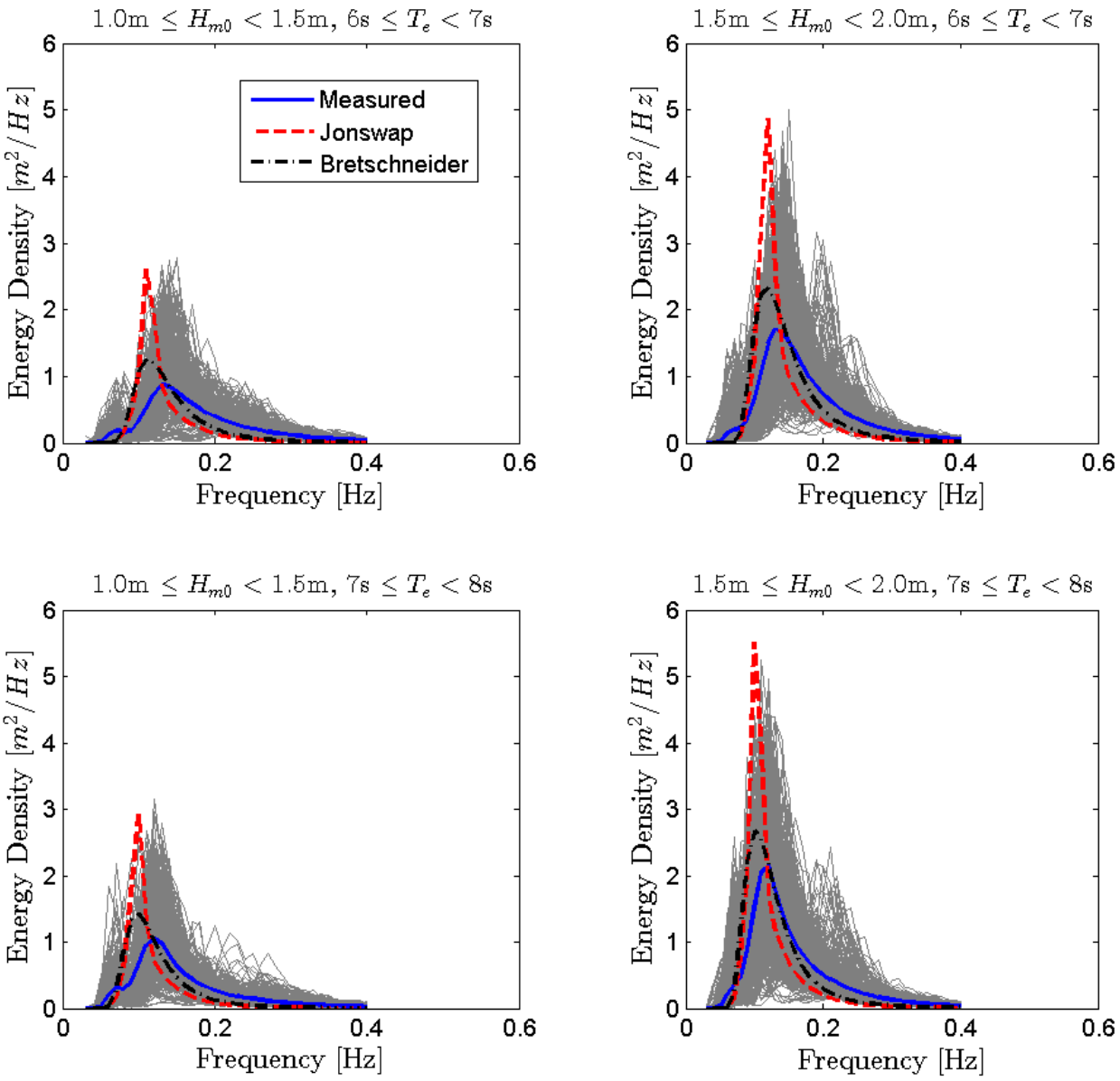

Figure 14. All hourly discrete spectra and the mean spectra measured at NDBC46050 within the sea state listed above each plot. The Bretschneider and JONSWAP spectra are represented by red and black dotted lines, respectively.

4. U.S. NAVY WAVE ENERGY TEST SITE (WETS)

4.1. Site Description

The United States' first grid-connected wave energy test site is being developed off the coast of the island of Oahu. The site, known as the U.S. Navy Wave Energy Test Site (WETS), is located on the windward side of the island at Marine Corps Base Hawaii (MCBH), at Kaneohe, as shown in Figure 15. The site infrastructure is being built by the U.S. Naval Facilities Engineering Command (NAVFAC) as a means of investigating the potential of wave energy to address the energy goals of the Navy. Through a cooperative effort between the Navy and the U.S. Department of Energy (DOE), the site will host companies seeking to test their pre-commercial WEC devices in an operational setting and advance their device transition readiness level. Now fully permitted and consisting of three berths, at water depths of 30 m (in place), 60 m, and 80 m (expected to be functional by July 2015), all within about 2 km of shore, the site will be capable of hosting point absorber and oscillating water column WEC devices up to a peak power of 1 MW.

The site is located in Hawaiian state waters at approximately 21.47 N, 157.75 W (Figure 15). The deep water mooring sites overlay a featureless sandy substrate on a slightly steeper slope (Department of the Navy 2014). Figure 16 shows the bathymetry near Mokapu and the surrounding area. The wave climate at the test site is dominated by swells from the North Pacific, which are more frequent in the winter, and year-round waves formed by the northeast trade winds, which peak in the summer months between May-October (Department of the Navy 2014). The wave environment at WETS is characterized by an annual average power flux of 10-15 kW/m, with a significant number of events exceeding 40 kW/m each year. Despite this reliable wave energy, quiet periods are likely throughout the year, providing year round access to WEC devices.

NAVFAC operates the site and handles the permitted berths, grid connection infrastructure, device-specific permits, and offers office space. Typically a Cooperative Research and Development Agreement (CRADA) or a Navy contract is set up.

The Hawaii National Energy Institute at the University of Hawaii (HNEI-UH) is working with NAVFAC and DOE to support efforts at WETS in three key areas: (1) independent WEC device performance analysis; (2) environmental impact monitoring; and, (3) outfitting of a site-dedicated at-sea support platform. Environmental monitoring consists of ongoing measurements and analysis of the device acoustic signature, device and cabling electromagnetic fields (EMF), and possible changes in the device/mooring-induced sediment transport, seawater chemistry, and the ecological environment. HNEI will independently assess the device performance through robust wave environment measurements using Waverider buoys and an ADCP, wave forecast modeling, comprehensive device power output monitoring, the creation of power matrices to characterize performance as a function of wave state, and regular diver and ROV inspections of the deployed devices and associated mooring and cabling infrastructure. An additional UH effort is aimed at utilizing the data from WETS to advance geophysical fluid dynamics-based models

of device performance to guide design improvements, as well to advance ongoing efforts to improve WEC array modeling.

Figure 15. WETS is located on the northeast shore of Oahu, Hawaii near the Marine Corps Base Hawaii (MCBH). The site is 1-2 km off-shore in 30–80 m depth water and has one operational berth and two berths under construction. One National Data Buoy Center ocean buoy and one National Data Buoy Center meteorological station are close to the site (see Table 2). The Heeia Kea Small Boat Harbor is located in Kaneohe Bay and a boatyard is accessible in Honolulu, HI. The hindcast simulation used two points of reference as shown. Image modified from Google Earth (2014).

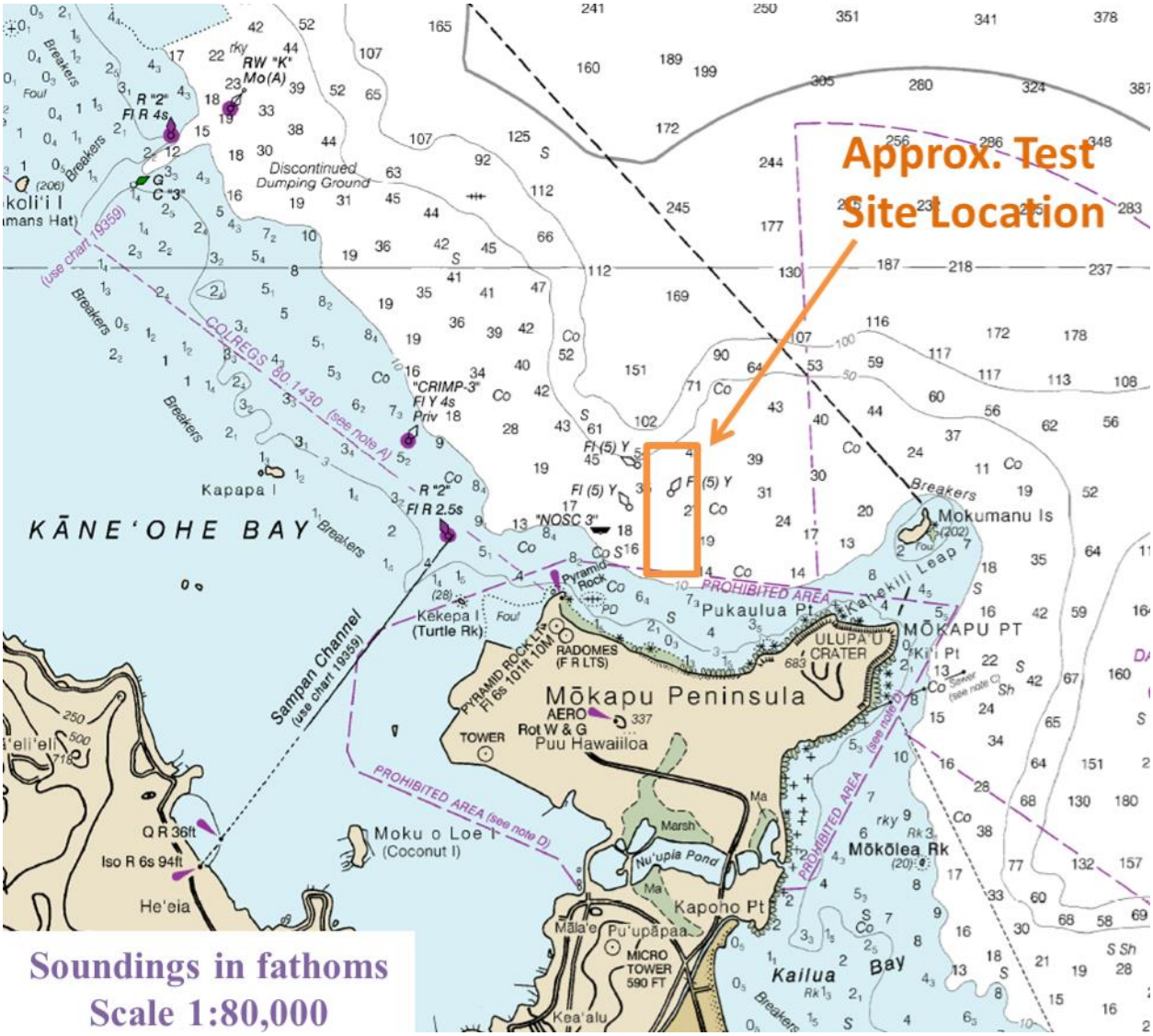

Figure 16. Nautical Chart of Mokapu Peninsula and surrounding area shows the gradually sloping bathymetry at WETS. Soundings in fathoms (1 fathom = 1.8288 m). Image modified from nautical chart #19357 (Office of Coast Survey 2013).

4.2. WEC Testing Infrastructure

4.2.1. Mooring Berths

There is one mooring berth at WETS and two under construction (Figure 17). The 30 m mooring berth uses a three point mooring system (a tri-moor configuration) with three sub-surface floats, two rock-bolted anchor bases and one gravity anchor. The mooring berth is fully functional and was used for testing a WEC device by Ocean Power Technologies between 2003 and 2011. Two deeper mooring berths at 60 m and 80 m are scheduled to be operational by July 2015. They also employ three point mooring systems and each utilizes three surface floats and three drag embedment anchors, with the majority of the mooring system components provided by the Navy, including the anchor, ground change, mooring chain, and surface buoy. Figure 18 shows a schematic of one of the three mooring legs for the 60 m and 80 m berths which were designed by Sound & Sea Technology.

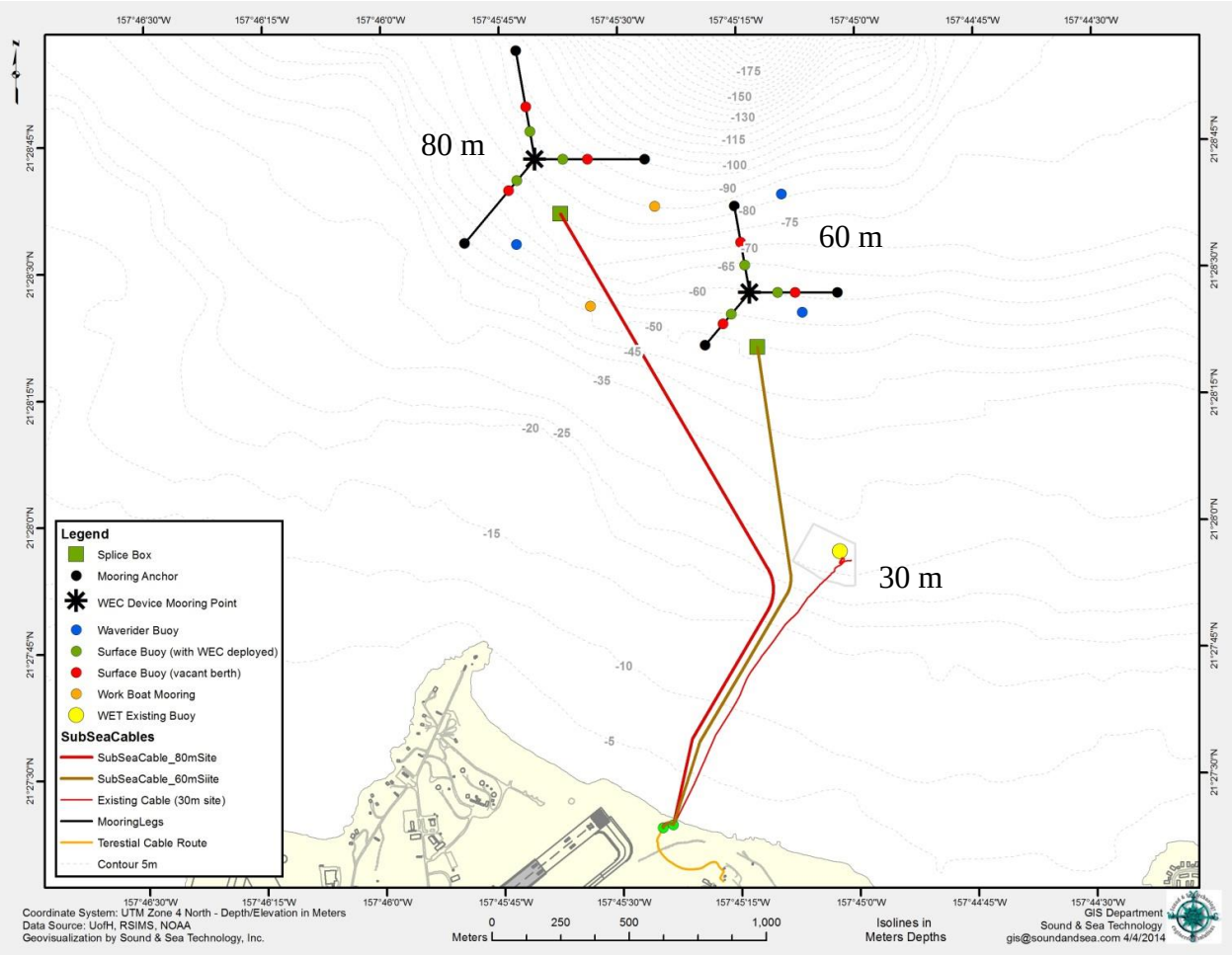

Figure 17. WETS mooring configuration and bathymetry map showing underwater cables and the three mooring sites at 30 m, 60 m, and 80 m depth (De Visser and Vega 2014).

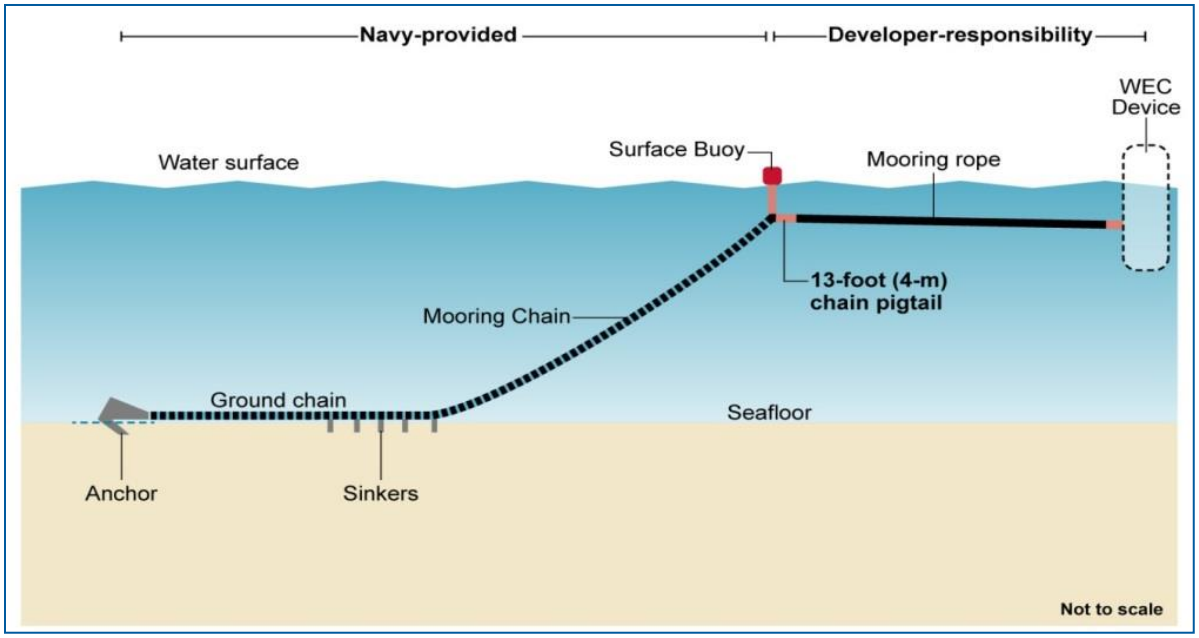

Figure 18. Sound & Sea Technology schematic of WETS 60 m and 80 m berths (De Visser and Vega 2014).

4.2.2. Electrical Grid Connection

WETS is a grid-accessible test site. An existing subsea cable with a maximum transmitting power of 250 kW at 4160 V services the 30 m mooring berth (De Visser and Vega 2014). Two additional cables are planned for installation by July 2015 to service the 60 m and 80 m mooring berths and will transmit up to 1 MW at 11,500 V (De Visser and Vega 2014).

4.2.3. Facilitating Harbor

To the West and to the East of WETS is Kaneohe Bay and Kailua Bay, respectively, which are both popular recreation destinations. For boat mooring, the Heeia Kea Small Boat Harbor (Waypoint #1 in Figure 15) offers 54 moorings, 21 berths and 3 boat ramps (State of Hawaii Division of Boating and Ocean Recreation 2014).

4.2.4. On-Shore Office Space

WETS is 1-2 km offshore of the Marine Corps Base Hawaii (MCBH), which encompasses the area of Mokapu Peninsula. Office space is available through MCBH (De Visser and Vega 2014).

4.2.5. Service Vessel and Engineering Boatyard

A key focus at WETS, by the Navy, DOE, and HNEI, is reducing the considerable costs to developers associated with at-sea testing of WEC devices. The regular device and mooring

inspections mentioned above are an important aspect of this. Additionally, HNEI plans to contract with a local ocean engineering company to provide a self-propelled barge equipped with cranes and hyperbaric chamber, dive and ROV facilities, an A-frame, and workspaces for WEC developers and UH scientists/engineers (Vega, 2014). To reduce mobilization costs and shorten emergency response time, this platform will be kept at Heeia Kea Small Boat Harbor, a state marina within an hour's transit from the site. Further, a limited amount of emergency maintenance response will be provided to tenants at WETS, furthering HNEI's ability to fully document device reliability issues and develop operational and maintenance protocols for DOE and the Navy. In addition, several engineering boatyards are available in Honolulu Harbor with a variety of services available (Vega 2014).

4.2.6. Travel and Communication Infrastructure

The Honolulu International Airport is only a half hour drive from MCBH. Cellular phone coverage is adequate and consistent, and cell phones may be used on MCBH.

4.2.7. Met-Ocean Monitoring Equipment

Real-time meteorological and wave data are collected by two met-ocean buoys from the CDIP database, one on-shore meteorological station available through the Automated-Surface-Observing-System (ASOS) and one maintained by NOAA. Instrument and data specifications for this monitoring equipment are summarized in Table 2. Buoy data is accessible online at the CDIP databases. CDIP198 (NDBC51207) (Figure 19 (a)) is located very close to the 80 m depth berth, and CDIP098 (NDBC51202) (Figure 19 (b)) is located approximately 12 km southeast. On-shore, there is a meteorological station on MCBH near the site.

Figure 19: a) CDIP198 Waverider, b) CDIP098 Waverider (Coastal Data Information Program 2013).

Table 2: Wave monitoring equipment in close proximity to WETS.

Instrument Name (Nickname)	CDIP198 / NDBC51207		CDIP098 / NDBC51202 (Mokapu Point, HI)		ASOS PHNG Kaneohe Bay Marine Corps Airfield	MOKH1 - 1612480 - Mokuoloe, HI
Type	Waverider Buoy		Waverider Buoy		Meteorological Station	Water Level Observation Network
Measured parameters	-std. met. data -spectral wave density data -spectral wave direction data		-std. met. data -spectral wave density data -spectral wave direction data		-wind dir & speed -barometric pressure -air temp -humidity	-wind dir & speed -gust -atmos press -air temp -water temp
Variables reported (includes derived variables)	*Std. Met.:* WVHT DPD APD MWD WTMP (30 min sampling period)	-Spectral Wave Density -Spectral Wave direction (30 min sampling period)	*Std. Met.:* WVHT DPD APD MWD WTMP (30 min sampling period)	-Spectral Wave Density -Spectral Wave direction (30 min sampling period)	WDIR WSPD (10 min sampling period) PRES ATMP (1 hour sampling period)	WDIR WSPD GST PRES ATMP WTMP (6 min sampling period)
Location	at WETS		directly east of Kailua Bay, 12 km southeast of WETS		Installed at MCBH, near the test site	on Coconut Island (farther west into Kaneohe Bay than WETS)
Coordinates	21.477 N 157.753 W (21°28'39" N 157°45'10" W)		21.417 N 157.668 W (21°25'1" N 157°40'4" W)		unknown	21.432 N 157.790 W (21°25'55" N 157°47'24" W)
Depth	81 m		82 m		unknown	-air temp height: 5.5 m above site elevation -anemometer height: 12.7 m above site elevation -barometer elev: 2.8 m above mean sea level
Data Start	10/27/2012		8/10/2000		unknown	6/25/2008
Data End	present		present		present	present
Period of Record	~2 yrs		~13 yrs		unknown	~6 yrs
Owner / Contact Person	Pacific Islands Ocean Observing System (PacIOOS) -- "Data provided by Scripps" Data reported at http://cdip.ucsd.edu/?xmg=search&xsearch=198&xsearch_type=Station_ID		Pacific Islands Ocean Observing System (PacIOOS) -- "Data provided by Scripps" Data reported at http://cdip.ucsd.edu/?ximg=search&xsearch=098&xsearch_type=Station_ID		http://www.aviationweather.gov/metar	NOAA Tides & Currents

4.2.8. Environmental Monitoring

Environmental conditions at WETS have been characterized by the Navy with support from HNEI. Background environmental data includes wave, current, and climate data, as well as bathymetry and sediment profiles (De Visser and Vega 2014). Environmental monitoring, provided by HNEI, consists of ongoing measurements and analysis of acoustics, electromagnetic fields (EMF), and ecological surveys (to determine possible changes in sediment transport, seawater chemical composition, and the ecological environment).

4.2.9. Permitting

The berths at the site are permitted for testing of generic point absorbers and oscillating water column (OWC) devices. Developers must individually complete device-specific categorical exclusion applications, and an Army Corp of Engineers permit.

4.3. Data Used

Researchers affiliated with the Hawaii National Marine Renewable Energy Center (HINMREC) at the University of Hawaii produced a 10 year hindcast dataset for the area offshore of Oahu (Li and Cheung 2014). This hindcast is an improved version of that by Stopa et al. (2013), and is currently being extended to a 30 year hindcast. The 10 year dataset was used to calculate statistics of interest for the characterization. The hindcast data at two grid points (21.472 N, 157.747 W and 21.4775 N, 157.7526 W) for the 60 m "Kaneohe II" and 80 m "WETS" berths, respectively, were analyzed by UH (see Figure 15 and Figure 17 for location).

In addition to the hindcast data set, historical data from buoy NDBC51202 was used to calculate estimates of extreme events because of its longer period of record (2001-2012). Historical data from buoy CDIP198/NDBC51207 was used to calculate representative spectra because of its location at WETS. Wind data from CFSR was used, as explained in Section 2.3. A high resolution wind data set for the Hawaiian Islands (in addition to the global CFSR data set) was utilized in the hindcast by Li and Cheung (2014), and therefore monthly averages will be provided in Appendix B as well. As with the other sites, current data was downloaded from OSCAR. See Figure 20 for data locations.

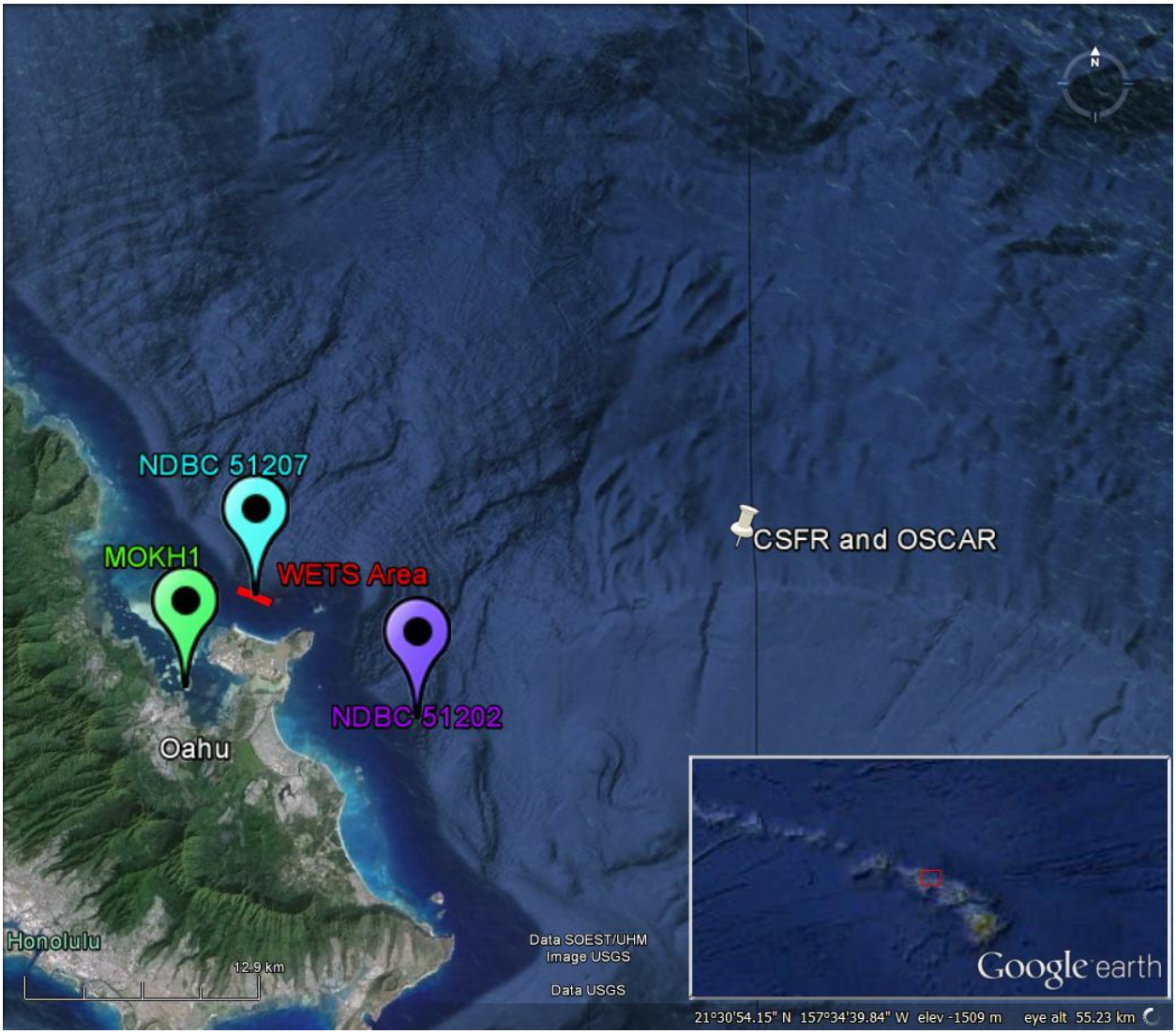

Figure 20. Two wave buoys and one met station surround the test site. The data points for OSCAR and CSFR overlap at 21.5 N, 157.5 W (Google Earth 2014).

4.4. Results

The following sections provide information on the joint probability of sea states, the variability of the IEC TS parameters, cumulative distributions, weather windows, extreme sea states, and representative spectra. This is supplemented by wave roses as well as wind and surface current data in Appendix B. The wind and surface current data provide additional information to help developers plan installation and operations & maintenance activities.

4.4.1. Sea States: Frequency of Occurrence and Contribution to Wave Energy

Joint probability distributions of the significant wave height, H_{m0}, and energy period, T_e, are shown in Figure 21 and 22. Figure 21 (top) shows the frequency of occurrence of each binned sea state and Figure 21 (bottom) shows the percentage contribution to the total wave energy for "Kaneohe II" berth (60 m depth). The same information is shown for the "WETS" berth (80 m depth) in Figure 22. Figure 21 (top) and Figure 22 (top) indicate that the majority of sea states are within the range 1 m < H_{m0} < 2.5 m and 5 s < T_e < 11 s. WETS experiences a minimal amount of extreme sea states, which rarely exceed 5 m. The site is well suited for testing WECs at various scales, and testing the operation of WECs under normal sea states. Year-round testing occurs at WETS and the winter storms may be considered for survival testing for scaled devices (compared to a full-scale devices deployed in a higher energy location).

As mentioned in the methodology (Section 2.2), previous studies show that sea states with the highest occurrence do not necessarily correspond to those with the highest contribution to total wave energy, as is the case in Figure 21 and Figure 22. The total wave energy in an average year is 102,849 kWh/m at the Kaneohe II berth and 113,439 kWh/m at the WETS berth, which corresponds to an average annual omnidirectional wave power of 11.7 kW/m and 12.9 kW/m. The most frequently occurring sea state is within the range 1 m < H_{m0} < 1.5 m and 6 s < T_e < 7 s, while the sea state that contributes most to energy is within the range 1.5 m < H_{m0} < 2 m and 7 s < T_e < 8 s for both Kaneohe II and WETS. Several sea states occur at a similar frequency, and sea states within 1 m < H_{m0} < 2 m and 6 s < T_e < 8 s contribute a similar amount to energy.

Frequencies of occurrence and contributions to energy of less than 0.01% are considered negligible and are not shown for clarity. For example, the sea state within 0.5 m < H_{m0} < 1 m and 4 s < T_e < 5 s has an occurrence of 0.02%. The contribution to total energy, however, is only 0.003% and, therefore, does not appear in Figure 21 (bottom). Similarly, the sea state within 3 m < H_{m0} < 3.5 m and 16 s < T_e < 17 s has an occurrence of 0.007%, but the contribution to total energy is 0.06%.

Curves showing the mean, 5th and 95th percentiles of wave steepness, H_{m0}/λ, are also shown in Figure 21 and Figure 22. The mean wave steepness is 0.0164 (≈1/61) at Kaneohe II and 0.0175 (≈1/57) at WETS. The 95th percentile is 0.0255 (≈1/39) at Kaneohe II and 0.0269 (≈1/37) at WETS.

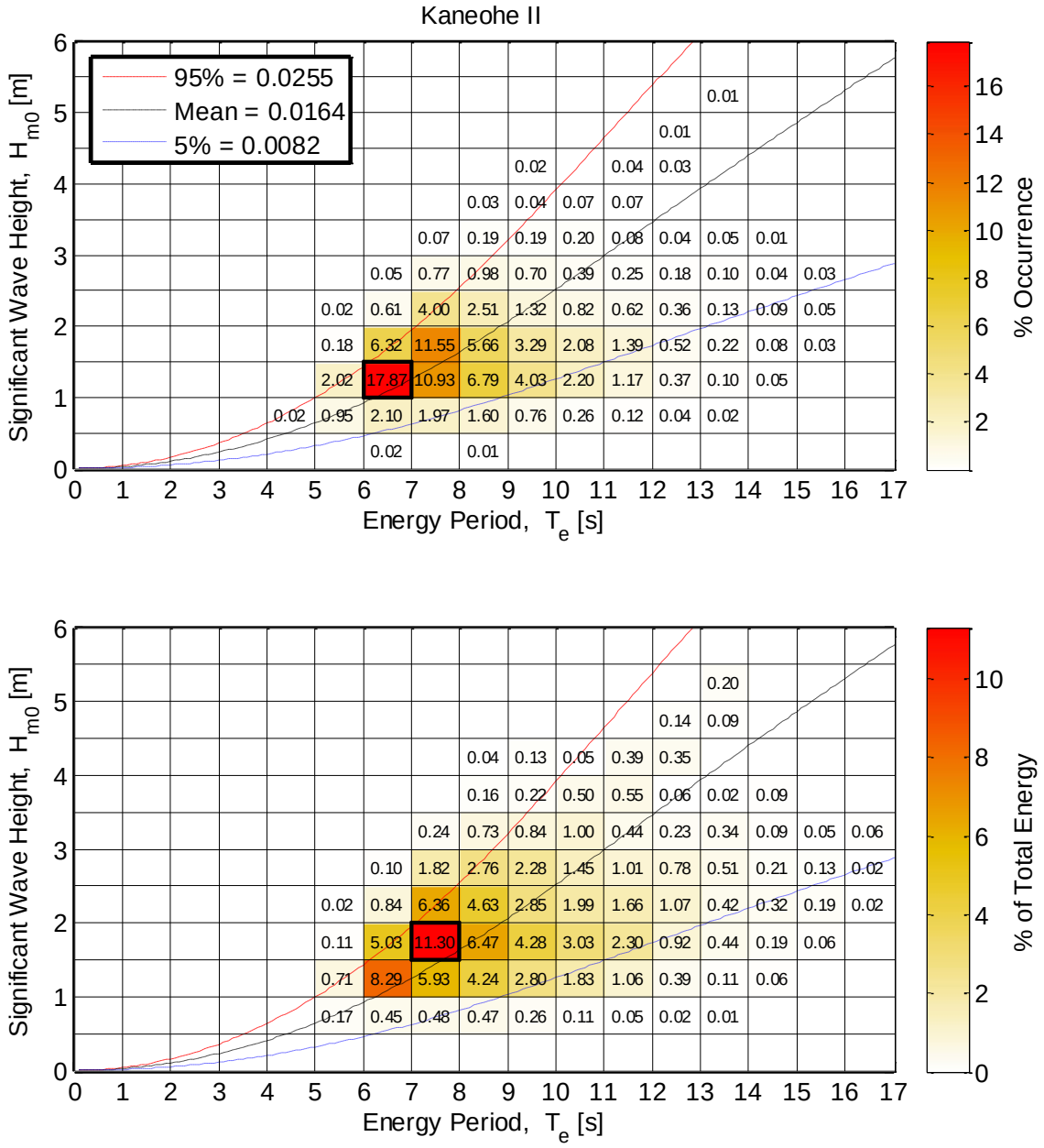

Figure 21. Joint probability distribution of sea states for the Kaneohe II berth (60 m depth). The top figure is frequency of occurrence and the bottom figure is percentage of total energy, where total energy in an average year is 102,849 kWh/m.

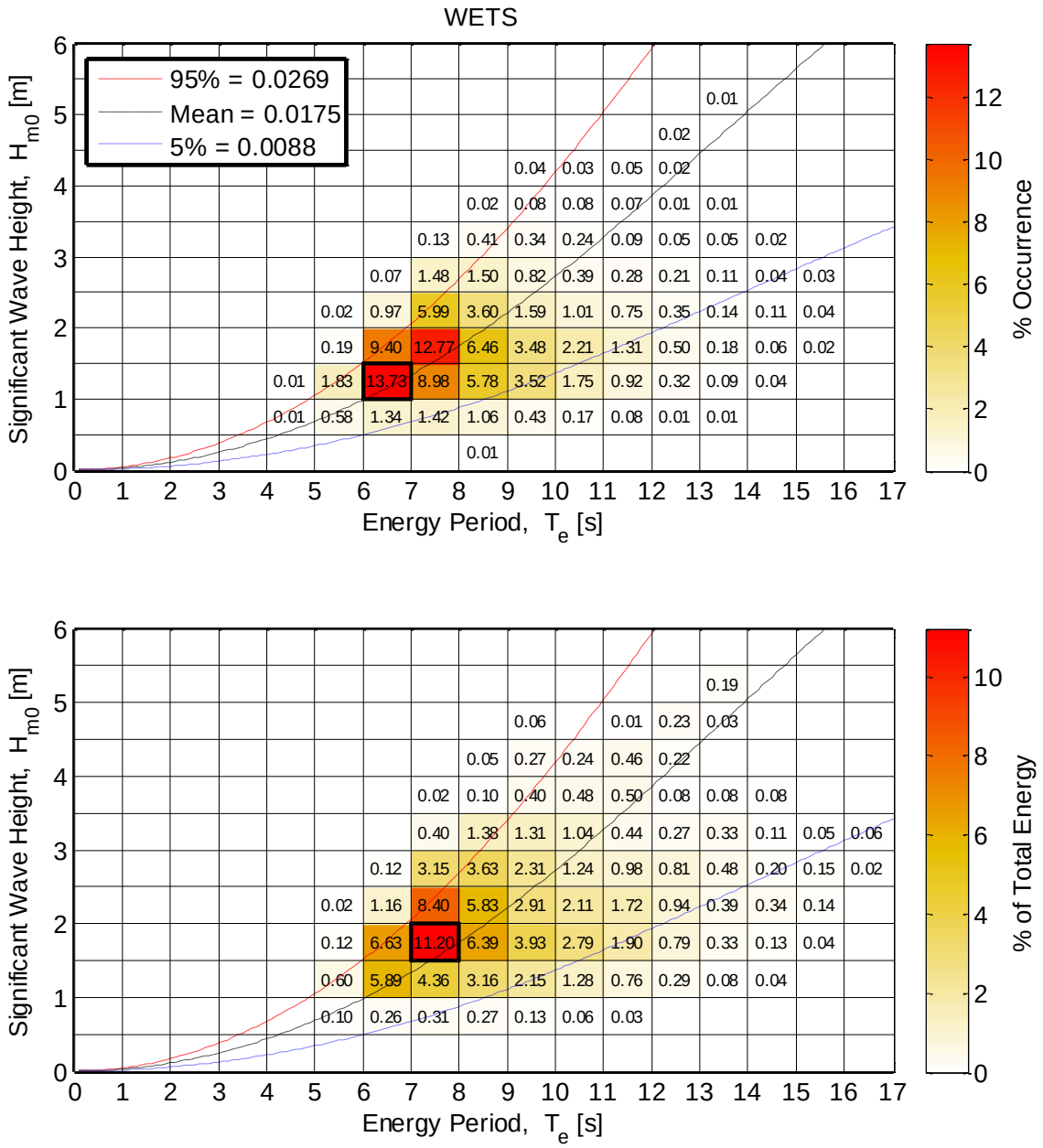

Figure 22. Joint probability distribution of sea states for the WETS berth (80 m depth). The top figure is frequency of occurrence and the bottom figure is percentage of total energy, where total energy in an average year is 113,439 kWh/m.

4.4.2. IEC TS Parameters

The monthly means of the six IEC TS parameters, along with the 5th and 95th percentiles, are shown in Figure 23 and Figure 24. The values in the figures are summarized in Table 8 and Table 9 in Appendix B.

Monthly means of the omnidirectional wave power, J, significant wave height, H_{m0}, and energy period, T_e, show the greatest seasonal variability compared to the other parameters. Values are largest and vary the most during the winter months. These observations are consistent with the relationship between wave power density, significant wave height and energy period, where wave power density, J, is proportional to the energy period, T_e, and the square of the significant wave height, H_{m0}.

The directionality coefficient (larger values indicate low directional spreading), is slightly larger in the summer, and it can be seen that the direction of maximum directionally resolved wave power (defined as the direction from which waves arrive in degrees clockwise from north), is most consistently from north/northeast during the summer, and varies more throughout the rest of the year. This is because summer months are dominated by wind waves from the northeast, while the winter months are made up of both wind waves and frequent swells from the North Pacific.

Seasonal variation of the spectral width, ϵ_0, is much less than the other parameters and barely discernable. Monthly means for ϵ_0 remain nearly constant between 0.35 and 0.4. In summary, the waves at both the Kaneohe II and WETS berths, from the perspective of monthly means, have a fairly consistent spectral width, are predominantly from the north/northeast, and exhibit a wave power that has a fairly narrow directional spread in the summer, and a wider directional spread in the winter.

Wave roses of wave power and significant wave height, presented in Appendix B, Figure 51 and Figure 52, also show the spread of direction of the maximum wave energy at WETS. The larger waves (with higher wave power), often come as swells from the North Pacific, while smaller waves usually come from the northeast as wind waves. Figure 51 shows two dominant wave direction sectors, northeast and approximately east-northeast (ENE). Along the predominant wave direction, which is northeast (45°), the omnidirectional wave power density is at or below 35 kW/m less than 25% of the time, and greater than 35 kW/m approximately 1% of the time. Along the ENE direction (60°), wave power density is at or below 35 kW/m over 25% of the time and rarely (less than 1% of the time) exceeds 35 kW/m.

Note that the wave climate is made up of swells from the North and South Pacific and year-round wind waves from the northeast. Therefore the direction of maximum directionally resolved wave power may not fully describe the origin of the wave power (i.e., the combination of swells and year-round wind waves from slightly different directions).

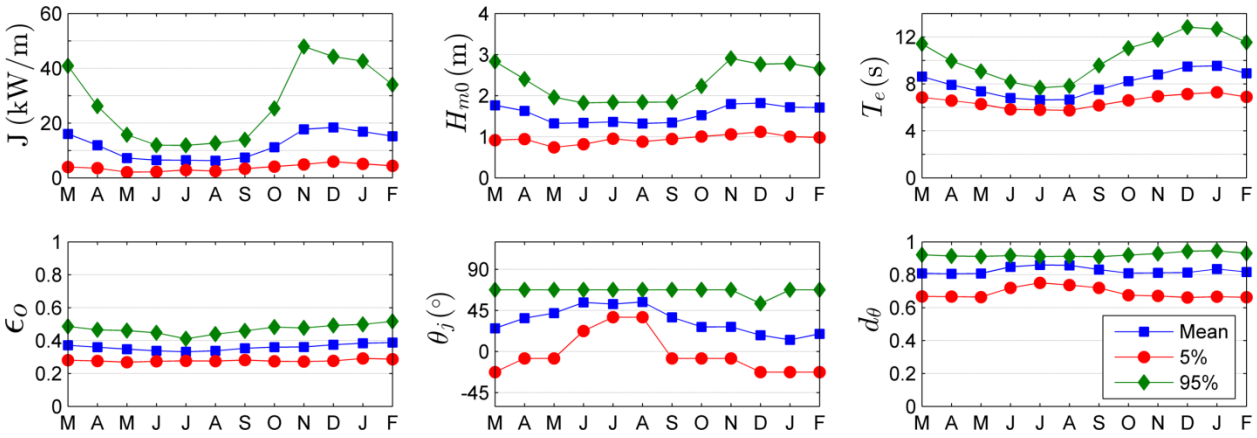

Figure 23. The average, 5th and 95th percentiles of the six parameters at Kaneohe II.

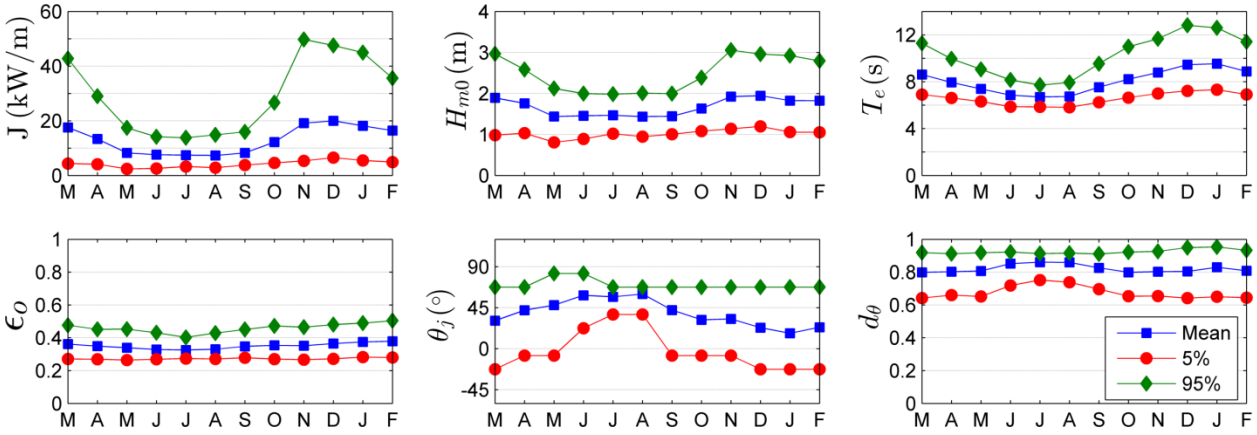

Figure 24. The average, 5th and 95th percentiles of the six parameters at WETS.

Monthly means, however, smear the significant variability of the six IEC parameters over small time intervals as shown in plots of the six IEC TS parameters at 1-hour intervals in Figure 25 for a representative year. While seasonal patterns described for Figure 23 and Figure 24 are still evident, these plots show how sea states can vary abruptly at small time scales with sudden changes, e.g., jumps in the wave power as a result of a storm. Note that the data in Figure 25 is from NDBC 51207, co-located at the WETS 80 m berth.

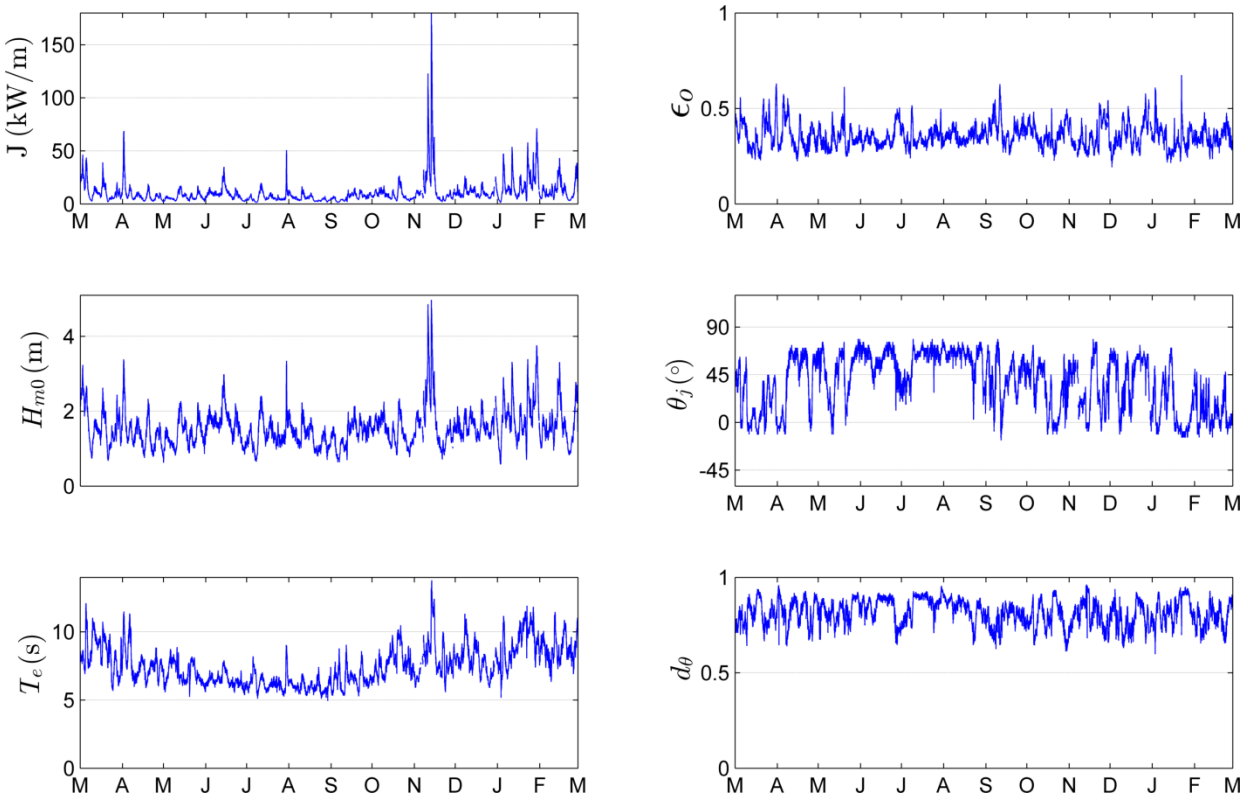

Figure 25. The six parameters of interest over a one-year period, March 2013 – February 2014 at NDBC51207 co-located at the WETS 80 m berth.

4.4.3. Cumulative Distributions

Annual and seasonal cumulative distributions (a.k.a., cumulative frequency distributions) at WETS are shown in Figure 26. Note that spring is defined as March – May, summer is June – August, fall is September – November, and winter is December – February. The cumulative distributions are another way to visualize and describe the frequency of occurrence of individual parameters, such as H_{m0} and T_e. A developer could use cumulative distributions to estimate how often they can access the site to install or perform operations and maintenance based on their specific device, service vessels, and diving operation constraints. For example, if significant wave heights need to be less than or equal to 1 m for installation and recovery, according to Figure 26, this condition occurs about 5% of the time on average within a given year. If significant wave heights need to be less than or equal to 2 m for emergency maintenance, according to Figure 26, this condition occurs about 79% of the time on average within a given year. Cumulative distributions, however, do not account for the duration of a desirable sea state, or weather window, which is needed to plan deployment and servicing of a WEC device at a test site. This limitation is addressed with the construction of weather window plots in the next section.

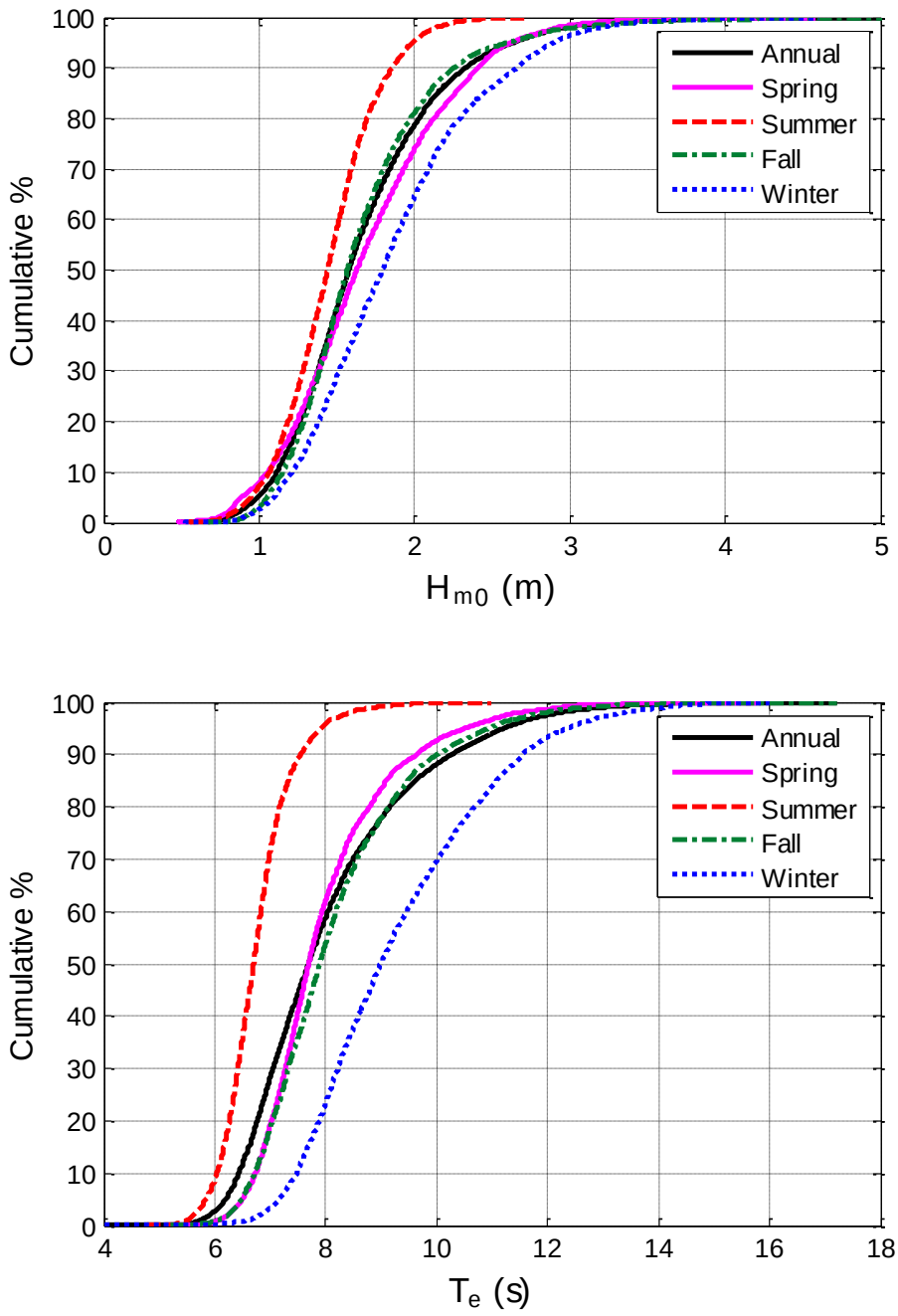

Figure 26. Annual and seasonal cumulative distributions of the significant wave height (top) and energy period (bottom) at WETS.

4.4.4. Weather Windows

Figure 27 shows the number of weather windows at WETS, when significant wave heights are at or below some threshold value for a given duration, for an averaged winter, spring, summer, and fall. In these plots, each occurrence lasts a duration that is some multiple of 6-hours. The minimum weather window is, therefore, 6-hours in duration, and the maximum is 96-hours (4 days). The significant wave height threshold is the upper bound in each bin and indicates the

maximum significant wave height experienced during the weather window. Note that the table is cumulative, so, for example, an occurrence of $H_{m0} \leq 1\ m$ for at least 36 consecutive hours in the fall is included in the count for 30 consecutive hours as well. It is clear that there are significantly more occurrences of lower wave heights during the summer than winter, which corresponds to increased opportunities for deployment or operations and maintenance.

Weather window plots provide useful information at test sites when planning schedules for deploying and servicing WEC test devices. For example, if significant wave heights need to be less than or equal to 1 m for at least 12 consecutive hours to service a WEC test device at WETS with a given service vessel, there would be, on average, eleven weather windows in the summer, but only four in the winter. When wind speed is also considered, Figure 28 shows the average number of weather windows with the additional restriction of wind speed, U<15 mph. Note that wind data was available from this hindcast, and was used herein (Ning and Cheung 2014), see Section B.4. For shorter durations (6- and 12-hour windows), daylight is necessary. Windows with U <15 mph and only during daylight hours are shown in Figure 29. Daylight was estimated as 5am – 10pm Local Standard Time (LST).

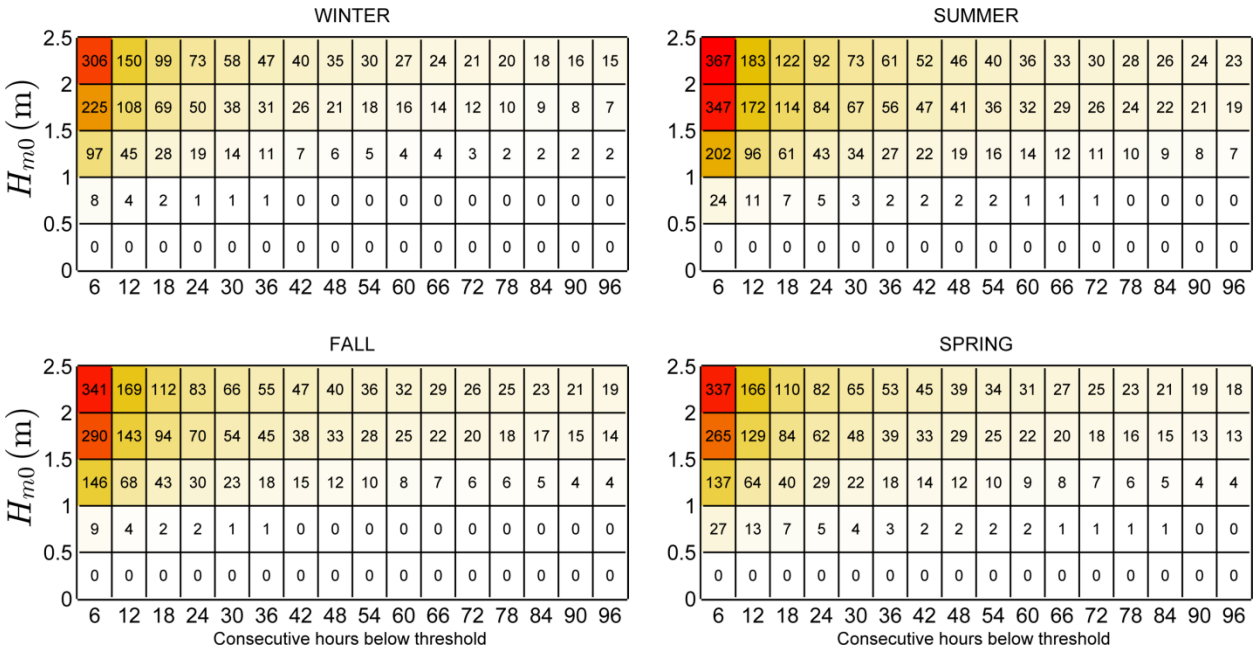

Figure 27. Average cumulative occurrences of wave height thresholds (weather windows) for each season at WETS. Winter is defined as December – February, spring as March – May, summer as June – August, and fall as September – November.

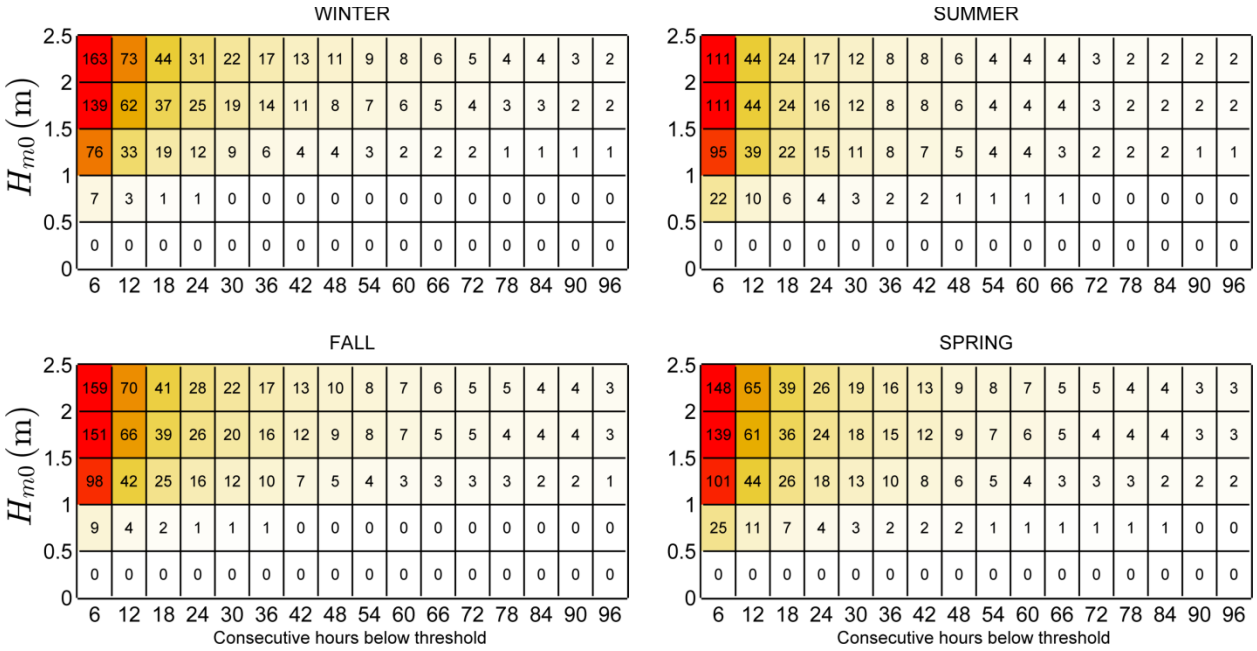

Figure 28. Average cumulative occurrences of wave height thresholds (weather windows) for each season at WETS with an additional restriction of U <15 mph.

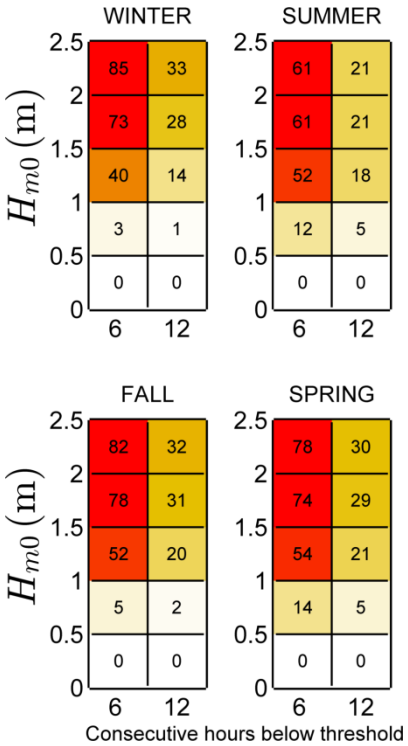

Figure 29. Average cumulative occurrences of wave height thresholds (weather windows) for 6- and 12-hour durations with U < 15 mph and only during daylight hours (5am – 10pm LST) at WETS.

4.4.5. Extreme Sea States

The modified IFORM was applied using CDIP098/NDBC51202 to generate the 100-year environmental contour for WETS shown in Figure 30. Although there is a buoy co-located at WETS (CDIP198/NDBC51207), the period of record is only two years, and therefore it was necessary to use a nearby buoy with a longer period of record (see Table 2 for buoy information). Selected sea states along this contour are listed in Appendix A, Table 10.

As stated in Section 1.2, environmental contours are used to determine extreme wave loads on marine structures and design these structures to survive extreme sea states of a given recurrence interval, typically 100-years. For WETS, the largest significant wave height estimated to occur every 100-years, is nearly 6.4 m, and has an energy period of about 12.8 s. However, significant wave heights lower than 6.4 m, with energy period less than or greater than 12.8 s, listed in Appendix B, Table 10, could also compromise the survival of the WEC test device under a failure mode scenario in which resonance occurred between the incident wave and WEC device, or its subsystem. For comparison, a 50-year return period results in a similar contour where the largest significant wave height is over 6.1 m with an energy period of about 12.5 s. A 25-year return period also results in a similar contour where the largest significant wave height is 5.9 m with an energy period of about 12.3 s.

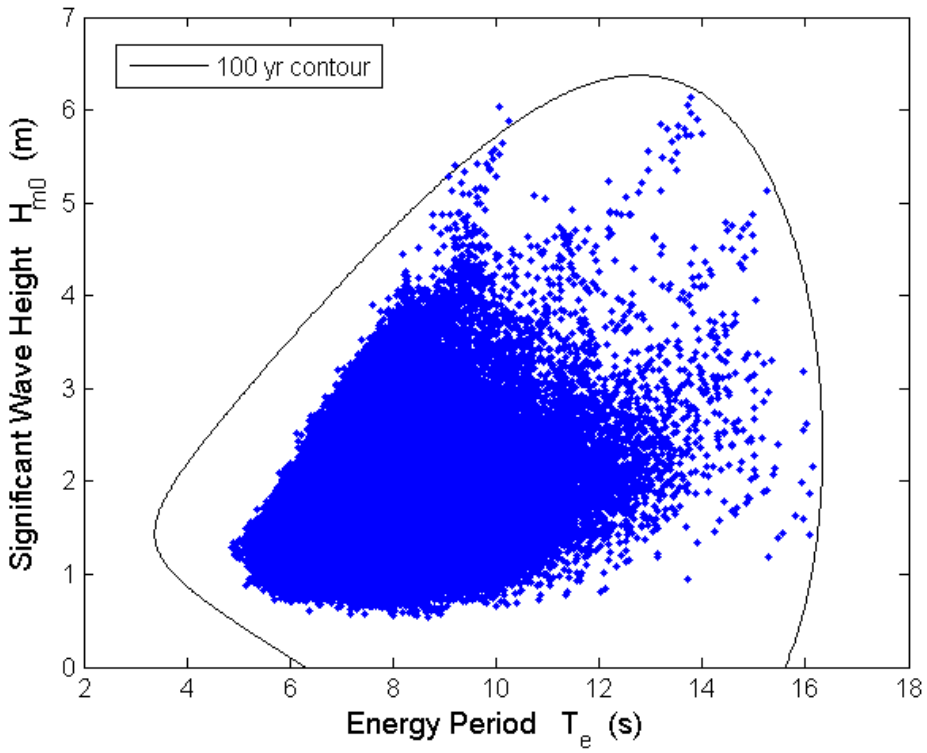

Figure 30. 100-year contour for CDIP098/NDBC51202 (2001-2012).

4.4.6. Representative Wave Spectrum

All hourly discrete spectra measured at CDIP198/NDBC51207 for the most frequently occurring sea states are shown in Figure 31. The most frequently occurring sea state, which is within the range 1.5 m < H_{m0} < 2 m and 6 s < T_e < 7 s, was selected from a JPD similar to Figure 22 in Section 4.4.1, but based on the CDIP198/NDBC51207 buoy data. As a result, the JPD, and therefore the most common sea states, generated from buoy data are slightly different from that generated from hindcast data. For example, the most frequently occurring sea state for the JPD generated from hindcast data is in the same range for T_e (6 s < T_e < 7 s), but a half-meter lower on bounds for H_{m0} (1 m < H_{m0} < 1.5 m). Often several sea states will occur at a very similar frequency, and therefore plots of hourly discrete spectra for several other sea states are also provided for comparison. Each of these plots includes the mean spectrum and standard wave spectra, including Bretschneider and JONSWAP, with default constants as described in Section 2.2.

For the purpose of this study, the mean spectrum is the 'representative' spectrum for each sea state, and the mean spectrum at the most common sea state, shown in Figure 31 (top-right plot), is considered the 'representative' spectrum at the site. The hourly spectra vary considerably about this mean spectrum, but this is partly reflective of the bin size chosen for H_{m0} and T_e. Comparisons of the representative spectra in all plots with the Bretschneider and JONSWAP spectra illustrate why modeled spectra with default constants, e.g., the shape parameter $\gamma = 3.3$ for the JONSWAP spectrum, should be used with caution. Using the constants provided in Section 2.2, the Bretschneider spectra are fair representations of the mean spectra in Figure 31. If these modeled spectra were to be used at this site, it is recommended that the constants undergo calibration against some mean spectrum, e.g., the representative spectrum constructed here.

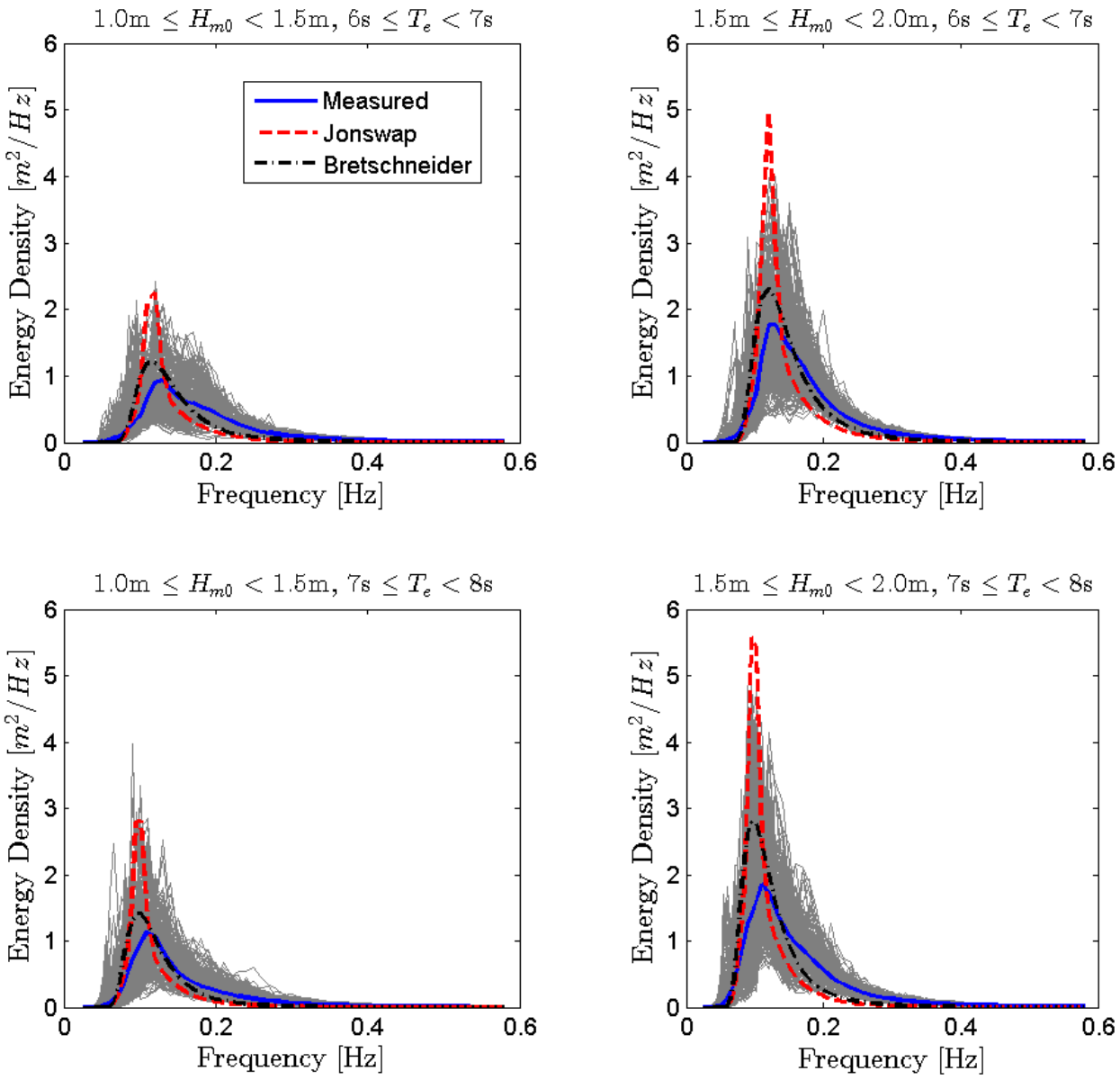

Figure 31. All hourly discrete spectra and the mean spectra measured at CDIP198/NDBC51207 within the sea state listed above each plot. The Bretschneider and JONSWAP spectra are represented by red and black dotted lines, respectively.

5. HUMBOLDT BAY, CALIFORNIA: POTENTIAL WEC TEST SITE

5.1. Site Description

For the purpose of this catalogue, the potential WEC site offshore of Humboldt Bay, referred to herein as the Humboldt Site, is located at 40.8418 N, 124.2477 W. As seen in Figure 32, the Humboldt Site lies in the footprint of the former Pacific Gas & Electric's (PG&E) pilot project test bed, the Humboldt WaveConnect (HWC), which was located in state waters to potentially ease permitting restrictions. PG&E considered this location for a WEC testing facility during the years 2008-2011 (Dooher et al. 2011). PG&E chose this test bed location based on numerous considerations, and the motivation for HWC's site placement is available in more detail in PG&E's Final Report (Dooher et al. 2011).

The Humboldt Site is approximately 9 km north/northwest of Humboldt Bay near the city of Eureka in Humboldt County, California (Figure 32). The site is at 45 m depth and lies over a sedimentary shelf consisting of sand and clay. As seen in Figure 33, the deployment site features a gently sloping seabed without many irregularities such as canyons that could disturb the local wave field (Dooher et al. 2011). The sediment and bathymetry are well suited for subsea cable burial and anchoring (Dooher et al. 2011).

The wave climate at the test site varies seasonally, with calmer seas in the summer compared to more energetic seas in the winter. The wave environment at the site is characterized by an annual average power flux of about 35 kW/m, including a number of events with significant wave heights exceeding 7 m each winter.

This site is the least developed site discussed in this catalogue, but it has the basic infrastructure needed to support WEC testing. The surrounding area offers port facilities, an electrical substation on shore, and an abundance of high quality met-ocean data.

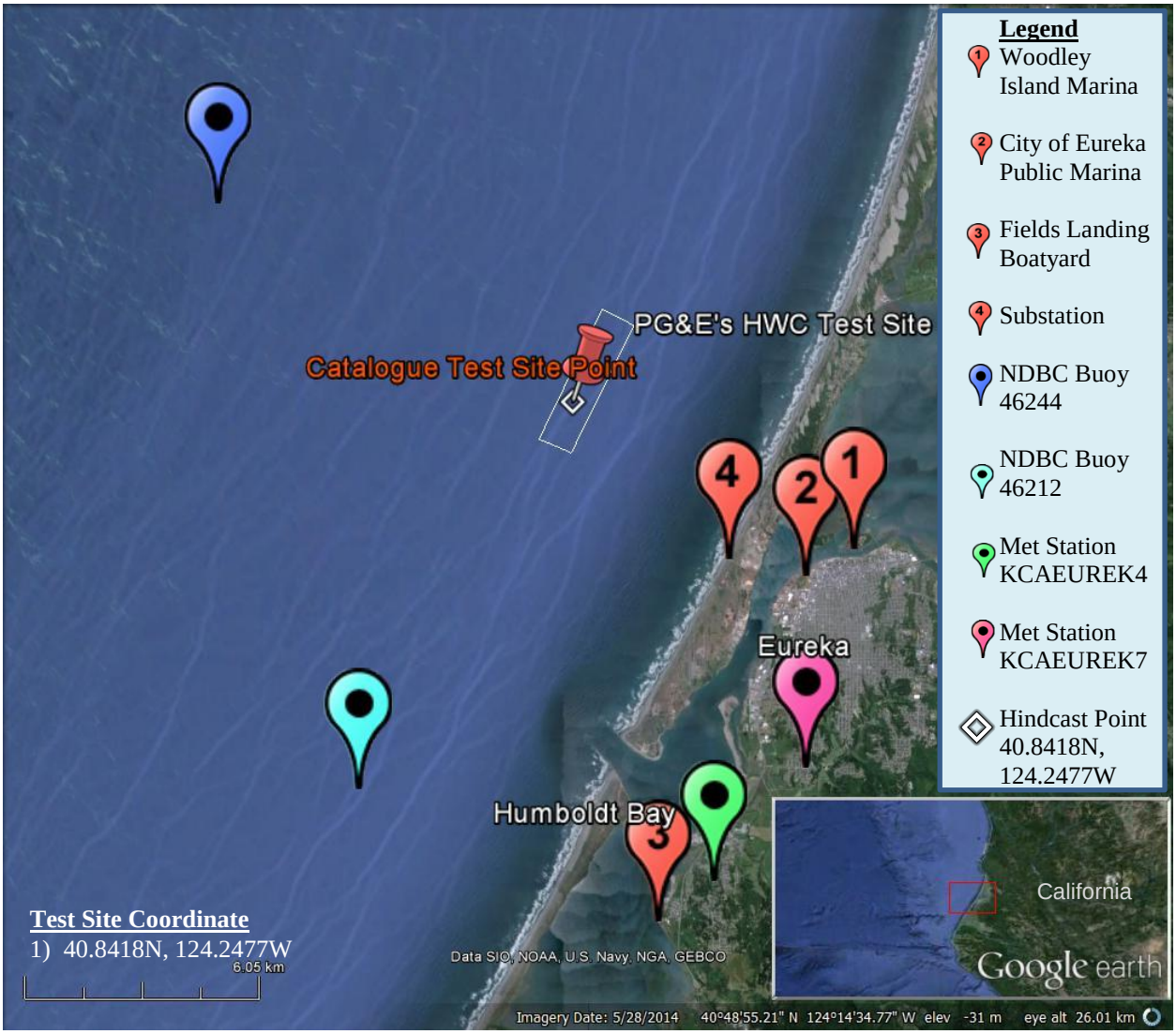

Figure 32. The proposed Humboldt Site is located on the coast of California near the city of Eureka. The test site is 5-6 km off-shore in 45 m depth water (~25 fathoms). No berthing or ocean infrastructure exist at this time. A future grid connection could be established at the existing substation. Two National Data Buoy Center (NDBC) ocean buoys and two National Weather Service (NWS) meteorological stations are close to the test site. The Woodley Island Marina and the City of Eureka Public Marina are located in Humboldt Bay and boatyard access is available at the Fields Landing Boatyard. The point of reference for the hindcast simulation is the primary coordinate for the proposed test site. Image modified from Google Earth (2014).

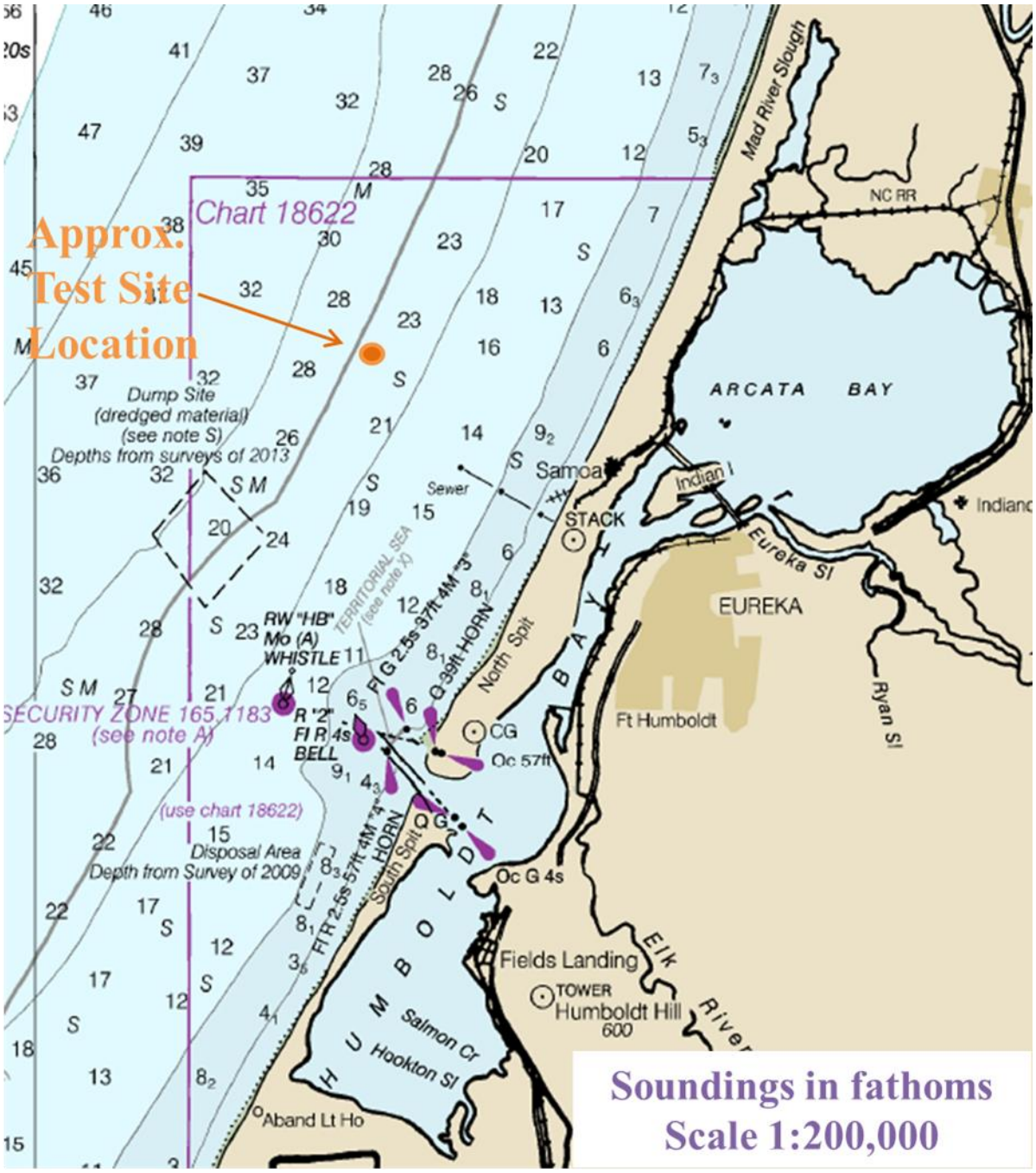

Figure 33. Nautical chart of Humboldt Bay and surrounding area shows the general bathymetry around the proposed test site. Sounds in fathoms (1 fathom = 1.8288 m). For a detailed map of Humboldt Bay, see Nautical chart #18622 (Office of Coast Survey 2013). Image modified from nautical chart #18620 (Office of Coast Survey 2012).

5.2. WEC Testing Infrastructure

5.2.1. Mooring Berths

As a potential test site, the Humboldt Site has no mooring berths installed or planned.

5.2.2. Electrical Grid Connection

There is currently no grid connection at the Humboldt Site. Future projects, however, may take advantage of the substation onshore directly landward of the test site (Waypoint #4 in Figure 32). The 60 kV PG&E Fairhaven Substation has three 60 kV lines connected to it, the highest of which accommodates 41 MW. The nearby former pulp mill facility also has a substation that interconnects to the same 60kV transmission lines and is capable of accommodating 30 MW.

5.2.3. Facilitating Harbor

The port nearest to the test site is located within Humboldt Bay, which is the only deep-water port on California's North Coast (Department of Transportation 2012). For boat mooring, there are two options in Humboldt Bay near the city of Eureka: the Woodley Island Marina (Waypoint #1 in) and the City of Eureka Public Marina (Waypoint #2 in Figure 32).

5.2.4. On-Shore Office Space

Humboldt Bay is situated by the city of Eureka. According to the U.S. census estimate, Eureka has a population of 26,000 residents in 2013. The Humboldt Bay Harbor Recreation and Conservation District recently acquired the site of the former Samoa pulp mill, located at 40.8061 N, 124.2003 W, which can serve as an onshore facility. The test site is approximately 6 km offshore from the pulp mill. The pulp mill is a large industrial facility with ~120,000 sqft of warehouse space, a machine building area with a 50-ton crane, an underutilized 30 MVA substation, and a dock (Redwood Terminal Berth #2) with quayside water depths ranging from 32-39 ft (9.8-11.9 m). The site also has office space and a large conference room.

5.2.5. Service Vessel and Engineering Boatyard Access

No dedicated service vessel is available at this time. Boats may be serviced at Fields Landing Boatyard (Waypoint #3 in Figure 32). This boatyard serves small to commercial-sized fishing boats with a travel lift. Repairs are made by the owner or hired external personnel. There may be companies such as Englund Marine & Industrial Supply Co. that can provide additional engineering services.

5.2.6. Travel and Communication Infrastructure

The Arcata/Eureka Airport services the Humboldt Bay area. The airport has several flights per day. Cellular phone service is available with moderate to full coverage.

5.2.7. Met-Ocean Monitoring Equipment

Real-time meteorological and wave data are collected by three met-ocean buoys and two meteorological stations. Instrument and data specifications for this monitoring equipment are summarized in Table 3. Buoy data is accessible online at the CDIP and NDBC databases. CDIP168 (NDBC46244) is operational and located approximately 8 km west of the test site. NDBC46022 (Figure 34 (a)), approximately 30 km southwest of the site, has been offline for repair and is expected to be operational in the fall of 2014. CDIP128 (NDBC46212) (Figure 34 (b)) is approximately 12 km from the test site, but was decommissioned in 2013. In addition to the met/ocean buoys, there are two land based meteorological stations located in Eureka, California.

Figure 34. (a) Discus buoy NDBC46022 located 30 km from site, (b) Waverider buoy CDIP128/NDBC46212 located 12 km south of test site (National Data Buoy Center 2014).

Table 3. Wave monitoring equipment in close proximity to the Humboldt proposed test site.

Instrument Name (Nickname)	CDIP128 / NDBC46212 - ("South Spit")		NDBC46022 (LLNR 500 / "Buoy 22")			CDIP168 / NDBC46244 - ("North Spit")		KCAEUREK4	KCAEUREK7
Type	Waverider Buoy		3-meter discus buoy			Waverider Buoy		Met station	Met station
Measured parameters	-std. met. data -spectral wave density data -spectral wave direction data		-std. met. data -continuous winds data -spectral wave density data -spectral wave direction data (only from 2007-2010)			-std. met data -spectral wave density data -spectra wave directional data		Meteorological data	Meteorological data
Variables reported, including derived variables (Sampling interval)	*Std. Met.:* WVHT DPD APD MWD WTMP (30 min)	-Spectral Wave Density -Spectral Wave Direction (30 min)	*Std. Met.:* WDIR WSPD GST WVHT DPD APD PRES ATMP WTMP (1 hr)	*Contin. Winds:* WDIR WSPD GDR GST GTIME (10 min)	-Spectral Wave Density -Spectral Wave Direction (1 hr)	*Std. Met:* WDIR WSPD GST WVHT DPD APD PRES ATMP WTMP (30 min)	-Spectral Wave Direction (30 min)	AirTemp DewPoint Pressure WDIR WSPD Humidity (5 min)	AirTemp DewPoint Pressure WDIR WSPD Humidity Precip (5 mins)
Location	12 km South of site, 6.5 km West of Humboldt Bay entrance		30 km West/Southwest of Test site			8 km West of Test Site		Humboldt Hill, Eureka, CA	Herrick Hill, Eureka, CA
Coordinates	40.753 N 124.313 W (40°45'12" N 124°18'48" W)		40.724 N 124.578 W (40°43'25" N 124°34'41" W)			40.888 N 124.356 W (40°53'18" N 124°21'22" W)		40.732 N 124.205 W (40° 43' 54'' N, 124° 12' 17'' W)	40.758 N 124.177 W
Depth	40 m		674.8 m			114 m		Elevation: 85 ft	Elevation: 102 ft
Data Start	1/22/2004		-wave data: 1982 -spectral wave data: 01/01/1996 -directional spectra: 06/01/2007			2/9/2010		3/7/2008	3/15/2011
Data End	4/3/2013		-11/13/2013 -dir. spectra ended 2/19/2010 -will be redeployed 8/2014			present		present	present
Period of Record	~9 yrs		-wave data: ~32 yrs -spectral data: ~18 yrs -directional spectra: ~4 yrs			~5.5 yrs		~6.5 yrs	~3.5 yrs
Owner / Contact Person	NOAA -- "Information Submitted by Scripps" http://cdip.ucsd.edu/?nav=recent&sub=observed&stn=128&xitem=info&stream=p1		National Data Buoy Center http://www.ndbc.noaa.gov/station_page.php?station=46022			NOAA-- "Information Submitted by Scripps" http://cdip.ucsd.edu/?ximg=search&xsearch=168&xsearch_type=Station_ID		National Weather Service; data download wundergroun d.com	National Weather Service; data download wundergro und.com

5.2.8. Environmental Monitoring

Environmental conditions have not been assessed at the Humboldt Site, and although some environmental studies were conducted as part of an environmental site assessment (ESA) for the HWC project site, the ESA was never completed (Dooher et al. 2011). PG&E partnered with Redwood Sciences Lab, Klamath Bird Observatory, and Humboldt State University (HSU) for their ESA related studies. Several ESA related studies reached completion including a marine life study conducted by Dr. Dawn Goley at HSU (Dooher et al. 2011: Appendix HSU E), a sediment dynamics study (Dooher et al. 2011: Appendix HSU C) and site placement in relation to local fishing economics study (Dooher et al. 2011: Appendix HSU D, Appendix HSU B). Future projects must further characterize the site and be responsible for environmental monitoring of the WEC device.

5.2.9. Permitting

The Humboldt Site has no federal, state or local permits to operate as a WEC test site. Future efforts to permit the Humboldt Site will require a substantial investment through the NEPA process, including outreach to various stakeholders, required permits for testing in California state waters, the development of an environmental impact report and monitoring, and adaptive management plans. The time required for this process is unknown and developers should be prepared for significant time uncertainty.

Although future projects must devote a significant effort to permitting at Humboldt Bay, developers can leverage the lessons learned from the HWC project site to ease the process. PG&E states in their report that they hope that their experiences may be informative for future test site developers and help future projects avoid some of the struggles they faced (Dooher et al. 2011). PG&E was issued preliminary permits for the HWC project site in 2008 through the Federal Energy Regulatory Commission (FERC), but a Pilot Project Licensing Process (PPLP) was never obtained (Dooher et al. 2011). Of all the obstacles, uncertainty regarding the expected impact of WEC devices on the environment was a major challenge in obtaining the permit. This uncertainty was partly due to the lack of specific information concerning WEC technologies to be tested at PG&E's site, and also the relative lack of understanding about the marine environment at the site. More information about PG&E's HWC project can be found in their final report, which is available from the Office of Science and Technical Information at http://www.osti.gov/scitech/biblio/1032845 (report ID 1032845).

5.3. Data used

Researchers at Sandia National Laboratories produced a 10 year hindcast dataset for the area offshore of Humboldt Bay, CA (Dallman et al. 2014). This dataset was used to calculate parameters of interest for the characterization at this site. The hindcast data at the grid point shown in Figure 35 was analyzed.

In addition to the hindcast data set, historical data from buoy CDIP128/NDBC46212 was used to calculate estimates of extreme events and representative spectra. As with the other sites, CFSR wind data and OSCAR current data were used.

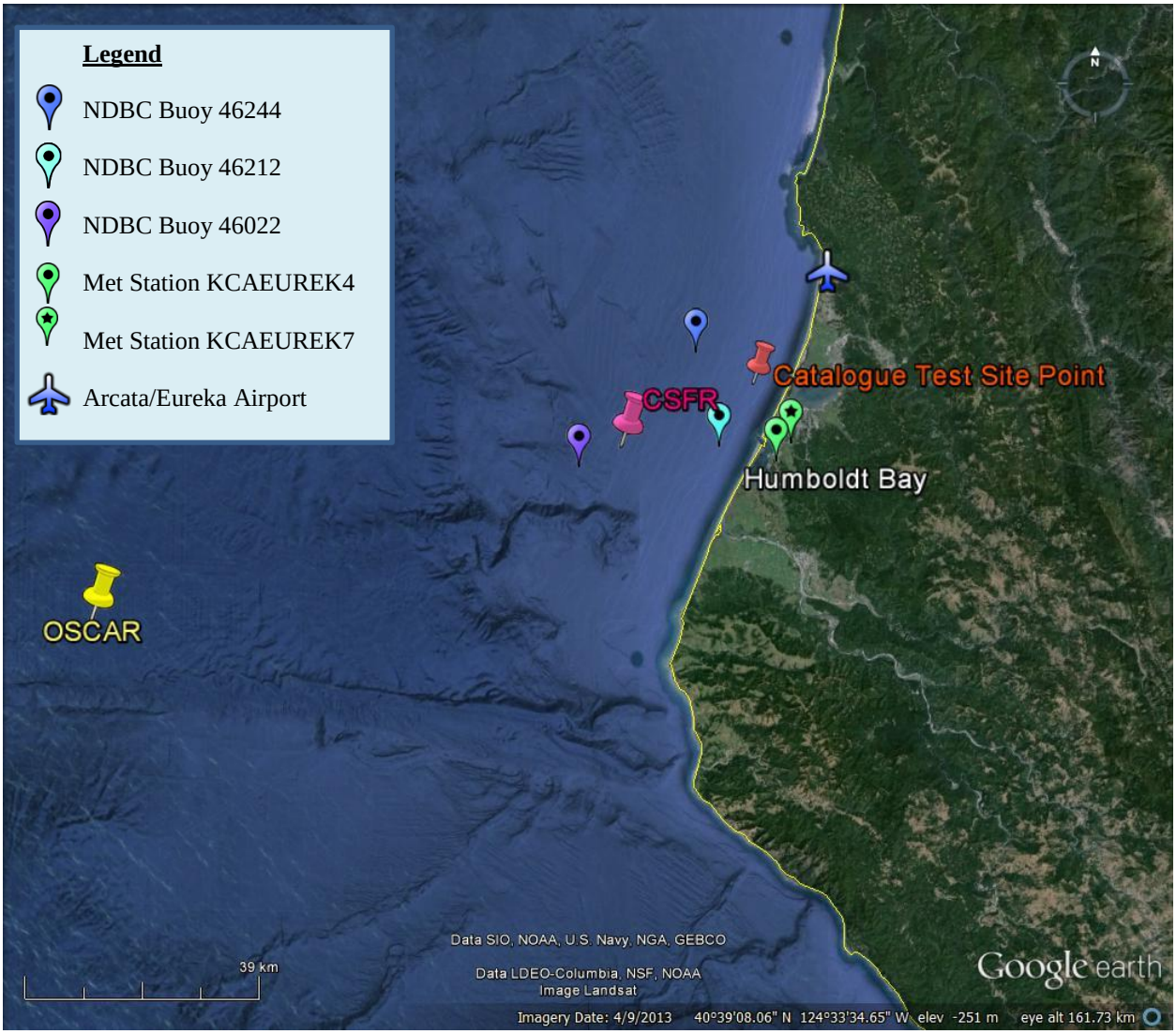

Figure 35. The catalogue test site location in relation to NDBC Buoys, OSCAR surface current data points, CSFR wind data points, and the nearest airport (Google Earth 2014).

5.4. Results

The following sections provide information on the joint probability of sea states, the variability of the IEC TS parameters, cumulative distributions, weather windows, extreme sea states, and representative spectra. This is supplemented by wave roses as well as wind and surface current data in Appendix C. The wind and surface current data provide additional information to help developers plan installation and operations & maintenance activities.

5.4.1. Sea States: Frequency of Occurrence and Contribution to Wave Energy

Joint probability distributions of the significant wave height, H_{m0}, and energy period, T_e, are shown in Figure 36. Figure 36 (top) shows the frequency of occurrence of each binned sea state and Figure 36 (bottom) shows the percentage contribution to the total wave energy. Figure 36 (top) indicates that the majority of sea states are within the range 1 m < H_{m0} < 3.5 m and 6 s < T_e < 11 s; but a wide range of sea states are experienced at the Humboldt Site, including extreme sea states caused by severe storms where H_{m0} exceeded 7 m. The site is well suited for testing WECs at various scales, including full-scale WECs, and testing the operation of WECs under normal sea states. This would also be a desirable site for commercial deployment. Although the occurrence of an extreme sea state for survival testing of a full scale WEC is unlikely during a normal test period, the Humboldt Site wave climate offers opportunities for survival testing of scaled model WECs.

As mentioned in the methodology (Section 2.2), previous studies show that sea states with the highest occurrence do not necessarily correspond to those with the highest contribution to total wave energy. The total wave energy in an average year is 302,200 kWh/m, which corresponds to an average annual omnidirectional wave power of 34.5 kW/m. The most frequently occurring sea state is within the range 1.5 m < H_{m0} < 2 m and 6 s < T_e < 7 s, while the sea state that contributes most to energy is within the range 3 m < H_{m0} < 3.5 m and 10 s < T_e < 11 s. Several sea states occur at a similar frequency, and sea states within 2 m < H_{m0} < 4.5 m and 9 s < T_e < 11 s contribute a similar amount to energy.

Frequencies of occurrence and contributions to energy of less than 0.01% are not shown in the figure for clarity. For example, the sea state within 0.5 m < H_{m0} < 1 m and 4 s < T_e < 5 s has an occurrence of 0.02%. The contribution to total energy, however, is only 0.001% and, therefore, does not appear in Figure 36 (bottom). Similarly, the sea state within 8 m < H_{m0} < 8.5 m and 13 s < T_e < 14 s has an occurrence of 0.007%, but the contribution to total energy is 0.11%.

Curves showing the mean, 5th and 95th percentiles of wave steepness, H_{m0}/λ, are also shown in Figure 36. The mean wave steepness at the Humboldt Site is 0.0185 (≈1/54), and the 95th percentile approaches 1/32.

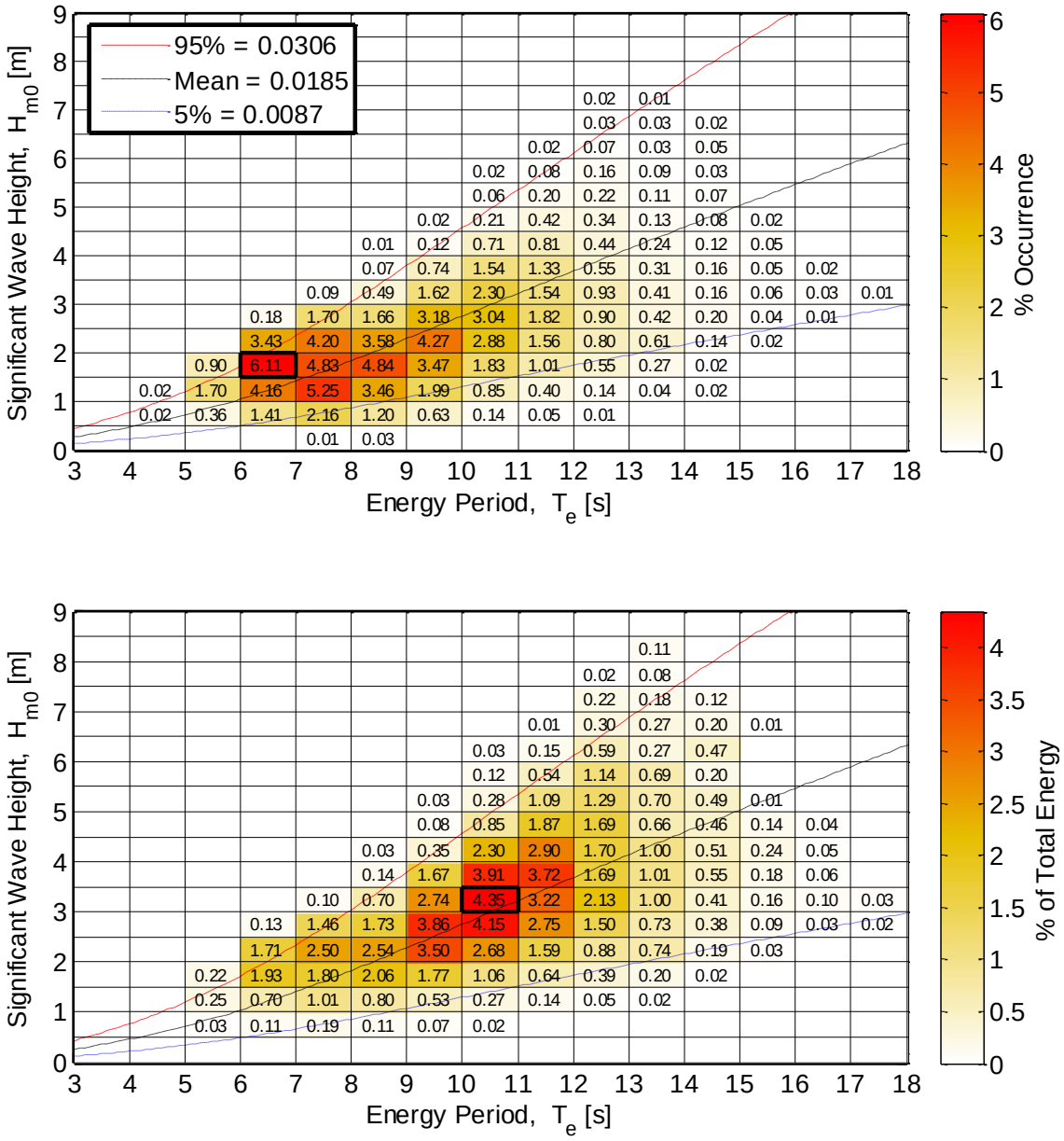

Figure 36. Joint probability distribution of sea states for the Humboldt Site. The top figure is frequency of occurrence and the bottom figure is percentage of total energy, where total energy in an average year is 302,200 kWh/m.

5.4.2. IEC TS Parameters

The monthly means of the six IEC TS parameters, along with the 5th and 95th percentiles, are shown in Figure 37. The values in the figure are summarized in Table 14 in Appendix C.

Monthly means of the omnidirectional wave power, J, significant wave height, H_{m0}, and energy period, T_e, show the greatest seasonal variability compared to the other parameters. Values are largest and vary the most during the winter months. These observations are consistent with the

relationship between wave power density, significant wave height and energy period, where wave power density, J, is proportional to the energy period, T_e, and the square of the significant wave height, H_{m0}.

The direction of maximum directionally resolved wave power (defined as the direction from which waves arrive in degrees clockwise from north), θ_j, is fairly consistent from west/northwest, and varies slightly between seasons. Seasonal variation of the spectral width, ϵ_0, and directionality coefficient (larger values indicate low directional spreading), is much less than the other parameters and barely discernable. Monthly means for ϵ_0 remain nearly constant between 0.3 and 0.35. Similarly, monthly means for d_θ remain nearly constant at ~0.93.

In summary, the waves at the Humboldt Site, from the perspective of monthly means, have a fairly consistent spectral width, are predominantly from the west/northwest, and exhibit a wave power that has a narrow directional spread.

Wave roses of wave power and significant wave height, presented in Appendix C, Figure 57 and Figure 58, also show the predominant direction of the wave energy at the Humboldt Site, with small shifts to the north and west. Figure 57 shows two dominant direction sectors from west/northwest: 285° and 300°. Along the first direction sector, 285°, the omnidirectional wave power density is at or below 35 kW/m approximately 18% of the time, and greater than 35 kW/m about 16% of the time. Along the second direction sector, 300°, the omnidirectional wave power density is at or below 35 kW/m approximately 26% of the time, but greater than 35 kW/m nearly 10% of the time.

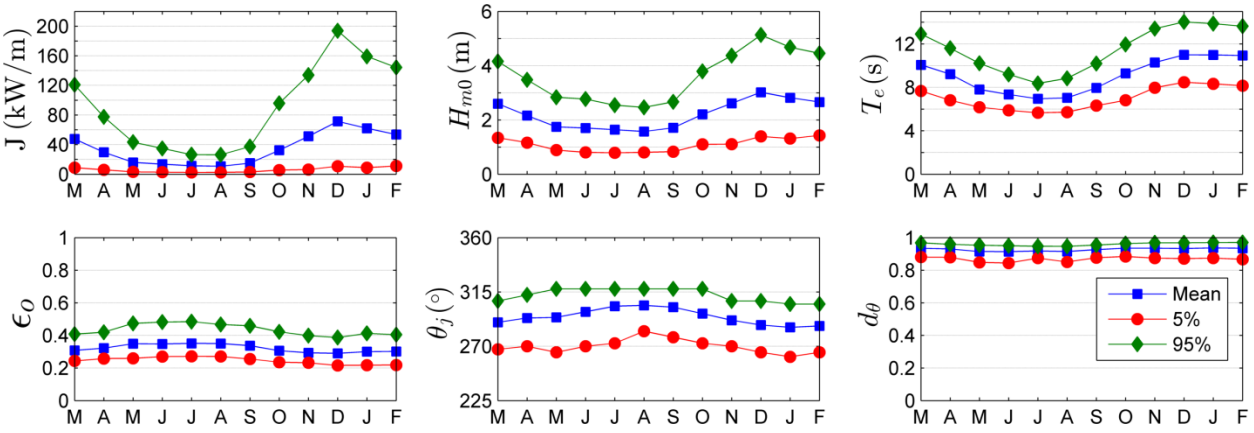

Figure 37. The average, 5th and 95th percentiles of the six parameters at the Humboldt Site.

Monthly means, however, smear the significant variability of the six IEC parameters over small time intervals as shown in plots of the parameters at 1-hour intervals in Figure 38 for a representative year. While seasonal patterns described for Figure 37 are still evident, these plots show how sea states can vary abruptly at small time scales with sudden changes, e.g., jumps in the wave power as a result of a storm.

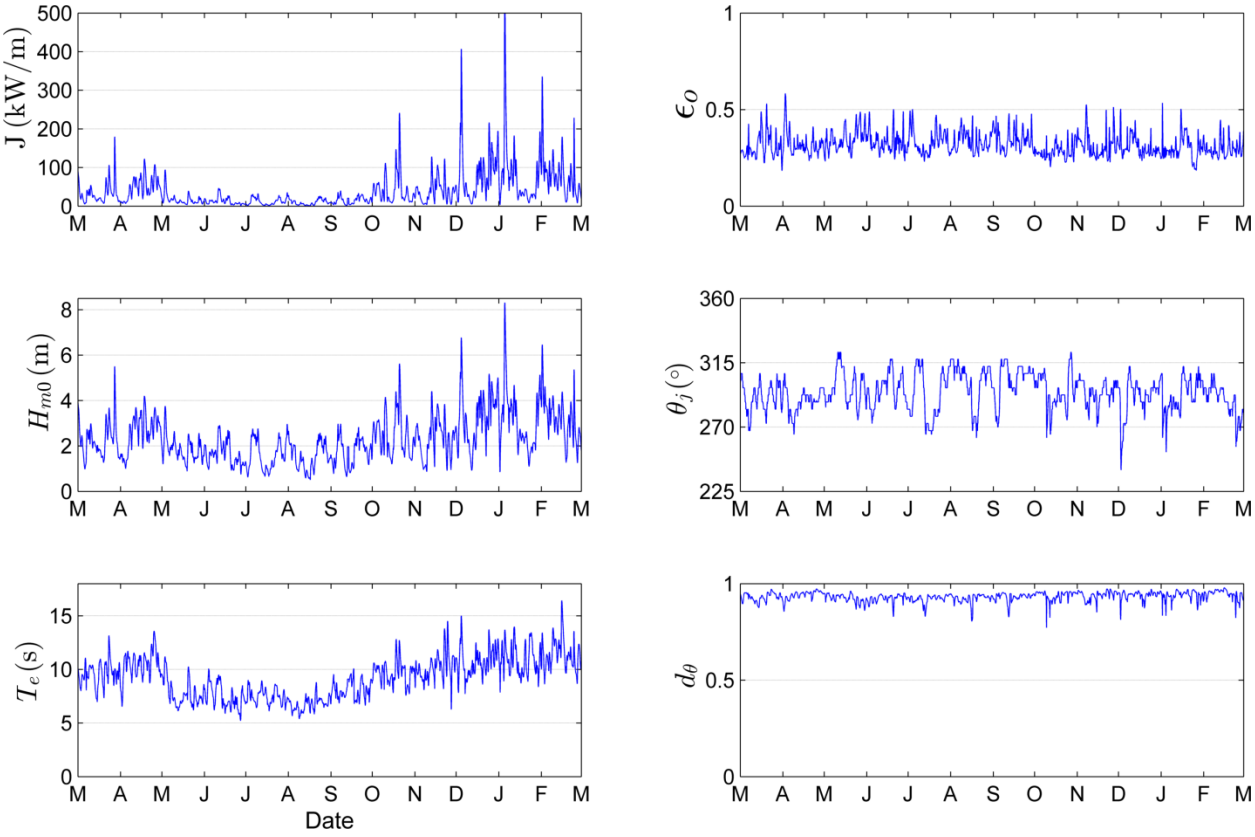

Figure 38. The six parameters of interest over a one-year period, March 2007 – February 2008 at the Humboldt Site.

5.4.3. Cumulative Distributions

Annual and seasonal cumulative distributions (a.k.a., cumulative frequency distributions) are shown in Figure 39. Note that spring is defined as March – May, summer as June – August, fall as September – November, and winter as December – February. The cumulative distributions are another way to visualize and describe the frequency of occurrence of individual parameters, such as H_{m0} and T_e. A developer could use cumulative distributions to estimate how often they can access the site to install or perform operations and maintenance based on their specific device, service vessels, and diving operation constraints. For example, if significant wave heights need to be less than or equal to 1 m for installation and recovery, according to Figure 39, this condition occurs about 6% of the time on average within a given year. If significant wave heights need to be less than or equal to 2 m for emergency maintenance, according to Figure 39, this condition occurs about 48% of the time on average within a given year. Cumulative distributions, however, do not account for the duration of a desirable sea state, or weather window, which is needed to plan deployment and servicing of a WEC device at a test site. This limitation is addressed with the construction of weather window plots in the next section.

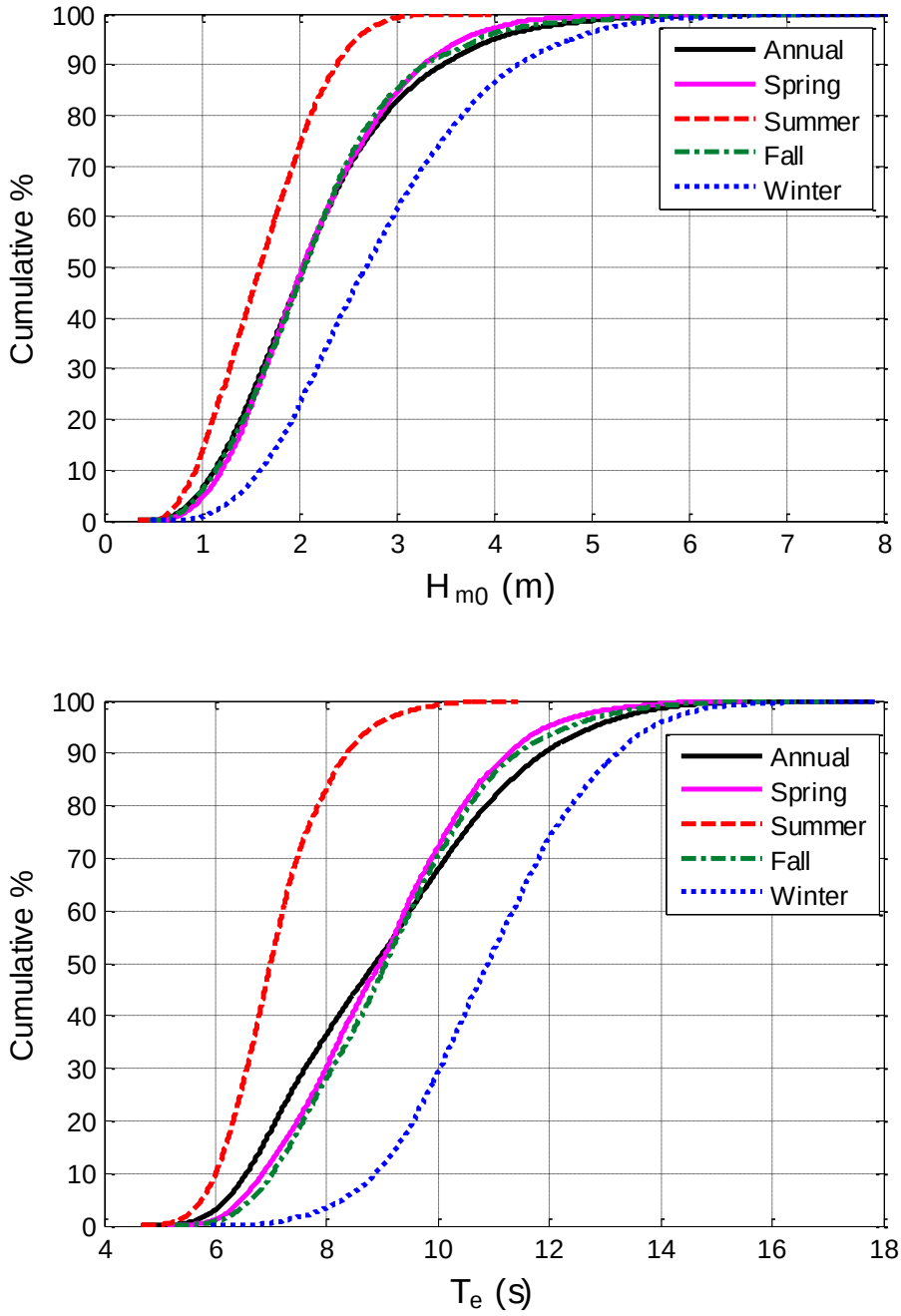

Figure 39. Annual and seasonal cumulative distributions of the significant wave height (top) and energy period (bottom) at the Humboldt Site.

5.4.4. Weather Windows

Figure 40 shows the number of weather windows at the Humboldt Site, when significant wave heights are at or below some threshold value for a given duration, for an averaged winter, spring, summer, and fall. In these plots, each occurrence lasts a duration that is some multiple of 6-hours. The minimum weather window is, therefore, 6-hours in duration, and the maximum is 96-hours (4 days). The significant wave height threshold is the upper bound in each bin and indicates the maximum significant wave height experienced during the weather window. Note that the table is cumulative, so, for example, an occurrence of $H_{m0} \leq 1\,m$ for at least 54 consecutive hours in the fall is included in the count for 48 consecutive hours as well. It is clear that there are significantly more occurrences of lower wave heights during the summer than winter, which corresponds to increased opportunities for deployment or operations and maintenance.

Weather window plots provide useful information at test sites when planning schedules for deploying and servicing WEC test devices. For example, if significant wave heights need to be less than or equal to 1 m for at least 12 consecutive hours to service a WEC test device at the Humboldt Site with a given service vessel, there would be, on average, twenty weather windows in the summer, but only one in the winter. When wind speed is also considered, Figure 41 shows the average number of weather windows with the additional restriction of wind speed, U<15 mph. Note that wind data was not available from the hindcast, so data from CFSR was used (see Section 2.3). For shorter durations (6- and 12-hour windows), daylight is necessary. Windows with U<15 mph and only during daylight hours are shown in Figure 42. Daylight was estimated as 5am – 10pm Local Standard Time (LST).

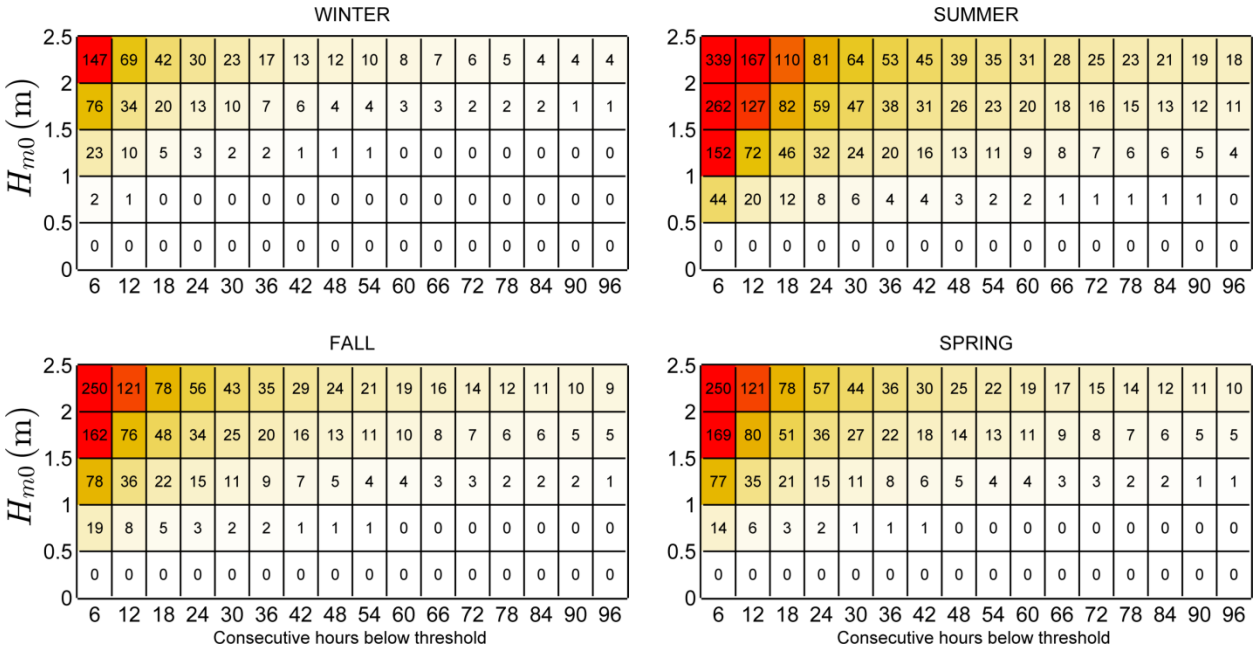

Figure 40. Average cumulative occurrences of wave height thresholds (weather windows) for each season at the Humboldt Site. Winter is defined as December – February, spring as March – May, summer as June – August, and fall as September – November.

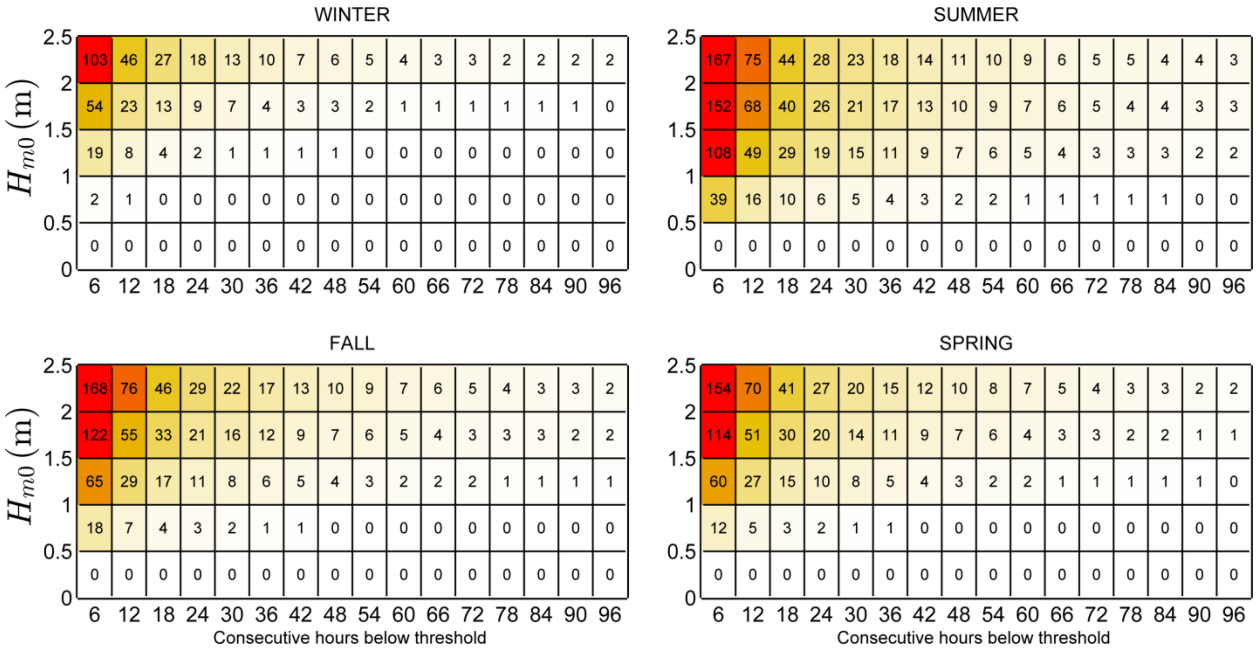

Figure 41. Average cumulative occurrences of wave height thresholds (weather windows) for each season at the Humboldt Site with an additional restriction of U < 15 mph.

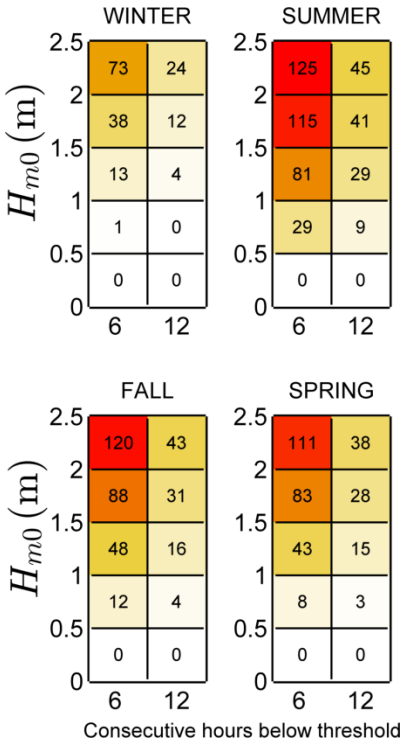

Figure 42. Average cumulative occurrences of wave height thresholds (weather windows) for 6- and 12-hour durations with U < 15 mph and only during daylight hours (5am – 10pm LST) at the Humboldt Site.

5.4.5. Extreme Sea States

The modified IFORM was applied using CDIP128/NDBC46212 to generate the 100-year environmental contour for the Humboldt Site shown in Figure 43. Selected sea states along this contour are listed in Appendix C, Table 15. As stated in Section 1.2, environmental contours are used to determine extreme wave loads on marine structures and design these structures to survive extreme sea states of a given recurrence interval, typically 100-years. For the Humboldt Site, the largest significant wave height estimated to occur every 100-years, is approximately 10.5 m, and has an energy period of about 17.7 s. However, significant wave heights lower than 10.5 m, with energy period less than or greater than 17.7 s, listed in Appendix C, Table 15, could also compromise the survival of the WEC test device under a failure mode scenario in which resonance occurred between the incident wave and WEC device, or its subsystem. For comparison, a 50-year return period results in a similar contour where the largest significant wave height is over 10.0 m with an energy period of about 17.3 s. A 25-year return period also results in a similar contour where the largest significant wave height is 9.6 m with an energy period of about 17.0 s.

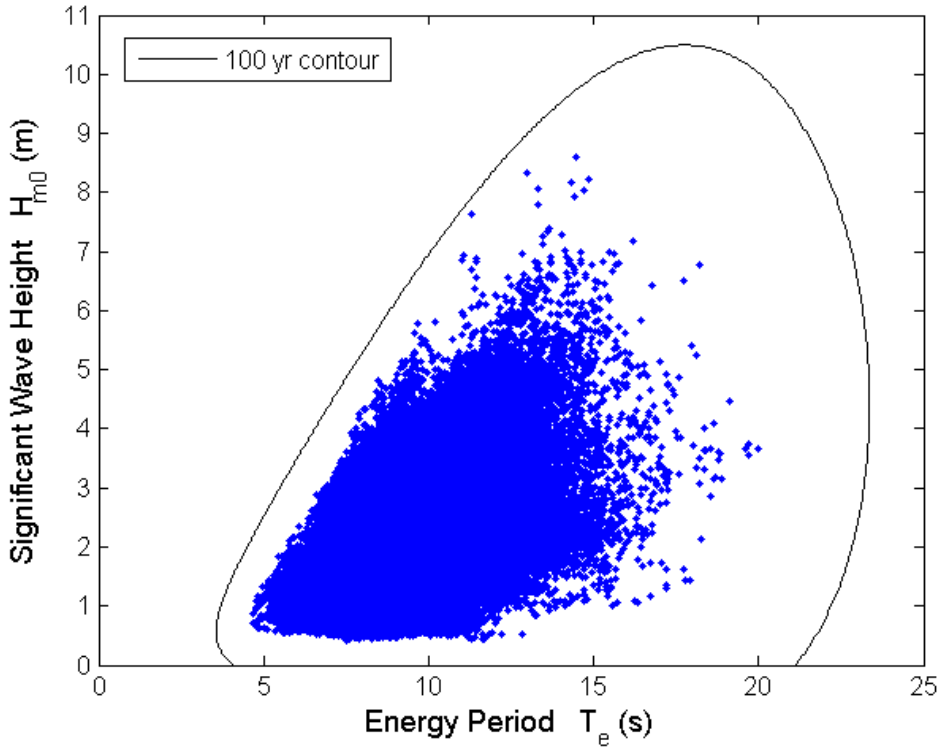

Figure 43. 100-year contour for CDIP128/NDBC46212 (2004-2012).

5.4.6. Representative Wave Spectrum

All hourly discrete spectra measured at CDIP128/NDBC46212 for the most frequently occurring sea states are shown in Figure 44. The most frequently occurring sea state, which is within the range 1 m < H_{m0} < 1.5 m and 7 s < T_e < 8 s, was selected from a JPD similar to Figure 36 in Section 5.4.1, but based on the CDIP128/NDBC46212 buoy data. As a result, the JPD, and therefore the most common sea states, generated from buoy data are slightly different from that generated from hindcast data. For example, the most frequently occurring sea state for the JPD generated from hindcast data is a half-meter higher on bounds for H_{m0} (1.5 m < H_{m0} < 2 m) and one second lower for T_e (6 s < T_e < 7 s). Often several sea states will occur at a very similar frequency, and therefore plots of hourly discrete spectra for several other sea states are also provided for comparison. Each of these plots includes the mean spectrum and standard wave spectra, including Bretschneider and JONSWAP, with default constants as described in Section 2.2.

For the purpose of this study, the mean spectrum is the 'representative' spectrum for each sea state, and the mean spectrum at the most common sea state, shown in Figure 44 (bottom-left plot), is considered the 'representative' spectrum at the site. The hourly spectra vary considerably about this mean spectrum, but this is partly reflective of the bin size chosen for H_{m0} and T_e. Comparisons of the representative spectra in all plots with the Bretschneider and JONSWAP spectra illustrate why modeled spectra with default constants, e.g., the shape

parameter $\gamma = 3.3$ for the JONSWAP spectrum, should be used with caution. Using the constants provided in Section 2.2, the Bretschneider spectra are, at best, fair representations of the mean spectra in Figure 14. If these modeled spectra were to be used at this site, it is recommended that the constants undergo calibration against some mean spectrum, e.g., the representative spectrum constructed here.

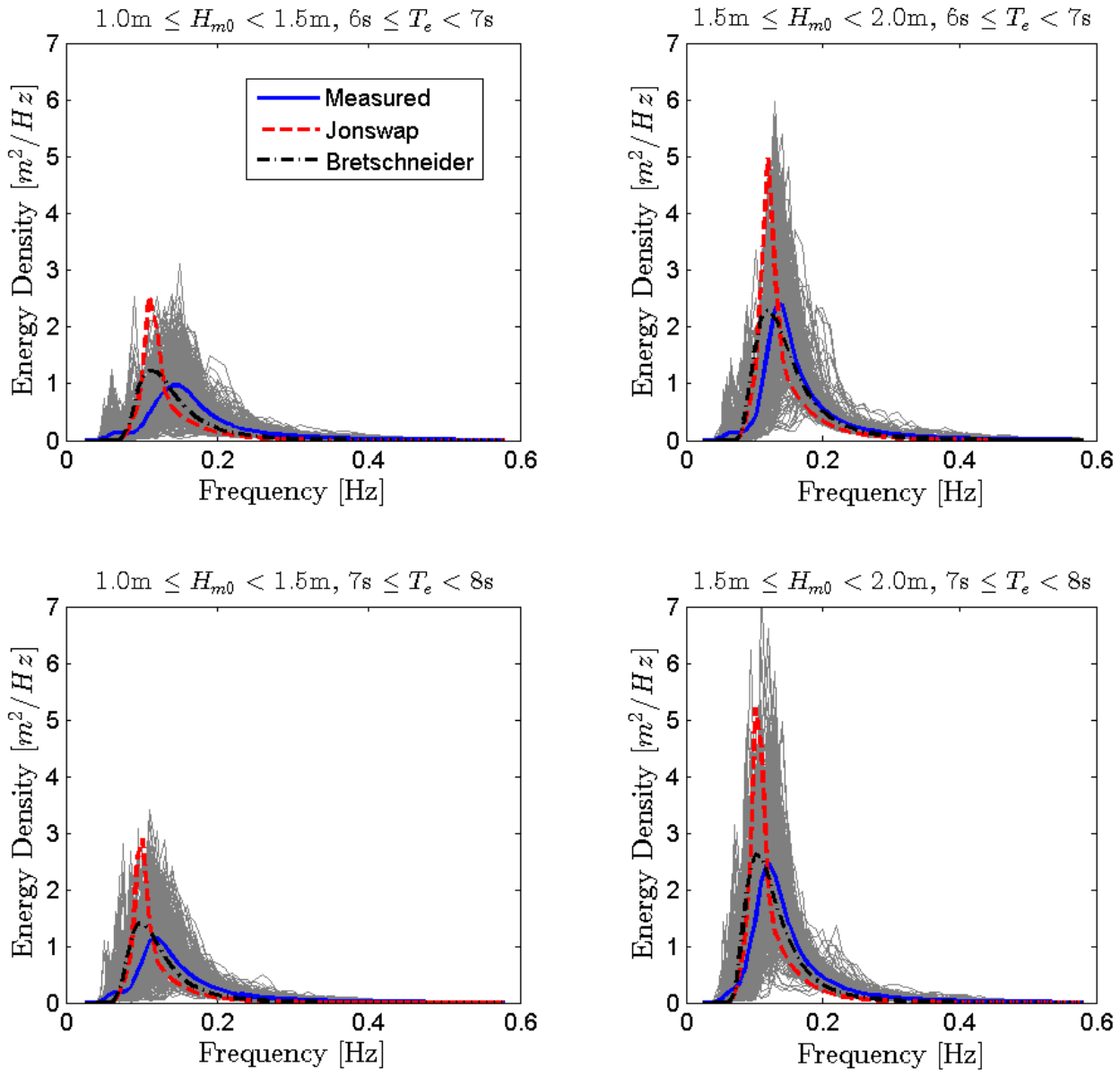

Figure 44. All hourly discrete spectra and the mean spectra measured at CDIP128/NDBC46212 within the sea state listed above each plot. The Bretschneider and JONSWAP spectra are represented by red and black dotted lines, respectively.

6. SUMMARY AND CONCLUSIONS

This study achieves a comprehensive characterization of three U.S. WEC test sites. It provides important information on test site infrastructure and services, and catalogues detailed met-ocean data and information derived from numerous data sources. Although there are some differences in the quality of the data sources, e.g., the location of the buoy observations with respect to the test site, and the period of record of the hindcast or buoy observations, the data are processed using uniform and consistent methods. The characterization results, therefore, allow reasonable comparisons between the wave resource characteristics among the different test sites, and selection of test sites that are most suitable for a given device or current testing needs and objectives.

Plots useful for designing WEC test devices include the JPDs, seasonal variation of the six IEC bulk parameters, representative wave spectra, and environmental contours (extreme sea states). They also provide a useful and comprehensive summary of the wave climate and wave energy resource. Cumulative distributions and weather windows can aid in planning WEC deployments and servicing schedules based on the requirements of the service vessel.

The characterization results also allow assessment of the opportunities and risks of testing at each site, how they vary seasonally, and how they can change abruptly within a matter of hours or days. Large waves, associated with both normal and extreme sea states, provide opportunities for testing full scale WEC devices, but they can increase the challenges and risks of testing at the site. These include reduced access to the test device, for deployment or operation and maintenance, and increased risk of damaging or destroying the test device.

NETS is a test site offshore of Newport, OR, where the average annual omnidirectional wave power is 36.8 kW/m. The wave climate at the site varies significantly by season. Calmer seas (lower significant wave heights and energy periods) occur in the summer, while energetic seas occur in the winter, dominated by swells further away in the North Pacific. Larger wave heights occur in the winter months, with a number of events each year exceeding 7 m, and some severe storms producing significant wave heights over 10 m.

WETS is a test site offshore of Oahu, HI, where the average annual omnidirectional wave power is nearly 13 kW/m at the 80 m berth. The wave climate varies seasonally, but with less variability than the Pacific Northwest. Calmer seas occur during the summer, produced by year-round trade winds from the northeast, while more energetic seas occur in the winter made up of both wind waves and swell from the North Pacific. Year-round testing has been done at the site because significant wave heights rarely exceed 3 m in the winter.

The Humboldt Site is a potential test or commercial deployment site, where the average annual omnidirectional wave power is 34.5 kW/m. Similarly to NETS, the wave climate varies significantly by season with calmer wind waves in the summer and much more energetic seas dominated by swell in the winter. A small percentage of sea states exceed 7 m each winter. Among all the sites, the Humboldt Site exhibits the most unidirectional waves.

The NETS and Humboldt sites exhibit similar wave characteristics. The average annual omnidirectional wave power at NETS and Humboldt is approximately three times higher than that at WETS, and seasonal variations are more pronounced. Winter storms are much more severe at NETS and Humboldt, with significant wave heights exceeding 5 m approximately 5% of the time in December.

Wave direction at each site generally does not align with the local wind direction because the waves are associated with swells and far-field winds, and they tend to align with the bathymetric contours as they approach shore. However, at each site there is a slight shift towards the wind direction in the summer when swells are less dominant. The local wind data is important for servicing, and is incorporated into the weather windows. It may also be important for determining loads on a low-draft device with a significant above-water profile.

The monthly mean surface currents at all sites are below 0.1 m/s, well below the IEC TS value of 1.5 m/s for depth-averaged current speed, which is recommended as the threshold beyond which it is important to account for ocean current effects in wave modeling. As surface currents are generally higher than depth-averaged currents, ocean currents at all three sites are not expected to significantly influence the wave dynamics.

Plans are underway to catalogue wave characteristics at additional WEC test sites over the next year, including Tier 1 test sites, where there is ample and high-quality observed data and validated hindcast model simulation data, as well as Tier 2 test sites, where data are relatively less comprehensive and of lower quality, but the sites have the potential to be of value to the WEC industry.

7. REFERENCES

Batten, Belinda. E-mail correspondence to Director of Northwest National Marine Renewable Energy Center, July 24 – September 9, 2014.

Batten, Belinda. Monitoring at North Ocean Test Site, Newport OR. [Powerpoint slides], 2013. Retreived from Tethys: http://tethys.pnnl.gov/sites/default/files/attachments/2013-04-09%201%20Belinda%20Batten.pdf.

Berg, J.C., *Extreme Ocean Wave Conditions for Northern California Wave Energy Conversion Device*, SAND 2011-9304. Sandia National Laboratories, Albuquerque, NM, 2011.

Bitner-Gregersen, E.M, 2001, *Extreme Wave Steepness Estimated from Environmental Contour Plots Contra Traditional Design Practice*, Proceedings of the 20th International Conference on Offshore Mechanics and Arctic Engineering, Rio de Janeiro, Brazil.

Cahill, B.G., and Lewis, A.W., 2011, *Wave Energy Resource Characterization of the Atlantic Marine Energy Test Site*. Proceedings of the 9th European Wave and Tidal Energy Conference, Southampton, United Kingdom.

Cahill, B.G., and Lewis, A.W., 2013 *Wave energy resource characterization of the Atlantic Marine Energy Test Site*, International Journal of Marine *Energy* 1, 3-15 p.

Chakrabarti, S.K., 1987, *Hydrodynamics of offshore structures*. WIT Press / Computational Mechanics, UK / Germany.

Coastal Data Information Program, "Station 198- Kaneohe Bay, HI." Photo taken November 18, 2013. http://cdip.ucsd.edu/?nav=historic&sub=data&units=metric&tz=UTC&pub=public&stn=198&stream=p1&xitem=stn_gallery3.

Coastal Data Information Program, "Station 098- Mokapu Point, HI." Photo taken November 18, 2013. http://cdip.ucsd.edu/?ximg=search&xsearch=098&xsearch_type=Station_ID.

Dallman, A.R., Neary, V.S., Stephenson, M., *Investigation of Spatial Variation of Sea States Offshore of Humboldt Bay, CA Using a Hindcast Model*, SAND2014-18207. Sandia National Laboratories, Albuquerque, NM, 2014.

Davey, T., Venugopal, V., Smith, H., Smith, G., Lawrence, J., Luigi, C., Bertotti, L., Prevosto, M., Girard, F., Holmes, B., *EquiMar D2.7 Protocols for wave and tidal resource assessment*, December 2010.

Department of the Navy, *Wave Energy Test Site: Final Environmental Assessment*, Prepared by Alan Suwa, Caroleen Toyama, Jeffrey Fong, Jackie Sanehira, Sean Hanser, Kate Winters, Justin

Fujimoto, T.A.F.,Thomas A. Fee, Gail Renard, Corlyn Olson Orr and John Clark, Marine Corps Base Hawaii: January 2014.

De Visser, A., and Vega, L.A., "*Wave Energy Test Site*," Proceedings of the 7th Annual Global Marine Renewable Energy Conference, April 15-18, 2014.

Det Norske Veritas, 2005, *Guidelines on design and operation of wave energy converters.* Det Norske Veritas, The Carbon Trust, 2005.

Det Norske Veritas, 2014, *Environmental Conditions and Environmental Loads.* Recommended Practice DNV-RP-C205.

Department of Transportation, 2012, *Port of Humboldt Bay*, Freight Planning Fact Sheet for Caltrans. http://dot.ca.gov/hq/tpp/offices/ogm/CFMP/Fact_Sheets/Seaports/Humboldt.pdf.

Dooher, B.P., Cheslak, E., Booth, R., Davy, D., Faraglia, A., Caliendo, I. Morimoto, G. and Herman, D. 2011, *PG&E WaveConnect Program Final Report*. DOE/GO/18170-1. Pacific Gas and Electric Company, San Francisco, CA, December 2011. doi: 10.2172/1032845.

Eckert-Gallup, A.C., Sallaberry, C.J., Dallman, A.R., Neary, V.S., *Modified Inverse First Order Reliability Method (I-FORM) for Predicting Extreme Sea State Estimation*, SAND2014-17550. Sandia National Laboratories, Albuquerque, NM, September 2014.

Feld, G., Mork, G., 2004, *A Comparison of Hindcast and Measured Wave Spectra Based on a Directional Spectral Fitting Algorithm*, Proceedings of the 8th International Workshop on Wave Hindcasting & Forecasting, North Shore, Oahu, HI, November 14-19.

Folley, M., Cornett, A., Holmes, B., Lenee-Bluhm, P., Liria, P., 2012, *Standardising resource assessment for wave energy converters*, Proceedings of the 4th Annual International Conference on Ocean Energy, Dublin.

García–Medina, G., Özkan-Haller, H.T., Ruggiero, P., 2014, *Wave resource assessment in Oregon and southwest Washington, USA*, Renew Energy 64, 203-214 p.

Google Earth, *Humboldt Bay*, 41°00'07.85" N 124°16'03.18" W. Data from SIO, NOAA, U.S. Navy, NGA, GEBCO, LDEO-Columbia, NSF. Image from Landsat. Accessed July 16, 2014.

Google Earth, *Newport, OR*, 44°50'37.26"N 124°12'15.47"W. Data from SIO, NOAA, U.S. Navy, NGA, GEBCO, MBARI, LDEO-Columbia, NSF. Image from Landsat. Accessed July 16, 2014.

Google Earth, *Newport, OR*, 44°50'37.26"N 124°12'15.47"W. Data from SIO, NOAA, U.S. Navy, NGA, GEBCO. Image from DigitalGlove. Accessed July 16, 2014.

Google Earth, *Kaneohe Bay*, 21°27'50.53" N 157°44'19.06"W. Data from USGS. Image from USGS. Accessed July 16, 2014.

Hasselmann, K., Barnett, T.P., Bouws, E., Carlson H., Cartwright D.E., Enke, K., Ewing J.A., Gienapp, H., Hasselmann, D.E., Kruseman, P., Meerburg, A., Müller, P., Olbers, D.J., Richter, K., Sell, W., Walden, H., 1973, *Measurements of Win-Wave Growth and Swell Decay During the Joint North sea Wave Project (JONSWAP)*, Deutschen Hydro-graphischen Institut, No. 12, Hamburg, Germany.

Hawaii National Marine Renewable Energy Center, "Kaneohe Site." April 25, 2013. Accessed July 14, 2014. http://hinmrec.hnei.hawaii.edu/.

Johnson, E.S., F. Bonjean, G.S.E. Lagerloef, J.T. Gunn, and G.T. Mitchum, 2007, *Validation and Error Analysis of OSCAR Sea Surface Currents*. Journal of Atmospheric and Oceanic Technology 24, 688–701 p. doi: 10.1175/JTECH1971.1.

Jouanne, Annette von, Lettenmaier, Terry, and Sean Moran, *Wave Energy Testing Using the Ocean Sentinel Instrumentation Buoy*. Presented at the 1st Marine Energy Technology Symposium, Washington, DC, April 10-11, 2013. http://www.globalmarinerenewable.com/images/wave%20energy%20testing%20using%20the%20ocean%20sentinel%20instrumentation%20buoy.pdf.

Lenee-Bluhm, P., Paasch, R., Özkan-Haller, H.T., 2011, *Characterizing the wave energy resource of the US Pacific Northwest*. Renew Energy 36, 2106-2119 p.

Lenee-Bluhm, P., 2010, *The Wave Energy Resource of the US Pacific Northwest*, MS Thesis, Oregon State University, http://ir.library.oregonstate.edu/xmlui/handle/1957/16384.

Li, N. and Cheung, K.F., 2014, *Wave Energy Resource Characterization at WETS*. Technical Report August 2014. http://hinmrec.hnei.hawaii.edu/.

National Data Buoy Center, "Station 46094: West of Newport NH-10, OR" http://www.ndbc.noaa.gov/station_page.php?station=46094.

National Data Buoy Center, "Station NWPO3: Newport, OR" http://www.ndbc.noaa.gov/station_page.php?station=NWPO3.

National Data Buoy Center, "Station 46212: Humboldt Bay South Spit, CA (128)" http://www.ndbc.noaa.gov/station_page.php?station=46212.

National Data Buoy Center, "Station 46022 (LLNR 500)- Eel River – 17 NM WSW of Eureka, CA" http://www.ndbc.noaa.gov/station_page.php?station=46022.

National Data Buoy Center, "Station MOKH1 – 1612480 – Mokuoloe, HI" http://www.ndbc.noaa.gov/station_page.php?station=mokh1.

National Data Buoy Center, "Station 51202 – Mokapu Point, HI (098)" http://www.ndbc.noaa.gov/station_page.php?station=51202.

National Data Buoy Center, "Station 51207 – Kaneohe Bay, HI (198)" http://www.ndbc.noaa.gov/station_page.php?station=51207.

National Oceanic Atmospheric Administration, "OSCAR: Ocean Surface Current Analysis- Real Time". Accessed June 26, 2014. http://www.oscar.noaa.gov/index.html.

NNMREC (Northwest National Marine Renewable Energy Center), Oregon State University. "Northwest National Marine Renewable Energy Center." Accessed July 14th, 2014. http://nnmrec.oregonstate.edu/.

O'Connor, M, Holmes, B., *EquiMar D4.3 Test Sites Catalogue*, April 2011.

Oregon State University, "Northwest National Marine Renewable Energy Center." Accessed July 14, 2014. http://nnmrec.oregonstate.edu/pmec-facilities.

Port of Newport. "South Beach Marina." Accessed July 28, 2014. http://www.portofnewport.com/recreational-marina/.

Port of Toledo, "Yaquina Boatyard." Accessed July 24, 2014. http://portoftoledo.org/yaquina-boatyard/.

State of Hawaii Division of Boating and Ocean Recreation, "Heeia Kea Small Boat Harbor." Accessed July 21, 2014. http://state.hi.us/dlnr/dbor/oahuharbors/heeiahrbr.htm.

Office of Coast Survey, *Chart 19357*. National Ocean and Atmospheric Association, printed March 1, 2013, accessed August 1, 2014. HTTP://WWW.NAUTICALCHARTS.NOAA.GOV/STAFF/CHARTSPUBS.HTML.

Office of Coast Survey, *Chart 18620*. National Ocean and Atmospheric Association, printed February 1, 2012, accessed August 1, 2014. http://www.nauticalcharts.noaa.gov/staff/chartspubs.html.

Office of Coast Survey, *Chart 18622*. National Ocean and Atmospheric Association, printed June 1, 2010, accessed August 1, 2014. http://www.nauticalcharts.noaa.gov/staff/chartspubs.html.

Office of Coast Survey, *Chart 18561*., National Ocean and Atmospheric Association, printed December 1, 2011, accessed August 1, 2014. http://www.nauticalcharts.noaa.gov/staff/chartspubs.html.

U.S. Census Bureau, *Newport (city) Oregon*, State & County QuickFacts, 2012. Retrieved from http://quickfacts.census.gov/qfd/states/41/4152450.html.

Saha, Suranjana, and Coauthors, 2010: *The NCEP Climate Forecast System Reanalysis*. Bull. Amer. Meteor. Soc., 91, 1015-1057 p. doi: 10.1175/2010BAMS3001.1

Saha, Suranjana and Coauthors, 2014: *The NCEP Climate Forecast System Version 2*. J. Climate, 27, 2185-2208 p. doi: http://dx.doi.org/10.1175/JCLI-D-12-00823.1

Stopa, J.E., Filipot, J.-F., Li, N., Cheung, K.F., Chen, Y.-L., Vega, L., 2013, *Wave energy resources along the Hawaiian Island chain*, Renew Energy 55, 305-321 p.

Winterstein, S.R., Ude, T.C., Cornell, C.A., Bjerager, P., Haver, S., *Environmental Parameters for Extreme Response: Inverse FORM with Omission Factors*, Proceedings of ICOSSAR-93, Innsbruck, Austria, 1993.

Vega, Luis: University of Hawaii, e-mail correspondence, July 23 – August 29, 2014.

DISTRIBUTION

1	MS1124	Ann R. Dallman	6122
1	MS1124	Vincent S. Neary	6122
1	MS0899	Technical Library	9536 (electronic copy)

APPENDIX A: NETS

A.1. IEC TS Parameter Values

Table 4. The average, 5th and 95th percentiles of the six parameters at NETS (see Figure 7).

	$J\ [kW/m]$			$H_{m0}\ [m]$			$T_e\ [s]$		
	5%	**Mean**	**95%**	**5%**	**Mean**	**95%**	**5%**	**Mean**	**95%**
March	9.4	52.2	141.6	1.46	2.86	4.75	7.65	9.92	12.80
April	6.5	36.8	96.3	1.16	2.39	4.03	7.65	9.75	12.04
May	3.6	16.1	42.1	0.87	1.71	2.84	7.01	8.76	10.84
June	3.7	12.2	33.6	0.88	1.52	2.68	6.89	8.84	11.39
July	2.3	9.3	19.0	0.73	1.39	2.05	6.72	8.41	10.46
August	2.8	8.7	20.5	0.83	1.33	2.09	6.60	8.45	10.70
September	4.3	18.1	52.7	0.98	1.74	3.04	7.37	9.31	11.78
October	7.8	38.5	106.5	1.26	2.43	4.19	7.86	9.79	12.28
November	9.1	62.4	162.8	1.35	3.09	5.10	7.75	10.05	12.90
December	8.6	69.3	203.0	1.25	3.13	5.45	8.12	10.66	13.95
January	11.3	66.6	173.5	1.43	3.08	5.06	8.19	10.88	14.13
February	11.1	52.4	141.4	1.43	2.77	4.70	8.24	10.70	13.44

	ϵ_0			$\theta_j\ [°]$			d_θ		
	5%	**Mean**	**95%**	**5%**	**Mean**	**95%**	**5%**	**Mean**	**95%**
March	0.33	0.43	0.54	242.5	276.0	297.5	0.82	0.91	0.96
April	0.33	0.45	0.55	252.5	280.3	297.5	0.79	0.91	0.96
May	0.32	0.43	0.55	247.5	274.6	302.5	0.80	0.89	0.95
June	0.33	0.45	0.59	242.5	272.1	302.5	0.79	0.88	0.94
July	0.34	0.45	0.56	242.5	278.6	302.5	0.75	0.86	0.93
August	0.33	0.44	0.58	252.5	279.0	302.5	0.78	0.86	0.94
September	0.31	0.43	0.57	247.5	280.6	302.5	0.81	0.89	0.95
October	0.30	0.41	0.52	247.5	281.2	302.5	0.84	0.92	0.96
November	0.29	0.41	0.51	247.5	280.2	302.5	0.83	0.92	0.97
December	0.27	0.41	0.53	237.5	276.5	297.5	0.82	0.92	0.97
January	0.28	0.42	0.53	242.5	275.4	297.5	0.85	0.93	0.97
February	0.27	0.41	0.54	237.5	276.8	302.5	0.82	0.92	0.97

A.2. Wave Roses

The annual wave rose of omnidirectional wave power, J, and direction of maximum directionally resolved wave power, θ_j, is shown in Figure 45, and essentially mirrors that for significant wave height, H_{m0}, and θ_j shown in Figure 46.

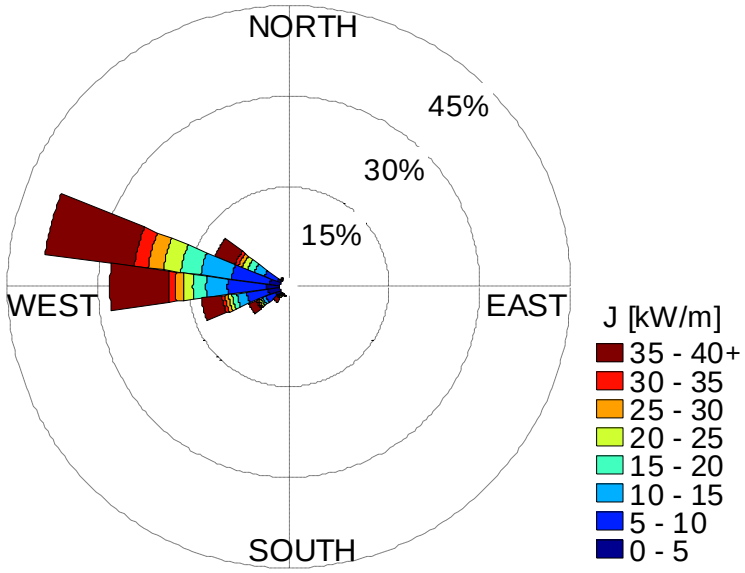

Figure 45. Annual wave rose of omnidirectional wave power and direction of maximally resolved wave power. Values of J greater than $60\,kW/m$ are included in the top bin as shown in the legend.

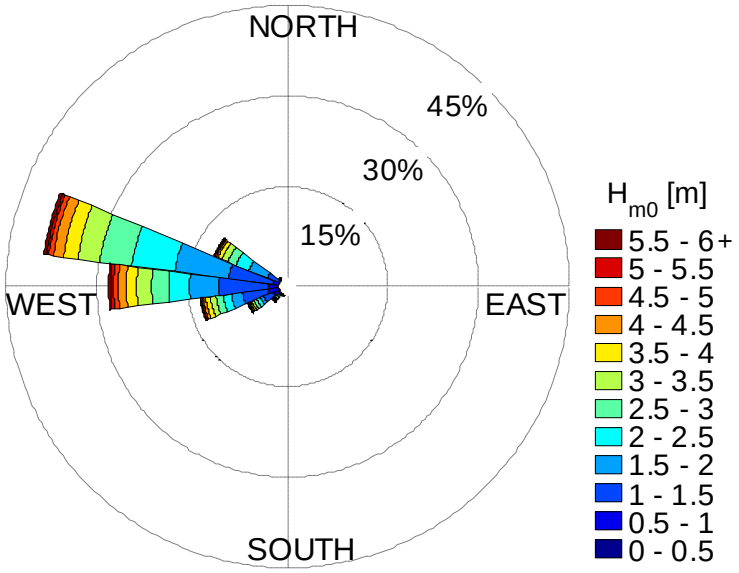

Figure 46. Annual wave rose of significant wave height and direction of maximally resolved wave power. Values of H_{m0} greater than $6\,m$ are included in the top bin as shown in the legend.

A.3. Extreme Sea States

Table 5. Selected values along the 100-year contour for NDBC46050 (see Figure 13).

Significant wave height [m]	Energy period [s]
1	3.89
2	4.63
3	5.32
4	5.96
5	6.56
6	7.13
7	7.67
8	8.21
9	8.73
10	9.26
11	9.79
12	10.34
13	10.92
14	11.56
15	12.27
16	13.14
17	14.39
17.55	16.32
17	18.27
16	19.66
15	20.66
14	21.47
13	22.17
12	22.80
11	23.35
10	23.86
9	24.32
8	24.73
7	25.09
6	25.42
5	25.69
4	25.92
3	26.08
2	26.18
1	26.20

A.4. Wind Data

The wind data for this site (obtained from CFSR), is the mean of magnitude and direction taken at 44.5 N, 124.5 W and 45 N, 124.5 W, which are the nearest data points to NETS. Note that the central location between these two points is approximately 30 km west/northwest of the test site (Figure 5). The average monthly values, along with the 5th and 95th percentiles, of wind are shown in Figure 47. The values are also tabulated in Table 6. The annual and seasonal wind roses are shown in Figure 48.

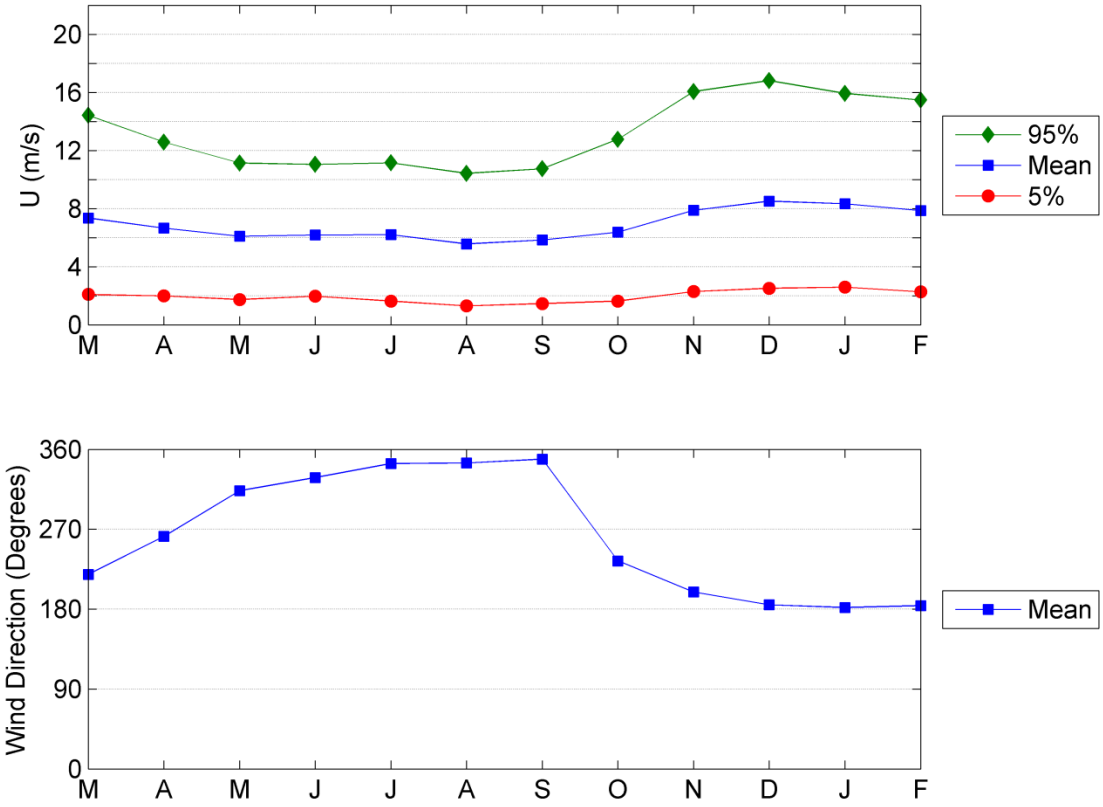

Figure 47. Monthly wind velocity and direction obtained from CSFR data during the period 1/1/1979 to 12/31/2012 at 44.75 N, 124.5 W, located 30 km west/northwest of NETS (Figure 5).

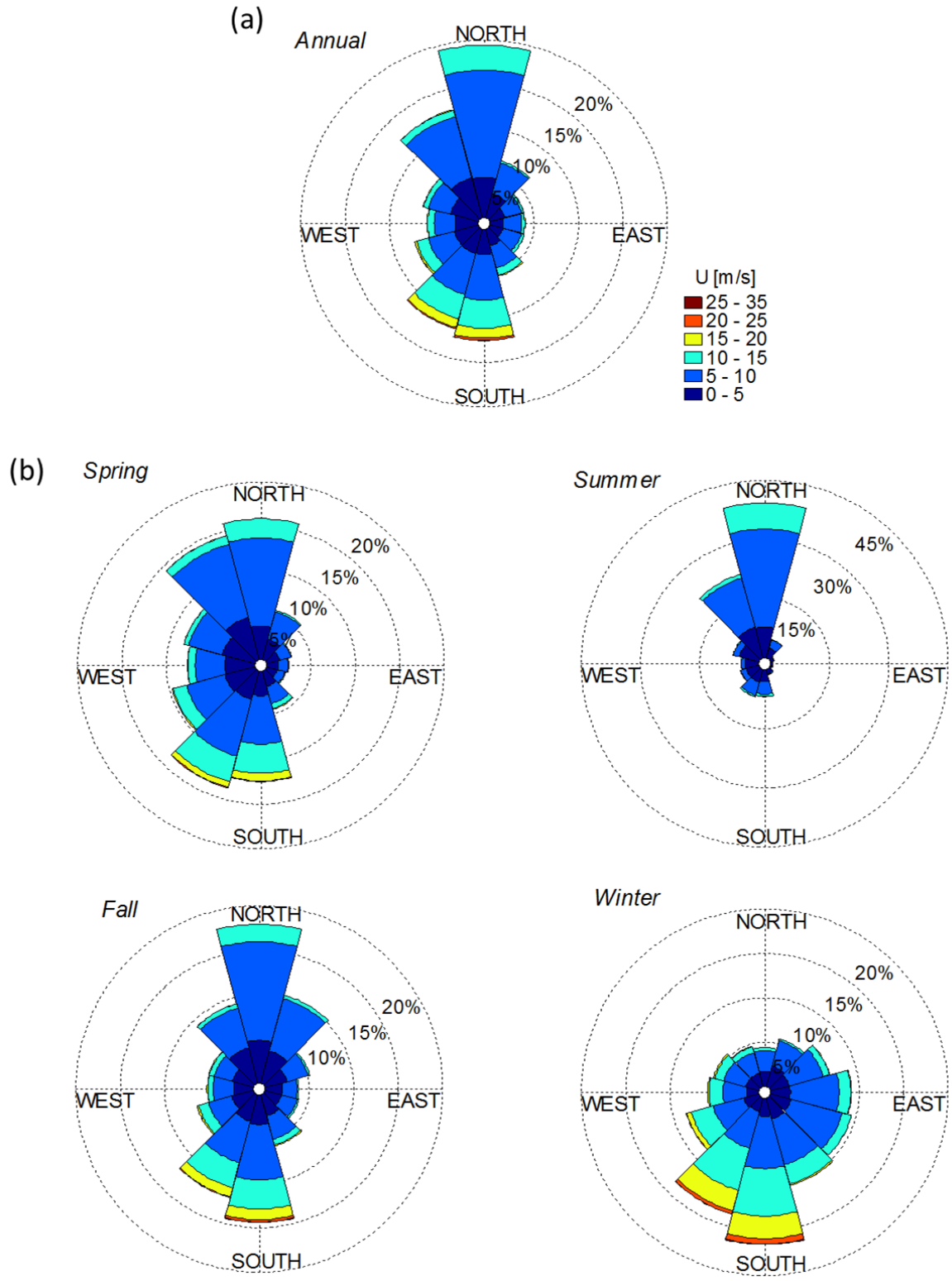

Figure 48. (a) Annual and (b) seasonal wind roses of velocity and direction obtained from CSFR data during the period 1/1/1979 to 12/31/2012. Data taken at 44.75 N, 124.5 W, located approximately 30 km west/northwest of NETS (Figure 5).

Table 6. Monthly wind velocity and direction obtained from CSFR data during the period 1/1/1979 to 12/31/2012 at 44.75 N, 124.5 W located 30 km west/northwest of NETS (Figure 5).

	$U\ [m/s]$			$Direction\ [°]$
	5%	**Mean**	**95%**	**Mean**
March	2.1	7.4	14.4	219
April	2.0	6.7	12.6	262
May	1.7	6.1	11.1	313
June	2.0	6.2	11.0	328
July	1.6	6.2	11.1	344
August	1.3	5.6	10.4	345
September	1.5	5.8	10.7	349
October	1.6	6.4	12.8	234
November	2.3	7.9	16.1	199
December	2.5	8.5	16.8	185
January	2.6	8.3	15.9	182
February	2.3	7.9	15.5	184

A.5. Ocean Surface Current Data

The surface current data (obtained from OSCAR), is located at 44.5 N, 125.5 W, the closest data point to shore. The average monthly values, along with the 5th and 95th percentiles, of current are shown in Figure 49. These data points are listed in Table 7. The annual and seasonal current roses are shown in Figure 50.

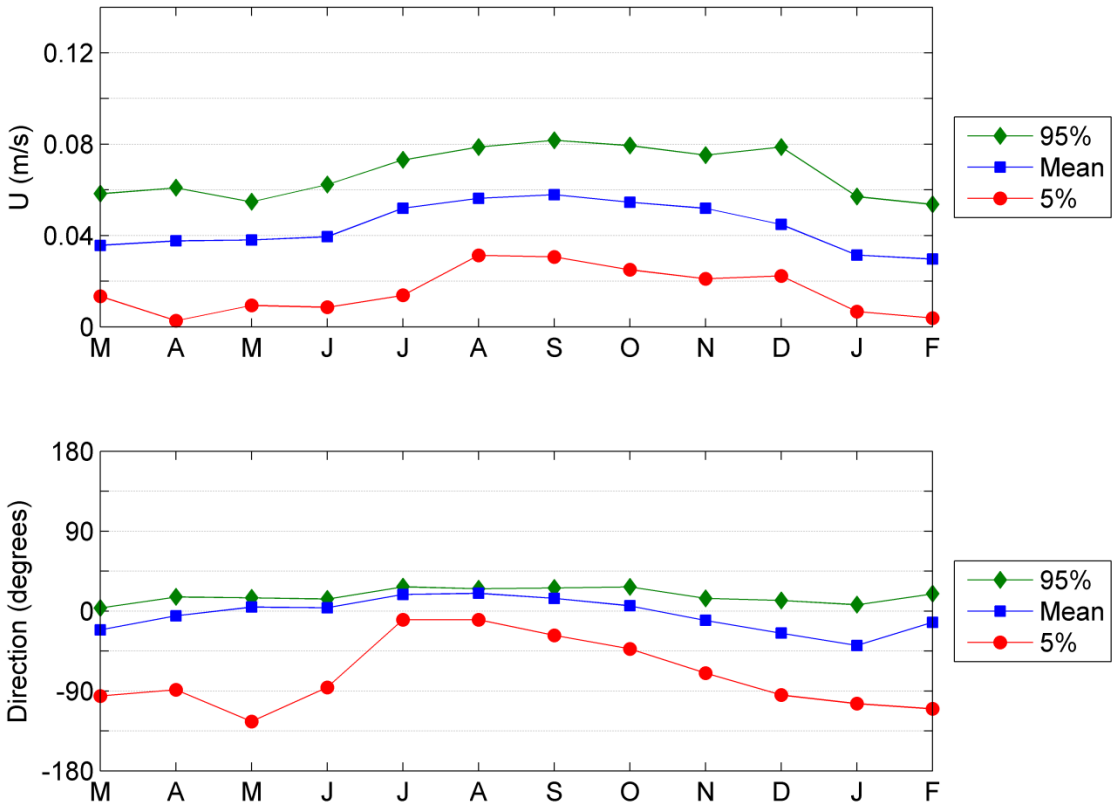

Figure 49. Monthly ocean surface current velocity and direction obtained from OSCAR at 44.5 N, 125.5 W, located approximately 35 km southwest of NETS. Data period 1/1/1993 to 12/30/2012.

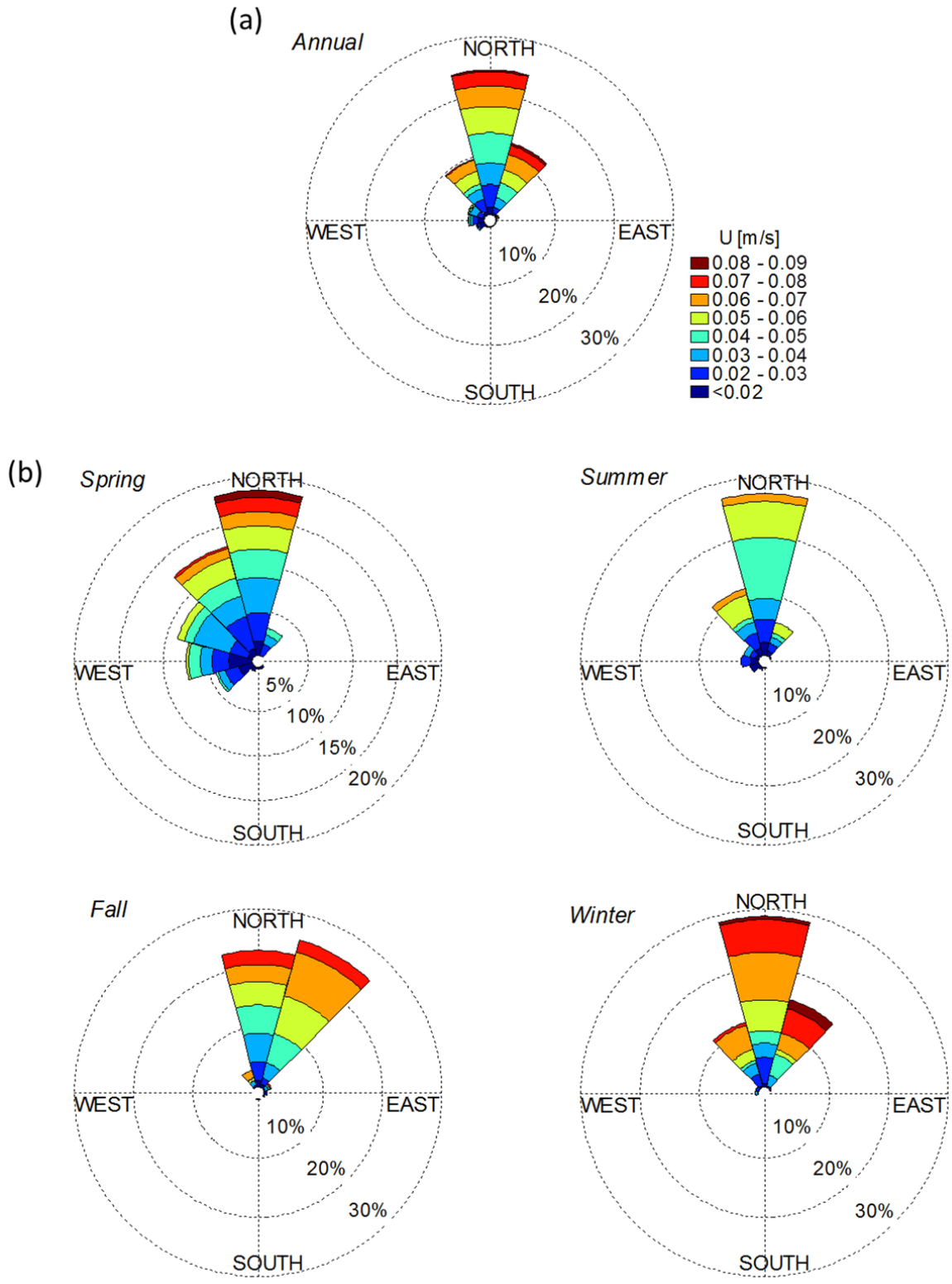

Figure 50. (a) Annual and (b) seasonal current roses of ocean surface current velocity and direction obtained from OSCAR at 44.5 N, 125.5 W, located approximately 35 km southwest of NETS. Data period 1/1/1993 to 12/30/2012.

Table 7. Monthly surface current velocity and direction obtained from OSCAR data during the period 1/1/1993 to 12/30/2012 at 44.5 N, 125.5 W located approximately 35 km southwest of NETS.

	$U\ [m/s]$			$Direction\ [°]$		
	5%	**Mean**	**95%**	**5%**	**Mean**	**95%**
March	0.013	0.036	0.058	-96	-21	3
April	0.003	0.038	0.061	-89	-5	16
May	0.009	0.038	0.055	-124	4	15
June	0.009	0.039	0.062	-86	4	14
July	0.014	0.052	0.073	-10	19	27
August	0.031	0.056	0.079	-10	20	25
September	0.031	0.058	0.082	-27	14	26
October	0.025	0.055	0.079	-43	6	27
November	0.021	0.052	0.075	-70	-11	14
December	0.022	0.045	0.079	-95	-25	12
January	0.007	0.031	0.057	-104	-39	7
February	0.004	0.030	0.054	-110	-13	19

APPENDIX B: WETS

B.1. IEC TS Parameter Values

Table 8. The average, 5th and 95th percentiles of the six parameters at Kaneohe II (see Figure 23).

	J $[kW/m]$			H_{m0} $[m]$			T_e $[s]$		
	5%	**Mean**	**95%**	**5%**	**Mean**	**95%**	**5%**	**Mean**	**95%**
March	3.9	16.0	40.9	0.92	1.76	2.83	6.85	8.62	11.41
April	3.5	11.9	26.2	0.94	1.63	2.40	6.58	7.92	9.95
May	2.1	7.2	15.7	0.74	1.32	1.96	6.28	7.36	9.06
June	2.2	6.5	11.9	0.82	1.34	1.82	5.83	6.79	8.17
July	2.9	6.4	11.8	0.95	1.36	1.84	5.79	6.63	7.66
August	2.4	6.3	12.7	0.88	1.32	1.84	5.75	6.66	7.83
September	3.4	7.4	13.9	0.95	1.34	1.84	6.17	7.51	9.57
October	4.1	11.2	25.3	1.01	1.52	2.23	6.60	8.24	11.04
November	4.9	17.7	47.9	1.06	1.80	2.91	6.95	8.80	11.76
December	5.9	18.4	44.2	1.12	1.82	2.76	7.14	9.48	12.83
January	5.1	16.8	42.6	1.00	1.72	2.78	7.28	9.54	12.66
February	4.4	15.2	34.0	0.98	1.71	2.66	6.89	8.90	11.53

	ϵ_0			θ_j [°]			d_θ		
	5%	**Mean**	**95%**	**5%**	**Mean**	**95%**	**5%**	**Mean**	**95%**
March	0.28	0.37	0.49	-22.5	25.4	67.5	0.67	0.81	0.92
April	0.28	0.36	0.47	-7.5	36.5	67.5	0.67	0.81	0.91
May	0.27	0.35	0.46	-7.5	42.0	67.5	0.66	0.81	0.91
June	0.27	0.34	0.45	22.5	53.7	67.5	0.72	0.85	0.92
July	0.28	0.33	0.41	37.5	52.0	67.5	0.75	0.86	0.91
August	0.28	0.34	0.44	37.5	54.2	67.5	0.74	0.86	0.91
September	0.28	0.35	0.46	-7.5	37.4	67.5	0.72	0.83	0.91
October	0.27	0.36	0.48	-7.5	26.9	67.5	0.68	0.81	0.92
November	0.27	0.36	0.48	-7.5	27.0	67.5	0.67	0.81	0.93
December	0.28	0.37	0.49	-22.5	17.9	52.5	0.66	0.81	0.94
January	0.29	0.38	0.50	-22.5	12.8	67.5	0.67	0.83	0.95
February	0.29	0.39	0.52	-22.5	19.3	67.5	0.66	0.82	0.93

Table 9. The average, 5th and 95th percentiles of the six parameters at WETS (see Figure 24).

	J $[kW/m]$			H_{m0} $[m]$			T_e $[s]$		
	5%	**Mean**	**95%**	**5%**	**Mean**	**95%**	**5%**	**Mean**	**95%**
March	4.3	17.5	42.7	0.98	1.89	2.96	6.91	8.61	11.28
April	4.1	13.3	29.0	1.03	1.76	2.58	6.61	7.94	9.95
May	2.4	8.2	17.4	0.81	1.44	2.12	6.31	7.39	9.06
June	2.6	7.6	14.1	0.89	1.45	2.00	5.87	6.85	8.15
July	3.3	7.4	13.8	1.02	1.47	1.98	5.85	6.70	7.71
August	2.8	7.3	14.8	0.95	1.43	2.01	5.81	6.74	7.93
September	3.8	8.3	15.9	1.00	1.44	1.99	6.24	7.53	9.54
October	4.6	12.2	26.6	1.08	1.63	2.38	6.64	8.22	10.99
November	5.3	19.1	49.7	1.14	1.92	3.06	7.00	8.78	11.66
December	6.5	20.0	47.5	1.20	1.94	2.96	7.22	9.45	12.82
January	5.5	18.1	44.9	1.06	1.82	2.92	7.31	9.54	12.59
February	4.9	16.4	35.6	1.05	1.82	2.79	6.91	8.88	11.41

	ϵ_0			θ_j [°]			d_θ		
	5%	**Mean**	**95%**	**5%**	**Mean**	**95%**	**5%**	**Mean**	**95%**
March	0.27	0.36	0.48	-22.5	30.8	67.5	0.64	0.80	0.92
April	0.27	0.35	0.45	-7.5	42.2	67.5	0.66	0.80	0.91
May	0.26	0.34	0.45	-7.5	47.7	82.5	0.65	0.81	0.92
June	0.27	0.33	0.43	22.5	58.6	82.5	0.72	0.85	0.92
July	0.27	0.33	0.40	37.5	56.9	67.5	0.75	0.86	0.91
August	0.27	0.33	0.43	37.5	59.9	67.5	0.74	0.86	0.92
September	0.28	0.35	0.45	-7.5	42.3	67.5	0.70	0.83	0.91
October	0.27	0.35	0.47	-7.5	31.7	67.5	0.65	0.80	0.92
November	0.27	0.35	0.46	-7.5	32.6	67.5	0.65	0.80	0.93
December	0.27	0.36	0.48	-22.5	23.1	67.5	0.64	0.80	0.95
January	0.28	0.37	0.49	-22.5	16.9	67.5	0.65	0.83	0.95
February	0.28	0.38	0.50	-22.5	23.5	67.5	0.64	0.81	0.93

B.2. Wave Roses

The annual wave rose of omnidirectional wave power, J, and direction of maximum directionally resolved wave power, θ_j, is shown in Figure 51, and essentially mirrors that for significant wave height, H_{m0}, and θ_j shown in Figure 52.

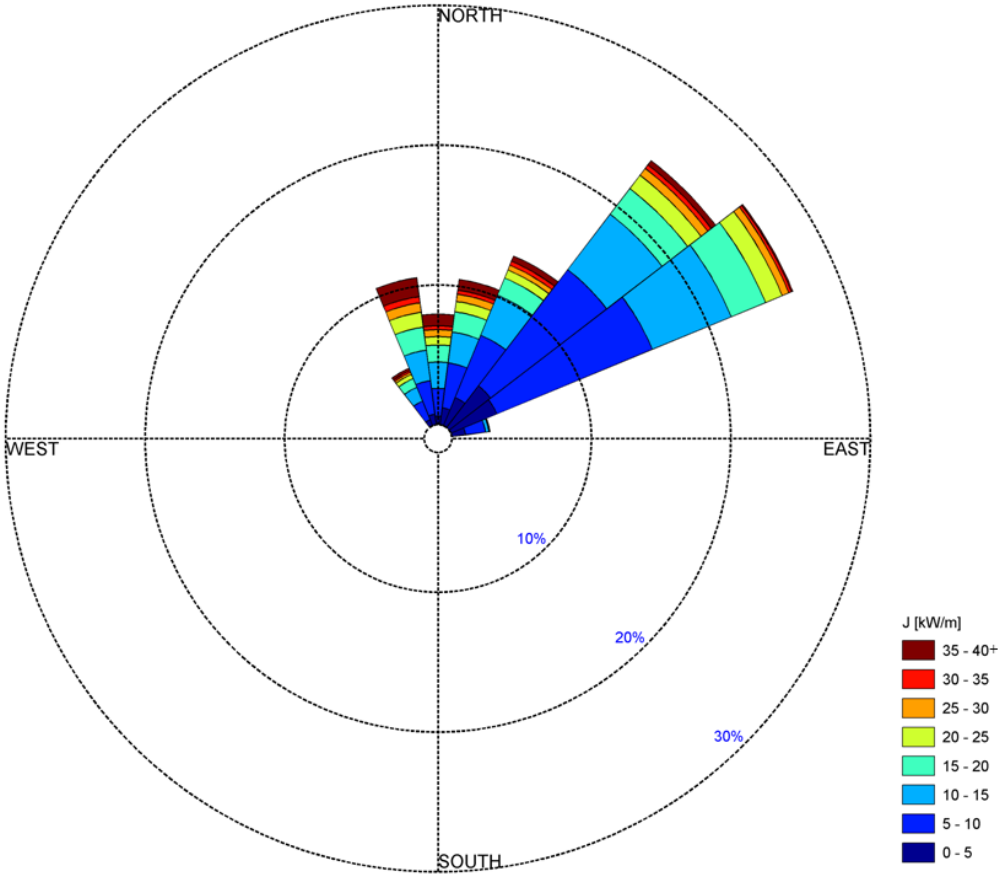

Figure 51. Annual wave rose of omnidirectional wave power and direction of maximum directionally resolved wave power. Values of J greater than $40\ kW/m$ are included in the top bin as shown in the legend. Figure produced by Ning Li (Li and Cheung 2014).

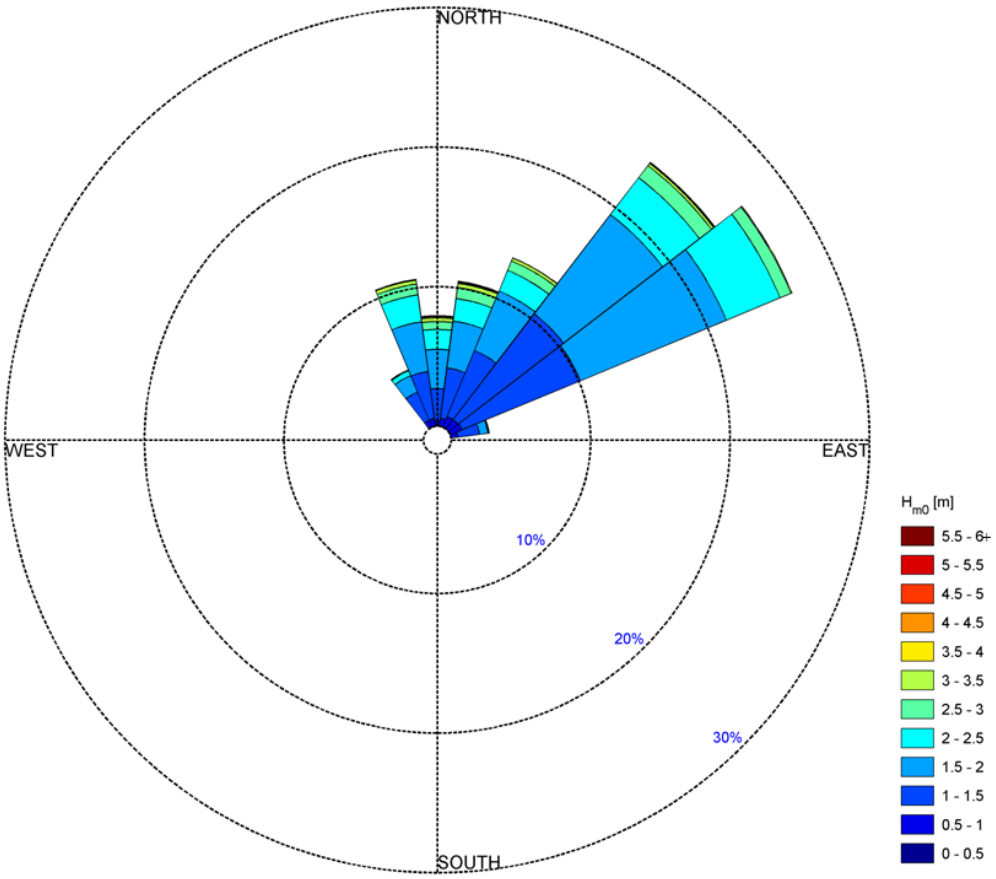

Figure 52. Annual wave rose of significant wave height and direction of maximum directionally resolved wave power. Values of H_{m0} greater than $6\ m$ are included in the top bin as shown in the legend. Figure produced by Ning Li (Li and Cheung 2014).

B.3. Extreme Sea States

Table 10. Selected values along the 100-year contour for CDIP098 (NDBC51202) (see Figure 30).

Significant wave height [m]	Energy period [s]
1	3.8
2	3.8
3	5.2
4	6.8
5	8.5
6	10.8
6.37	12.8
6	14.4
5	15.5
4	16.0
3	16.3
2	16.3
1	16.1

B.4. Wind Data

The wind data for this site (obtained from CFSR), is taken at 21.5 N, 157.5 W located approximately 25 km east of WETS (Figure 20), which is the nearest data point to the site. The average monthly values, along with the 5^{th} and 95^{th} percentiles, of wind are shown in Figure 53. The values are also tabulated in Table 11. The annual and seasonal wind roses are shown in Figure 54.

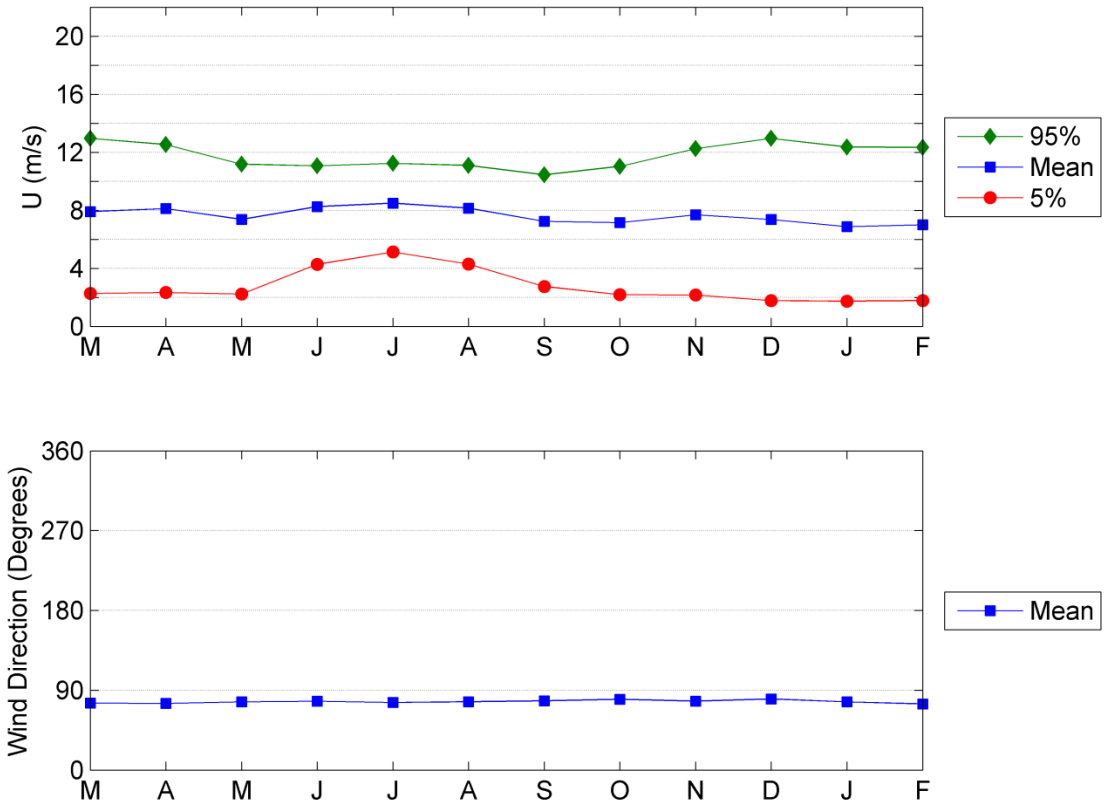

Figure 53. Monthly wind velocity and direction obtained from CSFR data during the period 1/1/1979 to 12/31/2012 at 21.5 N, 157.5 W, located approximately 25 km east of WETS (Figure 20).

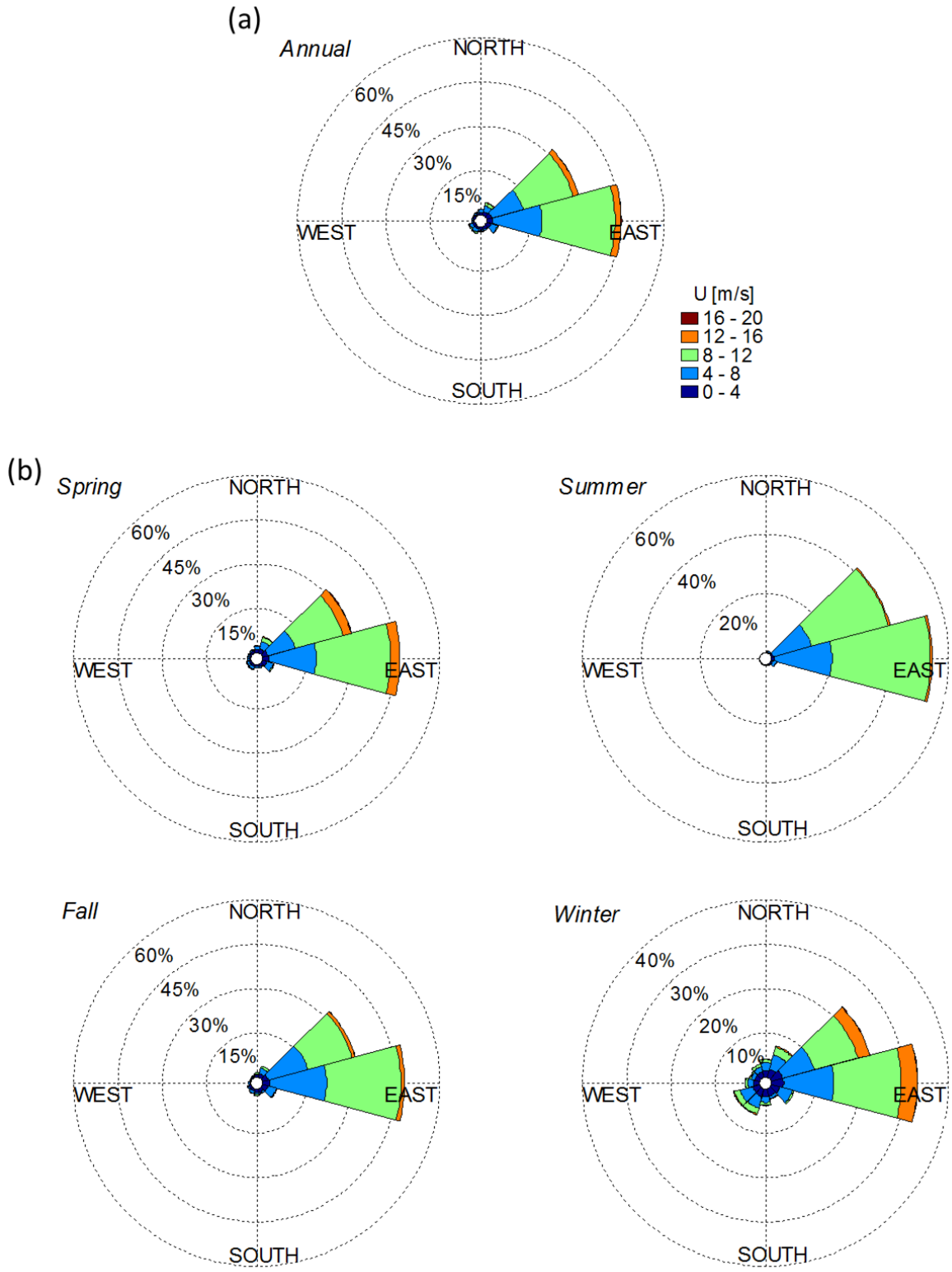

Figure 54. (a) Annual and (b) seasonal wind roses of velocity and direction obtained from CSFR data during the period 1/1/1979 to 12/31/2012. Data taken at 21.5 N, 157.5 W, located approximately 25 km east of WETS (Figure 20).

Table 11. Monthly wind velocity and direction obtained from CSFR data during the period 1/1/1979 to 12/31/2012 at 21.5 N, 157.5 W, located approximately 25 km east of WETS (Figure 20).

	$U\ [m/s]$			$Direction\ [°]$
	5%	Mean	95%	Mean
March	2.3	7.9	13.0	75
April	2.3	8.1	12.5	75
May	2.2	7.4	11.2	77
June	4.3	8.3	11.1	77
July	5.1	8.5	11.2	76
August	4.3	8.1	11.1	77
September	2.7	7.2	10.4	78
October	2.2	7.1	11.0	80
November	2.2	7.7	12.2	78
December	1.8	7.4	13.0	80
January	1.7	6.9	12.4	77
February	1.8	7.0	12.3	75

Table 12. Monthly wind velocity from the UH high resolution WRF data set used in their hindcast and for weather window calculations, located at the 80 m depth berth.

	$U\ [m/s]$
March	7.0
April	7.0
May	6.2
June	7.1
July	7.2
August	6.9
September	6.2
October	6.2
November	6.5
December	6.4
January	6.2
February	6.4

B.5. Ocean Surface Current Data

The surface current data (obtained from OSCAR), is located at 21.5 N, 157.5 W, the closest data point to shore. The average monthly values, along with the 5th and 95th percentiles, of current are shown in Figure 55. These data points are listed in Table 13. The annual and seasonal current roses are shown in Figure 56.

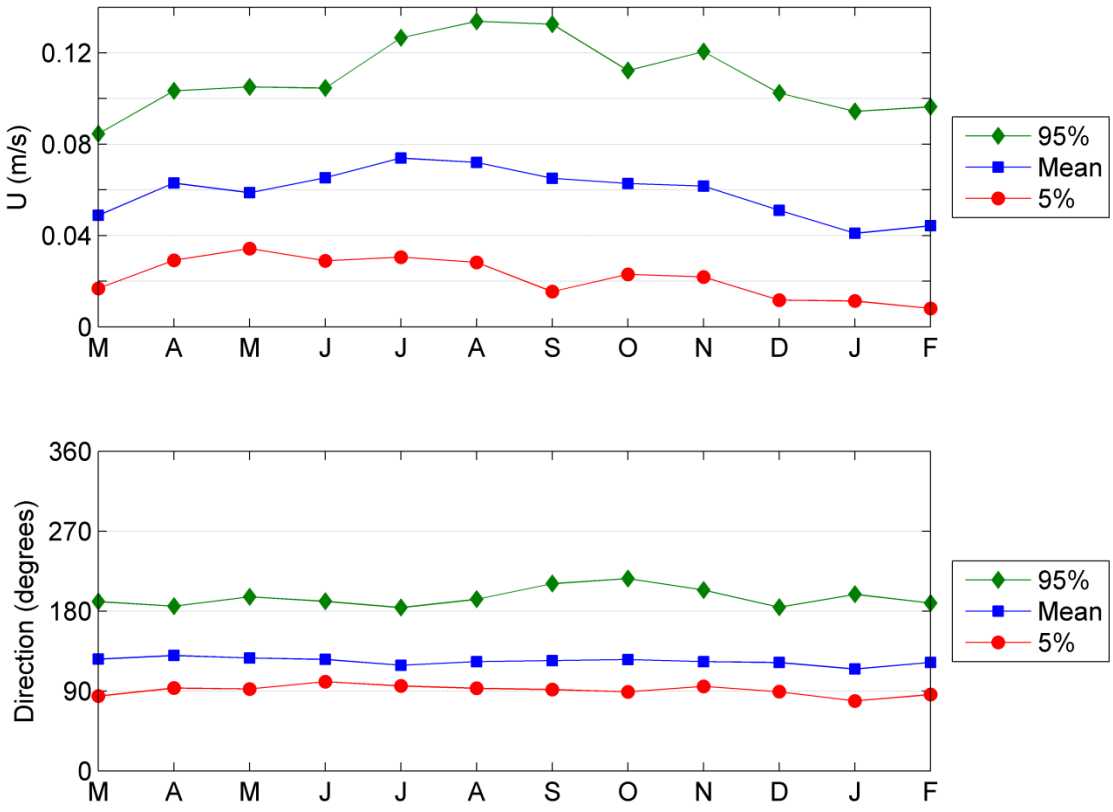

Figure 55. Monthly ocean surface current velocity and direction obtained from OSCAR at 21.5 N, 157.5 W, located approximately 25 km east of NETS. Data period 1/1/1993 to 12/30/2012.

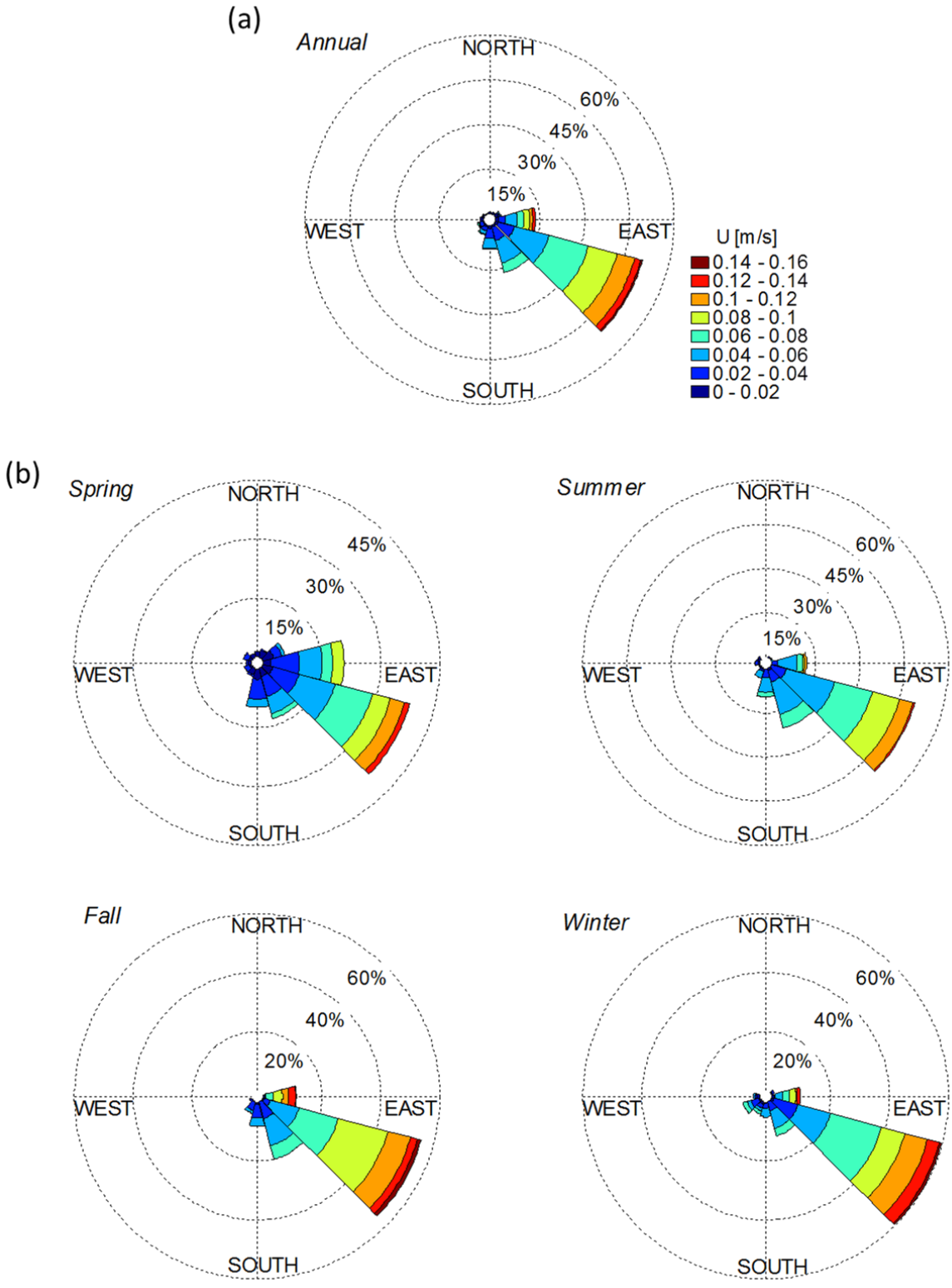

Figure 56. (a) Annual and (b) seasonal current roses of ocean surface current velocity and direction obtained from OSCAR at 21.5 N, 157.5 W, located approximately 25 km east of WETS. Data period 1/1/1993 to 12/30/2012.

Table 13. Monthly surface current velocity and direction obtained from OSCAR data during the period 1/1/1993 to 12/30/2012 at 21.5 N, 157.5 W, located approximately 25 km east of WETS.

	$U\ [m/s]$			$Direction\ [°]$		
	5%	**Mean**	**95%**	**5%**	**Mean**	**95%**
March	0.017	0.049	0.085	84	126	191
April	0.029	0.063	0.103	93	130	185
May	0.034	0.059	0.105	92	127	196
June	0.029	0.065	0.105	100	126	191
July	0.031	0.074	0.127	96	119	184
August	0.028	0.072	0.134	93	123	193
September	0.015	0.065	0.133	92	124	211
October	0.023	0.063	0.112	89	125	217
November	0.022	0.062	0.121	95	123	204
December	0.012	0.051	0.102	89	122	184
January	0.011	0.041	0.094	79	115	199
February	0.008	0.044	0.096	86	122	189

APPENDIX C: HUMBOLDT SITE

C.1. IEC TS Parameter Values

Table 14. The average, 5th and 95th percentiles of the six parameters at the Humboldt Site (see Figure 37).

	J $[kW/m]$			H_{m0} $[m]$			T_e $[s]$		
	5%	**Mean**	**95%**	**5%**	**Mean**	**95%**	**5%**	**Mean**	**95%**
March	8.9	47.6	120.8	1.34	2.60	4.16	7.66	10.07	12.91
April	6.0	29.7	77.4	1.16	2.16	3.48	6.81	9.21	11.61
May	3.1	16.0	43.3	0.89	1.74	2.84	6.17	7.81	10.21
June	2.8	13.5	34.8	0.81	1.70	2.77	5.89	7.35	9.19
July	2.4	11.4	26.3	0.79	1.64	2.54	5.66	6.95	8.36
August	2.5	10.8	26.2	0.80	1.57	2.46	5.71	7.03	8.83
September	3.1	14.9	37.3	0.83	1.71	2.67	6.32	7.95	10.19
October	5.6	32.4	95.8	1.10	2.20	3.79	6.81	9.28	11.95
November	6.3	51.2	133.9	1.11	2.61	4.37	7.96	10.28	13.41
December	10.8	71.4	193.8	1.39	3.02	5.13	8.47	11.00	14.02
January	8.9	62.0	159.2	1.31	2.82	4.67	8.33	10.99	13.87
February	11.1	53.6	144.2	1.43	2.66	4.45	8.15	10.93	13.63

	ϵ_0			θ_j [°]			d_θ		
	5%	**Mean**	**95%**	**5%**	**Mean**	**95%**	**5%**	**Mean**	**95%**
March	0.24	0.31	0.41	267.5	289.8	307.5	0.88	0.93	0.97
April	0.26	0.32	0.42	270.0	293.4	312.5	0.88	0.93	0.96
May	0.26	0.35	0.47	265.0	293.9	317.5	0.85	0.91	0.95
June	0.27	0.35	0.48	270.0	298.5	317.5	0.84	0.91	0.95
July	0.27	0.35	0.48	272.5	303.2	317.5	0.87	0.92	0.95
August	0.27	0.35	0.47	282.5	303.9	317.5	0.85	0.91	0.95
September	0.26	0.34	0.46	277.5	302.4	317.5	0.88	0.93	0.95
October	0.24	0.31	0.42	272.5	297.0	317.5	0.88	0.93	0.96
November	0.23	0.29	0.40	270.0	291.5	307.5	0.87	0.93	0.97
December	0.22	0.29	0.39	265.0	287.6	307.5	0.87	0.93	0.97
January	0.22	0.30	0.41	261.3	285.7	305.0	0.87	0.94	0.97
February	0.22	0.30	0.40	265.0	286.9	305.0	0.87	0.93	0.97

C.2. Wave Roses

The annual wave rose of omnidirectional wave power, J, and direction of maximum directionally resolved wave power, θ_j, is shown in Figure 57, and essentially mirrors that for significant wave height, H_{m0}, and θ_j shown in Figure 58.

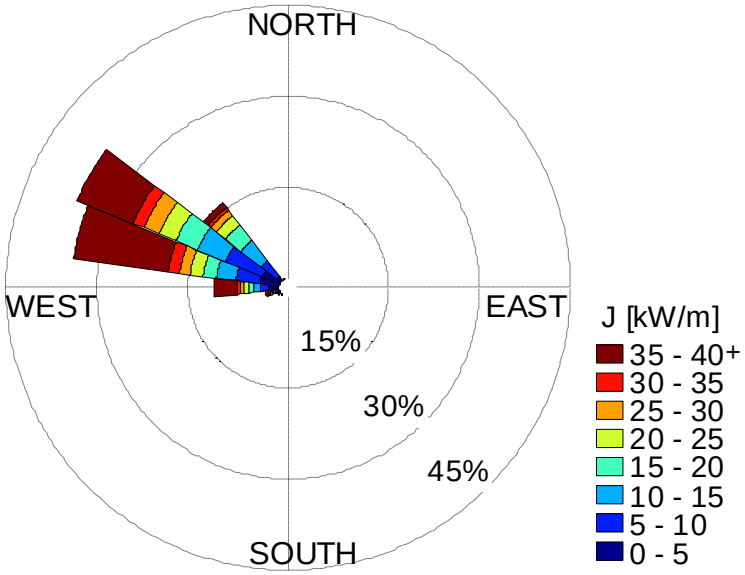

Figure 57. Annual wave rose of omnidirectional wave power and direction of maximum directionally resolved wave power. Values of J greater than $40\ kW/m$ are included in the top bin as shown in the legend.

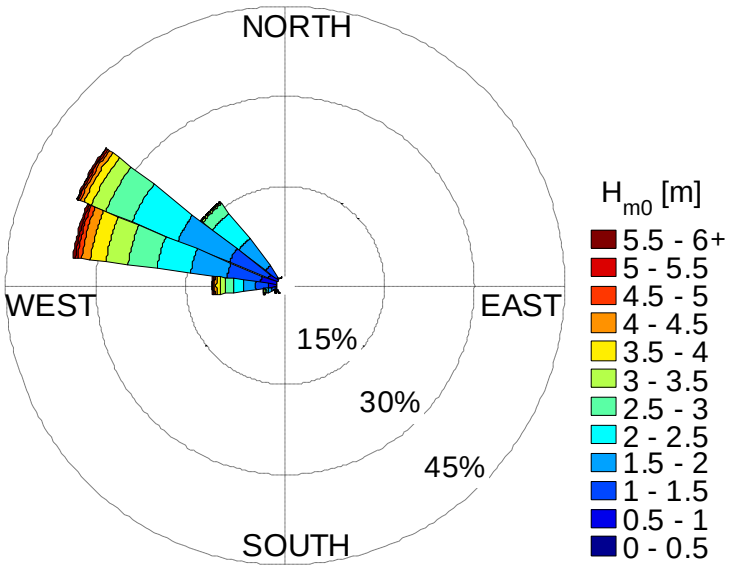

Figure 58. Annual wave rose of significant wave height and direction of maximum directionally resolved wave power. Values of H_{m0} greater than $6\ m$ are included in the top bin as shown in the legend.

C.3. Extreme Sea States

Table 15. Selected values along the 100-year contour for CDIP128 (NDBC46212) (see Figure 43).

Significant wave height [m]	Energy period [s]
1	3.7
2	4.5
3	5.5
4	6.5
5	7.6
6	8.8
7	10.1
8	11.4
9	13.0
10	15.1
10.49	17.7
10	20.0
9	21.5
8	22.3
7	22.8
6	23.2
5	23.3
4	23.3
3	23.2
2	22.8
1	22.2

C.4. Wind Data

The wind data for this site (obtained from CFSR), is the mean of magnitude and direction taken at 40.5 N, 124.5 W and 41 N, 124.5 W. Note that the central location between these two points is approximately 25 km southwest of the test site (Figure 35). The average monthly values, along with the 5^{th} and 95^{th} percentiles, of wind are shown in Figure 59. The values are also tabulated in Table 16. The annual and seasonal wind roses are shown in Figure 60. In the summer, the predominant direction of winds and waves correlate well. In the winter, the waves are dominated by distant swells, and the local winds have little effect.

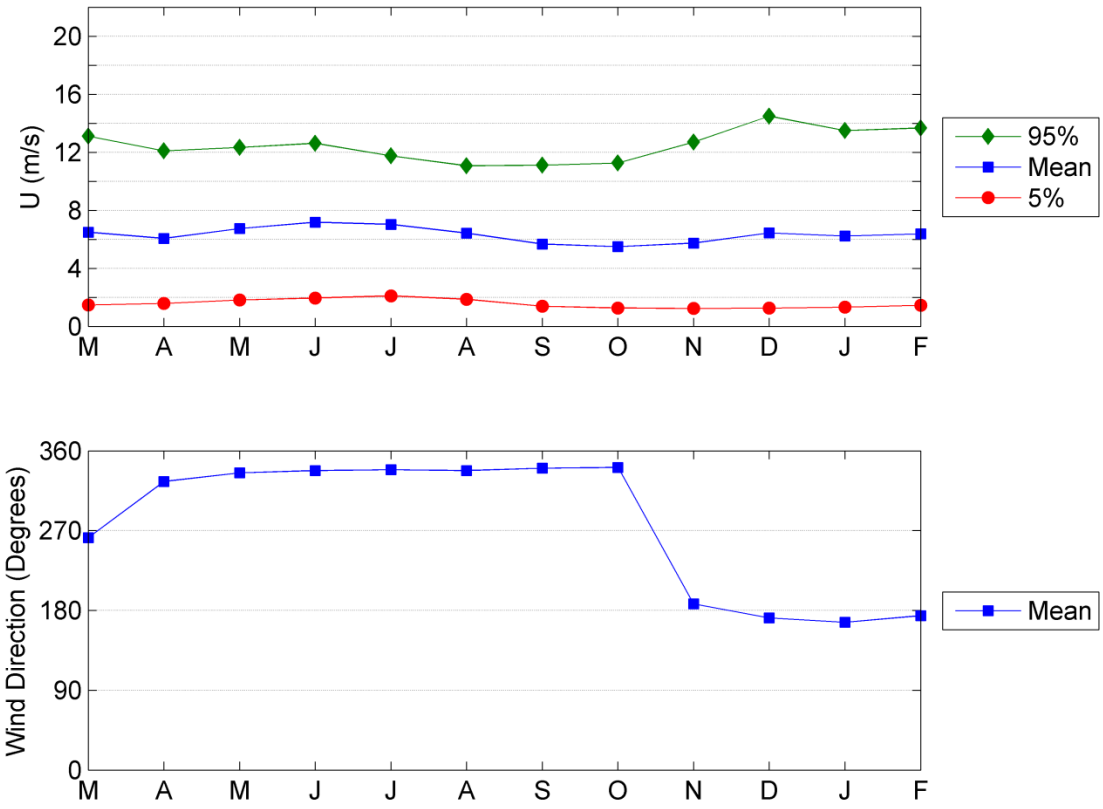

Figure 59. Monthly wind velocity and direction obtained from CSFR data during the period 1/1/1979 to 12/31/2012 at 40.75 N, 124.5 W, located approximately 25 km southwest of the test site (Figure 35).

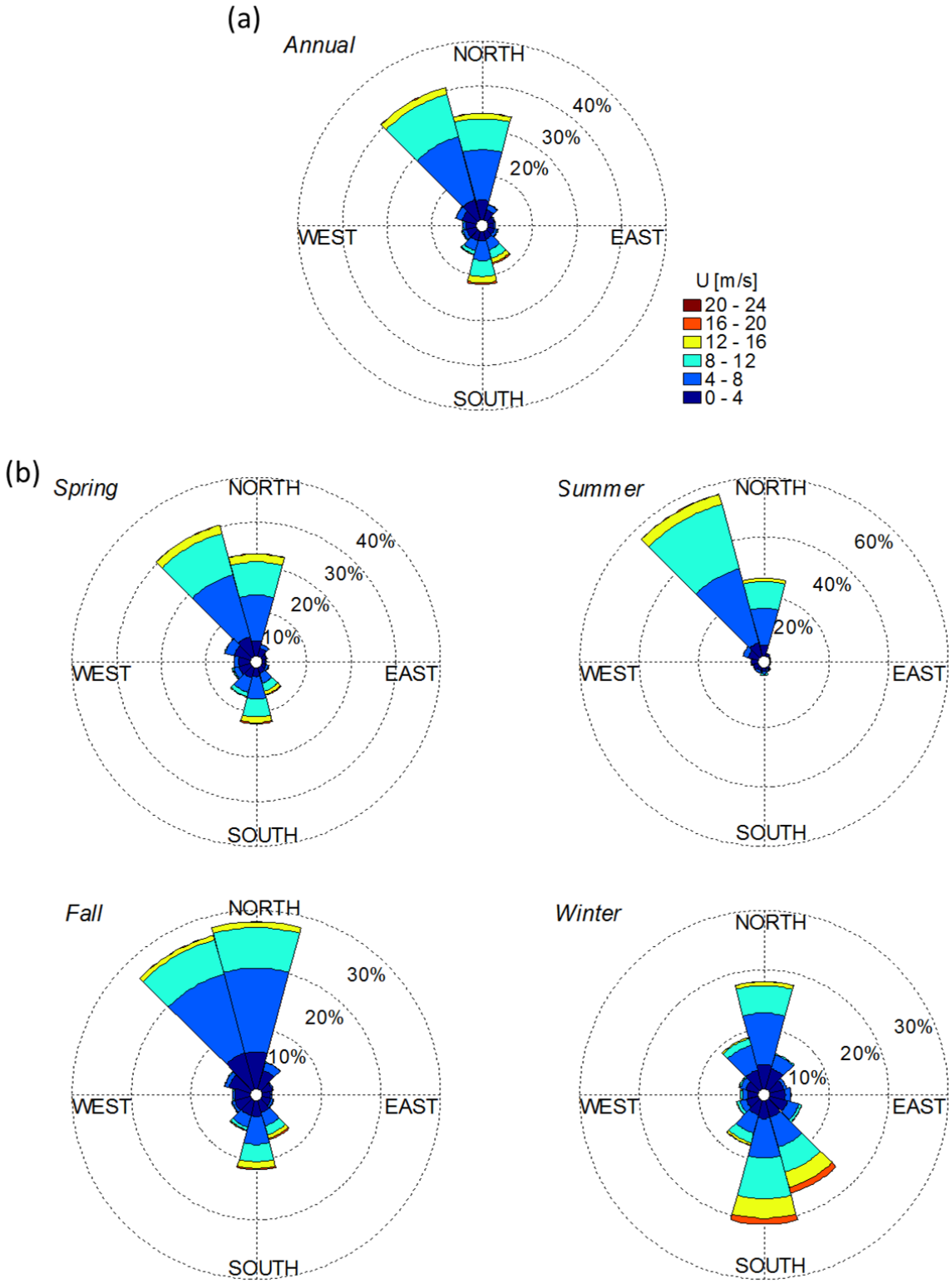

Figure 60. (a) Annual and (b) seasonal wind roses of velocity and direction obtained from CSFR data during the period 1/1/1979 to 12/31/2012. Data taken at 40.75 N, 124.5 W, located approximately 25 km southwest of the test site (Figure 35).

Table 16. Monthly wind velocity and direction obtained from CSFR data during the period 1/1/1979 to 12/31/2012 at 40.75 N, 124.5 W located approximately 25 km southwest of the Humboldt Site (Figure 35).

	$U\ [m/s]$			$Direction\ [°]$
	5%	**Mean**	**95%**	**Mean**
March	1.5	6.5	13.1	262
April	1.6	6.1	12.1	325
May	1.8	6.7	12.3	335
June	2.0	7.2	12.6	338
July	2.1	7.0	11.8	339
August	1.9	6.4	11.1	338
September	1.4	5.7	11.1	340
October	1.3	5.5	11.3	341
November	1.2	5.7	12.7	187
December	1.3	6.4	14.5	171
January	1.3	6.2	13.5	167
February	1.5	6.4	13.7	174

C.5. Ocean Surface Current Data

The current data (obtained from OSCAR), is located at 40.5 N, 125.5 W, the closest data point to shore. The average monthly values, along with the 5^{th} and 95^{th} percentiles, of current are shown in Figure 61. These data points are listed in Table 17. The annual and seasonal current roses are shown in Figure 62.

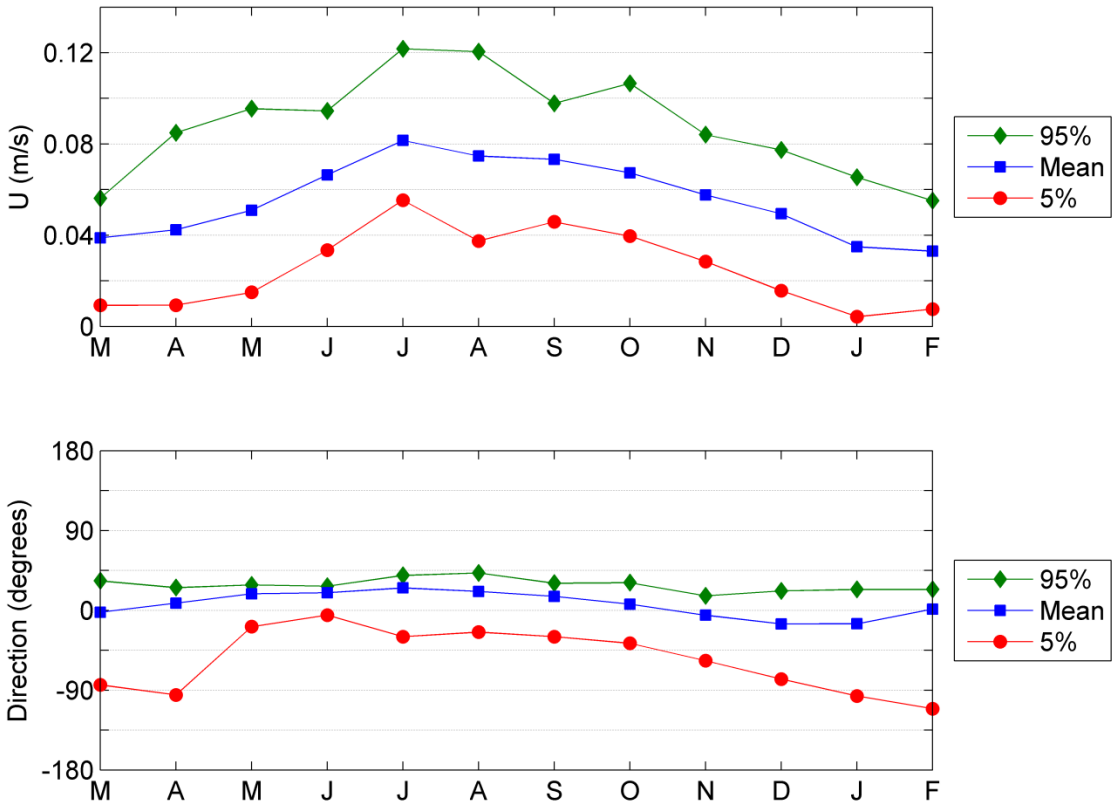

Figure 61. Monthly ocean surface current velocity and direction obtained from OSCAR at 40.5 N, 125.5 W, located approximately 110 km southwest of the Humboldt Site. Data period 1/1/1993 to 12/30/2012.

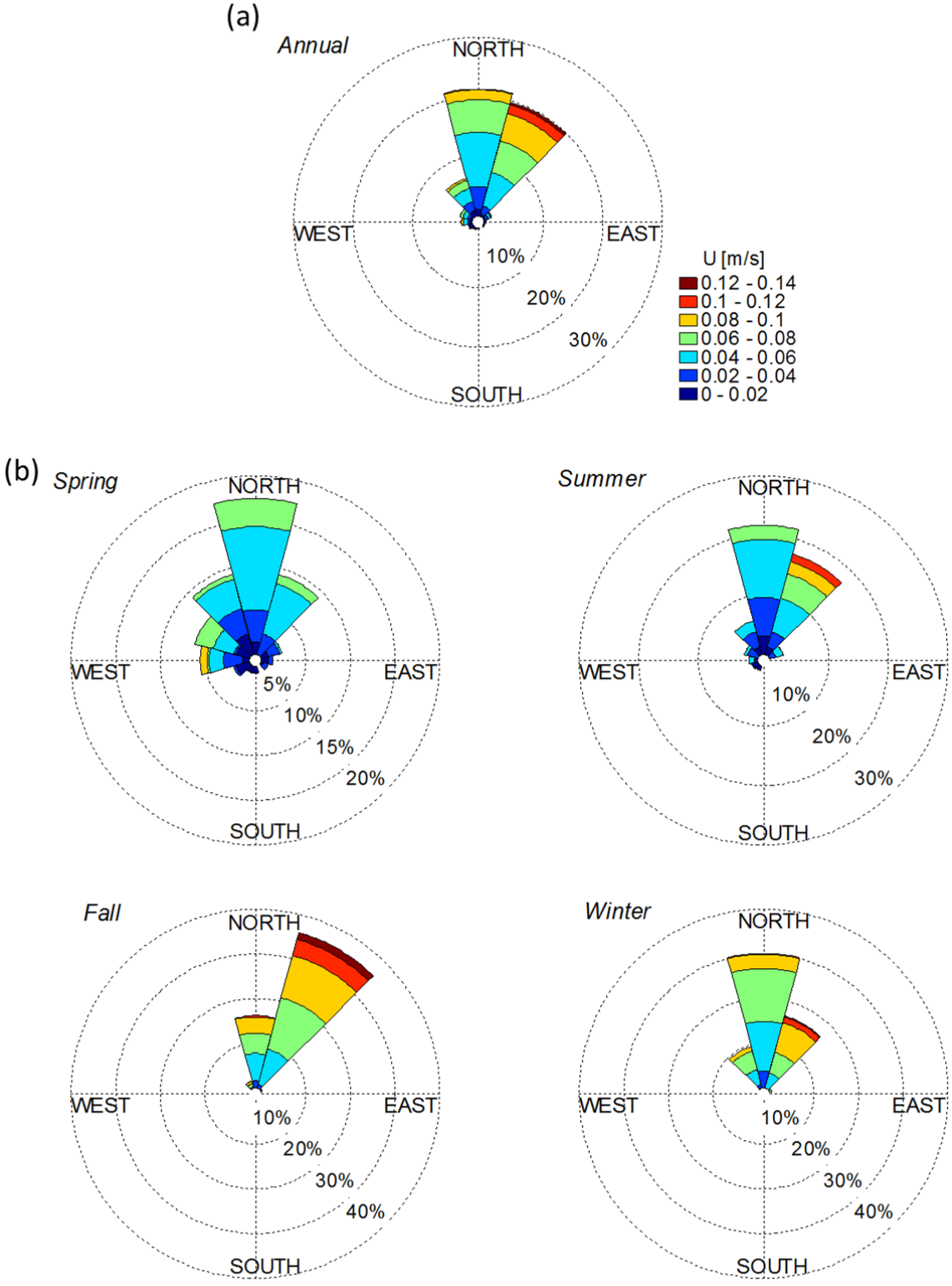

Figure 62. (a) Annual and (b) seasonal current roses of ocean surface current velocity and direction obtained from OSCAR at 40.5 N, 125.5 W, located approximately 110 km southwest of the Humboldt Site. Data period 1/1/1993 to 12/30/2012.

Table 17. Monthly surface current velocity and direction obtained from OSCAR data during the period 1/1/1993 to 12/30/2012 at 40.5 N, 125.5 W located approximately 110 km northwest of the Humboldt Site.

	$U\ [m/s]$			$Direction\ [°]$		
	5%	**Mean**	**95%**	**5%**	**Mean**	**95%**
March	0.009	0.039	0.056	-84	-2	33
April	0.009	0.042	0.085	-95	8	26
May	0.015	0.051	0.095	-18	19	29
June	0.033	0.066	0.094	-5	20	27
July	0.055	0.082	0.122	-30	25	39
August	0.037	0.075	0.120	-25	21	42
September	0.046	0.073	0.098	-30	16	31
October	0.040	0.067	0.107	-37	7	31
November	0.028	0.058	0.084	-57	-5	16
December	0.016	0.049	0.077	-78	-15	22
January	0.004	0.035	0.065	-96	-15	24
February	0.008	0.033	0.055	-111	1	23


Sandia National Laboratories